Università degli Studi di Modena e Reggio Emilia

PhD School in Molecular and Regenerative Medicine

XXXII CYCLE

Crosstalk between iron homeostasis, metabolic syndrome and pathways involved in metabolic adaptation

Candidate: Dr Elena Buzzetti

Supervisor: Prof. Antonello Pietrangelo

Coordinator: Prof. Michele De Luca

Contents

1. INTRODUCTION

Iron is a microelement of pivotal importance for both cells and organisms: indeed, it is essential for several vital processes, such as energy production, biosynthesis, replication and locomotion. From ancient times iron has been recognized as having an important role in humans, both in health and disease. Iron medicinal use was reported by Egyptians, Hindus, Greeks, and Romans (1). The importance of iron was finally settled in 1932 by the convincing evidence that inorganic iron was needed for hemoglobin synthesis (2). Iron is in fact primarily used by developing red blood cells for the synthesis of heme, a prosthetic group deputized to link oxygen contained in hemoglobin, allowing oxygen transportation to tissue and organs via the bloodstream. Over more recent years, it has been demonstrated how iron, its metabolism and its regulatory pathways can influence many processes involved in the regulation of overall metabolism, as well as disease outcomes when it is in abundance or deficiency.

The term 'hemochromatosis' is used to indicate a heterogeneous group of either inherited or idiopathic conditions (3). Hereditary Hemochromatosis (HH) is a disorder in which a genetic defect contributes to uncontrolled iron adsorption from food, resulting in excess iron excess over requirements, as the body lacks an adequate excretory system. Over time, this excess leads to a state of iron overload, with accumulation and consequential damage, especially in the liver, heart and endocrine glands (4). Although it was initially believed that the pathogenic homozygous mutation (C282Y) of the HFE gene was 'the culprit' in most of patients with HH (5), it rapidly became clear that not all the carriers of such mutation show the typical phenotypic manifestations, but rather C282Y was found to have low penetrance. Moreover, other 'iron genes' have been identified, which mutations have been associated with hereditary iron overload syndromes with similar, if not the same, phenotypic features seen in classical hemochromatosis: transferrin receptor 2 (TfR2) (6), hepcidin (HAMP) (7, 8),hemojuvelin (HJV) (7,

8) and ferroportin (FPN) (9, 10). The OMIM (Online Mendelian Inheritance in Man) database subcategorizes hemochromatosis according to the chronological order of discovery of the affected genes [13]: type 1, the classic form due to HFE mutations; type 2, comprising subtypes 2A (due to HAMP mutations) and 2B (due to HJV mutations); type 3 (caused byTfR2 mutations); and type 4 (due to FPN mutations). According to several experts such classification is simplistic and incomplete and does not consider the peculiarity or similarity of phenotypes within subtypes. This said, what is certain is that each type involves the alteration of a gene which is either involved in iron adsorption (directly or as a regulator, such as FPN or HAMP), or in iron sensing (HFE, TfR2, HJV).

1.1 IRON BIOCHEMISTRY

Iron is one of the most abundant microelements on earth, although its availability for organisms is limited by its high insolubility in aqueous environment. In fact, iron chemistry in aqueous solution translates mainly in the presence of two isoforms, Fe^{2+} and Fe^{3+}, which have the ability to mediate electron transfer, changing between the ferrous (+2) and ferric (+3) oxidation states, and therefore being involved in acid-base reactions.

The one-electron transfer between these oxidation states is achieved in a way that reducing agents perform the reduction of aqueous Fe^{3+} to Fe^{2+}, while dioxygen (O2) promotes the reverse reaction (Fig. 1). The most stable form of iron under physiological O2 concentrations is Fe^{3+}. Such iron capacity to participate in one-electron transfer reactions, makes iron indispensable for life. Indeed, some iron-containing proteins and enzymes are the key components of many essential biological processes, such as energy metabolism and oxygen transport. Another fundamental free radical reaction, rate-determining in DNA synthesis, is the reduction of ribonucleotides to their corresponding deoxy ribonucleotides, catalyzed by ribonucleotides reductases (RNRs) all of which are metalloenzymes.

Other functions encompass the detoxification of reactive oxygen species (ROS) and their reaction products, as well as numerous other reactions catalyzed by enzymes such as oxygenases or peroxygenases.

On the other hand, the reduction of O2 by Fe^{2+} may result in the formation of superoxide radicals, some of which are responsible for the attack to proteins, nucleic acids and carbohydrates, and may trigger lipid peroxidation and cell apoptosis.

For these reasons and with the aim of preventing free iron toxicity, the human body has evolved mechanisms to tightly regulate iron homeostasis.

Figure 1. Scheme of Fenton and Haber-Weiss reaction.

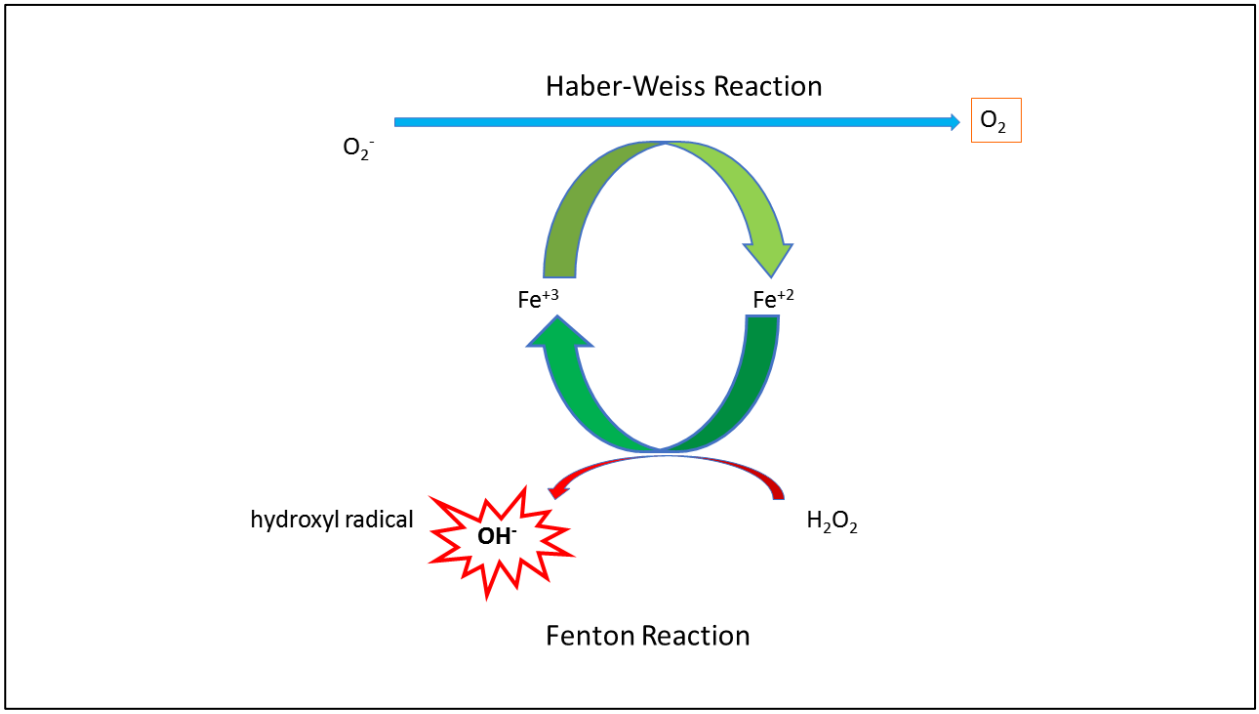

1.2 IRON IN THE HUMAN BODY

In the human body, iron is found mainly in heme compounds, such as hemoproteins (hemoglobin, approximately corresponding to 2 g of iron in men and 1.5 g in women, or myoglobin, both oxygen transport proteins) or heme enzymes (cytochromes and catalases) but also in nonheme enzymes (flavin-iron enzymes) and bound to iron transport and storage proteins (such as transferrin and ferritin).

Such an iron reservoir in the body comes primarily from two sources: senescent red blood cells, through the phagocytic activity of macrophages in a sort of 'recycling mechanism', and dietary iron absorption, which particularly tends to compensate in cases of iron loss or increased need (such as bleeding, pregnancy, hypoxia).

The liver is the main storage site for iron and, as such, the main target of iron toxicity in case of iron overload.

Iron excretion is an unregulated process which occurs through loss in sweat, menstruation, hair and skin cells shedding, and through enterocytes turnover.

Therefore, according to current knowledge, the body's iron exchange with the environment is only actively controlled at the absorption level.

Figure 2. Estimated iron amount in the main organs involved in its metabolism

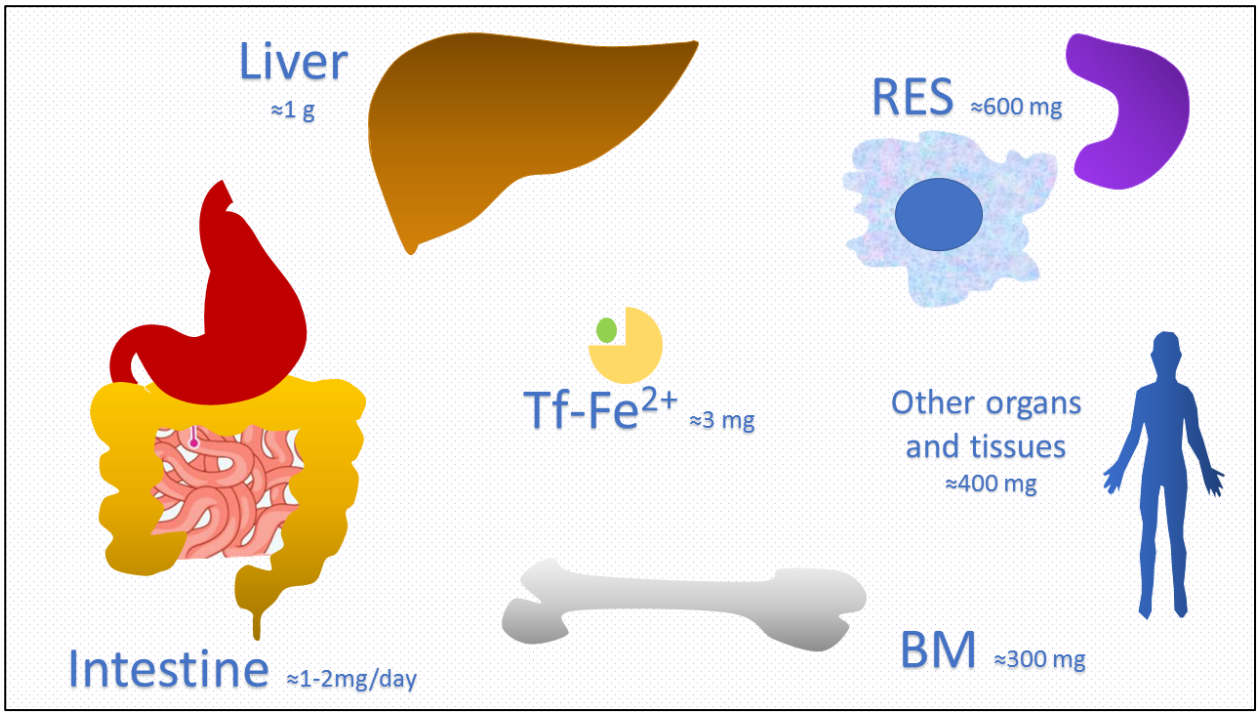

Abbreviations: Tf, transferrin; RES, reticuloendothelial system; BM, bone marrow. Adapted from (11).

1.2.a Dietary iron absorption

Despite its relative abundance in the environment and its relatively low daily dietary requirements (10mg ingested/1 mg absorbed) for humans, iron is often a growth-limiting nutrient in the human diet (12). Absorbable dietary iron can be divided in two types, heme and non-heme iron.

The former is derived from heme-proteins of animal food sources and it has high absorbability (ranging from 15 to 35% of the amount which is introduced in the gastrointestinal tract) and makes up for the 10% of the adsorbed iron (12). Non-heme iron is contained in vegetables and iron-fortified foods and is less well absorbed. Low intake of iron accounts for most anemia cases in developed countries and is responsible for nearly half of the anemias in non-industrialized nations. One reason for the lack of adequate iron absorption is that, upon exposure to oxygen, iron forms highly insoluble oxides which are not available for absorption in the human gastrointestinal tract (12).

The absorption of iron is limited by oxalates, phytates, polyphenols, phosphates and calcium. Therefore, certain food products such as milk and dairy products, eggs, coffee, tea, spinach, dry legume seeds (i.e. rich sources of the above-mentioned components), hinder the utilisation of dietary iron. Hence, the bioavailability of non-heme iron varies according to dietary composition.

The absorption of most dietary iron occurs in duodenum and proximal jejunum and depends heavily on the physical state of the iron atom. At physiological pH, iron is present in the oxidized, ferric (Fe^{3+}) state. To be absorbed, iron must be in the ferrous (Fe^{2+}) state or bound to a protein. The low pH of gastric acid arriving in the proximal duodenum allows duodenal cytochrome B (Dcytb), a ferric reductase enzyme on the brush border of the enterocytes, to convert the insoluble ferric (Fe^{3+}) to absorbable ferrous (Fe^{2+}) ions. As a consequence, gastric acid production

plays an important role in plasma iron homeostasis: when proton-pump inhibitors such as omeprazole are used, iron absorption can be significantly reduced.

Once ferric iron is reduced to ferrous iron in the intestinal lumen, a protein on the apical membrane of enterocytes called divalent metal cation transporter 1 (DMT1) transports iron across the apical membrane and into the cell (13). DMT1 and Dcytb levels are upregulated in the hypoxic environment of the intestinal mucosa by hypoxia-inducible factor-2 (HIF-2α) (14).

As for heme, at acidic pH in the stomach, it is dissociated from hemoproteins (15) and absorbed mainly in the proximal intestine, with the mediation of Heme Carrier Protein 1 (HCP1) and the involvement of specific proteins such as hephaestin. HCP1 mRNA expression is elevated in the duodenum and appears to be regulated by hypoxia and by Iron Responsive Proteins (IRPs) (16).

Inside enterocyte, the heme molecule is catabolized by a microsomal enzyme called heme oxygenase (HO). The by-products derived from HO-catalysed heme degradation include bivalent ferrous ions (Fe^{2+}), carbon oxide (CO), and biliverdin IXa, which is subsequently reduced to bilirubin by biliverdin reductase (17). To date, two different isoforms of heme oxygenase, encoded by two separate genes, have been described in humans, HO-1 and HO-2. HO-1 can be induced by a series of factors such as cellular stress, reactive oxygen species, heme, thermal shock, UV radiation, nitric oxide (NO), pro-inflammatory cytokines, and heavy metals, in order to protect cells from the harmful and oxidizing nature of free heme. Conversely, HO-2 is constitutively expressed and plays a pivotal role in the catabolism of heme in absorptive enterocytes (18).

Ionic iron released in the process of heme degradation is further metabolized on a common pathway with non-heme iron. Depending on the actual demand, iron ions present inside absorbent enterocytes can be either stored as ferritin and eliminated from the organism with

exfoliated enterocytes or transported further through the basolateral membrane of the enterocyte.

It has been shown that control of enterocytic iron transfer involves ferritin, because mice with an intestinal ferritin H gene deletion show increased intestinal iron absorption and iron overload (19).

1.2.b Iron recycling

Dietary iron absorption alone cannot sustain erythropoiesis and the regular need for iron of the human body , therefore recycling of heme iron by HO-1 in the macrophages and its release by ferroportin are of great importance (20) (21).

It is well known that senescent red blood cells are recognized and phagocytised by specialized macrophages found mostly in the bone marrow and spleen (22), with a special role for hepatic macrophages, which contribute significantly to the elimination of erythrocytes and iron recycling when the number of damaged red cells is increased (i.e., in hemolytic anemia) (23). RBCs are degraded in erythrophagolysomes, and following the breakdown of hemoglobin, heme is exported into the cytosol and iron released from protoporphyrin thanks to HO-1. At this point, iron can either be stored in ferritin or exported for re-use by FPN.

1.2.c Iron export in the bloodstream

It is now well established that, once at the basolateral side of the enterocytes, inorganic iron is exported into the bloodstream via a specific exporter, named ferroportin (FPN) (24).

Ferroportin is a multi-pass protein which is expressed in placenta, intestinal cells, reticuloendothelial macrophages and hepatocytes (25); in polarised cells, it is found at the basolateral membrane. Its complete inactivation in mice leads to embryonic lethality, while its selective inactivation causes iron accumulation in enterocytes, macrophages, and hepatocytes, consistent with a key role for ferroportin in those cell types (24). Ferroportin is organised in two

transmembrane lobes separated by a cytoplasmic loop (26), and it binds iron in its ferrous form and exports it outside the cell by an inward/outward-facing conformation change mechanism. Over-expression of FPN is induced by cellular iron, and it is suppressed by hepcidin. Hepcidin binds to FPN on the cell surface, inducing its internalization which is followed by lysosomal degradation (27). Therefore, iron efflux from enterocytes or macrophages is suppressed, leading to reduced iron release. Once exported by FPN, iron needs to be transformed from ferrous into ferric form by ferroxidases such as ceruloplasmin (Cp) or the trans-membrane ferroxidase hephaestin (HEPH, which co-localizes with FPN), in order to be bound to serum transferrin (Tf) (28). The ferroxidases at the cell surface mediate the stability of FPN. In humans with aceruloplasminemia, anemia is associated with impaired cellular iron export, while disruption of the Cp gene in mice leads to an impaired release of iron from the reticuloendothelial cells and hepatocytes (29).

1.2.d Iron plasmatic transport, cellular uptake and storage

Transferrin (Tf) is the specific protein that binds and transports iron once it is exported from duodenal enterocytes into the bloodstream; Tf is also involved in the transport of iron from reticuloendothelial cells and the liver to the other cells of the body, thereby controlling the levels of “labile iron” (30).

Human Tf is a glycoprotein of ∼65,000 kDa, synthesized in hepatocytes and secreted into the plasma, (4) composed of single bi-lobal chains connected by a hinge, forming a cleft that contains the iron-binding domains (each binds one atom of Fe^{+3}). Iron binding and release are coordinated by conformational shifts (31, 32): Tf releases iron at acidic pH because of major conformational changes including a 54- to 63-degree rotation between the two domains on each lobe (33).

Cellular iron uptake happens after iron bound-Tf (Fe-Tf) binds to its receptor on the cellular surface (TfR).

There are two distinct TfRs, TfR1 and TfR2. TfR1 consists of a core, a transmembrane and a cytoplasmic domain. Two molecules of Fe-Tf bind to the TfR homodimer on a conserved arginine-glycine-aspartate sequence located in the TfR helical domain (34). A study using cryoelectronic microscopy showed that Tf binds across the TfR1 dimer and extends into the space between the receptor ectodomain terminus and the cell membrane (35). Once Fe-Tf is bound to TfR1, the complex is endocytosed into the cell, in an acidic endosome. The change in pH in the endosome causes the iron to disassociate from Tf, and it is then exported from the endosome into the cytosol by a divalent metal transporter after reduction by a ferric reductase.

TfR2 has been identified more recently and has been shown to be involved in the import of cellular iron, but has a different expression pattern fromTfR1 (36). TfR2 is expressed primarily in hepatocytes and in iron-absorbing duodenal and intestinal cells (37), has a lower affinity for Fe-Tf than TfR1 (36, 38) and is not redundant for TfR1 (TfR1 knockout is embryonically lethal (39), despite the presence of TfR2). Deficiencies in TfR1 or TfR2 have different phenotypic outcomes: TfR1 deficiency results in low tissue iron levels, while TfR2 inadequacy leads to the development of hemochromatosis (6, 40). TfR1 mRNA contains five iron-regulatory elements (IREs) that convey posttranscriptional regulation of expression by cellular iron concentration (41). IREs are structures located in untranslated regions (UTR) of mRNAs that are regulated by iron levels and are recognized by specific proteins, called iron-regulatory proteins (IRPs). The activity of the two IRPs, IRP1 and IRP2, is controlled by the amount of iron in the cell. Both IRP1 and IRP2 are activated under iron-deficient conditions, leading to their binding of the target IREs (42).

IRE-IRP influences the translation and stability of various target mRNAs, including TfR, ferritin, eLAS, Fpn, and DMT1. If iron concentrations are high, IRPs are degraded or inactivated, causing the downregulation of TfR1. Once iron is depleted, iron is withdrawn from the IRP-1 iron–sulphur cluster (ISC), and its mRNA-binding activity is restored. TfR1 is also regulated at the

transcriptional level. The TfR1 promoter contains a hypoxia-responsive element (HRE) located upstream of the transcription start site and which is bound by hypoxia inducible factor (HIF-1α and HIF-1β) in hypoxic conditions (43).

Unlike TfR1, TfR2 does not contain an IRE in its mRNA and does not appear to be iron-dependently regulated (44, 45). Studies of TfR2 expression in a mouse model for hemochromatosis revealed that TfR2 was not downregulated under iron overload (44), which supported the absence of an iron-mediated posttranscriptional regulatory mechanism. In addition, TfR2 was not upregulated in response to iron deficiency (44). The time- and dose-dependent increase in TfR2 expression in hepatocytes in response to the addition of exogenous Fe-Tf was observed only at the protein level, suggesting that such upregulation may be a result of protein stabilization (46). These results suggest that TfR1 and TfR2 are differentially regulated and may therefore serve diverse roles in terms of iron sensing and regulation.

Ferritin is the main protein for iron storage at the cellular and organism levels. It is responsible for the capture of potentially harmful, reactive iron. Ferritin stores iron in its unreactive Fe^{3+} form inside its shell as a result of a strong equilibrium between ferritin-bound iron (Fe^{3+}) and the labile iron pool in the cells (Fe^{2+}), by which ferritin prevents the formation of ROS mediated by Fenton reaction. Because of its important function in the storage of iron, ferritin is ubiquitous in tissues, serum, and in other multiple locations within the cell. It is regulated at the transcriptional and post-transcriptional level by various pathways in response to diverse stimuli.

In the cells, ferritin is found in the cytoplasm, nucleus, and mitochondria). In vertebrates, cytoplasmic ferritin is expressed in almost all tissues. This ubiquitous protein consists of 24 subunits of heavy (H) and light (L) chains, encoded by two different genes (47), in various ratios and can sequester up to 4,500 iron atoms (48). The H subunit has ferroxidase activity, which converts Fe^{2+} to Fe^{3+} for storage inside the shell (49). The ferritin L subunit, on the other hand,

stabilizes ferritin structure and facilitates the absorption of iron into the shell (50). The ratio of H and L subunits in the ferritin protein is not fixed and is tissue dependent (51): for instance, H chain is abundant in the heart, whereas the L subunit is predominant in the liver and spleen (48). Accumulating evidence shows that ferritin may act as an antioxidant protein. Indeed, overexpression or knockdown of ferritin expression in mammalian cells has proven the cytoprotective role of ferritin under pro-oxidative conditions (52-57). Ferritin H is induced by NF-κB in response to TNF-α treatment, resulting in suppression of ROS and inhibition of apoptosis (57). . Consistently, induction of ferritin mRNA was observed in mouse liver (58) and erythroid cells (54) treated with oxidative stress–inducing compounds. The regulation would happen at the transcriptional level through an antioxidant-responsive element (ARE) (59).

Lysosome-mediated ferritin degradation uses the autophagy system under particular conditions (60, 61) and iron chelator treatment (62)). Amino acid and serum depletion stimulate autophagy, resulting in ferritin degradation, which sensitized cells to H_2O_2-induced oxidative stress due to of an increased "labile iron" pool, with consequent ROS production (61). Iron-mediated ferritin regulation is primarily achieved through post-translational mechanisms (63-65) through the binding of IRP1 and IRP2 to an IRE located in the 5′ UTR of ferritin mRNA (41); however, iron depletion by chelators has also been shown to enhance lysosome-mediated ferritin degradation (62).

Fpn expression appears to enhance ferritin degradation through a proteasome-dependent pathway, as it has been seen that in presence of proteasome inhibitors ferritin degradation is prevented (66). Thus, besides lysosome-mediated ferritin degradation, an unknown but important proteasome-mediated ferritin-degradation mechanism may exist.

.

Serum ferritin is identical to cytoplasmic ferritin, but its primary component is the L subunit, which contains little iron (67). Serum ferritin levels have been thought to reflect the true iron stores in the body and to increase proportionally to intracellular ferritin synthesis (68, 69)., and for this reason it is usually measured in patients undergoing screening for iron-related disorders (70-72). Several lines of evidence suggested that ferritin may bind to the surface of certain cells and may be endocytosed. Elevated serum ferritin H levels were shown to be correlated with increased $CD4^+$, $CD25^+$, $CD69^-$ regulatory T cells (73). In addition, the recombinant ferritin H protein was reported to activate T cells (74). Given that ferritin is a circulating protein that binds to the cell surface, ferritin may have its own receptor (75) (76).

Figure 3. **Summary of iron homeostasis**

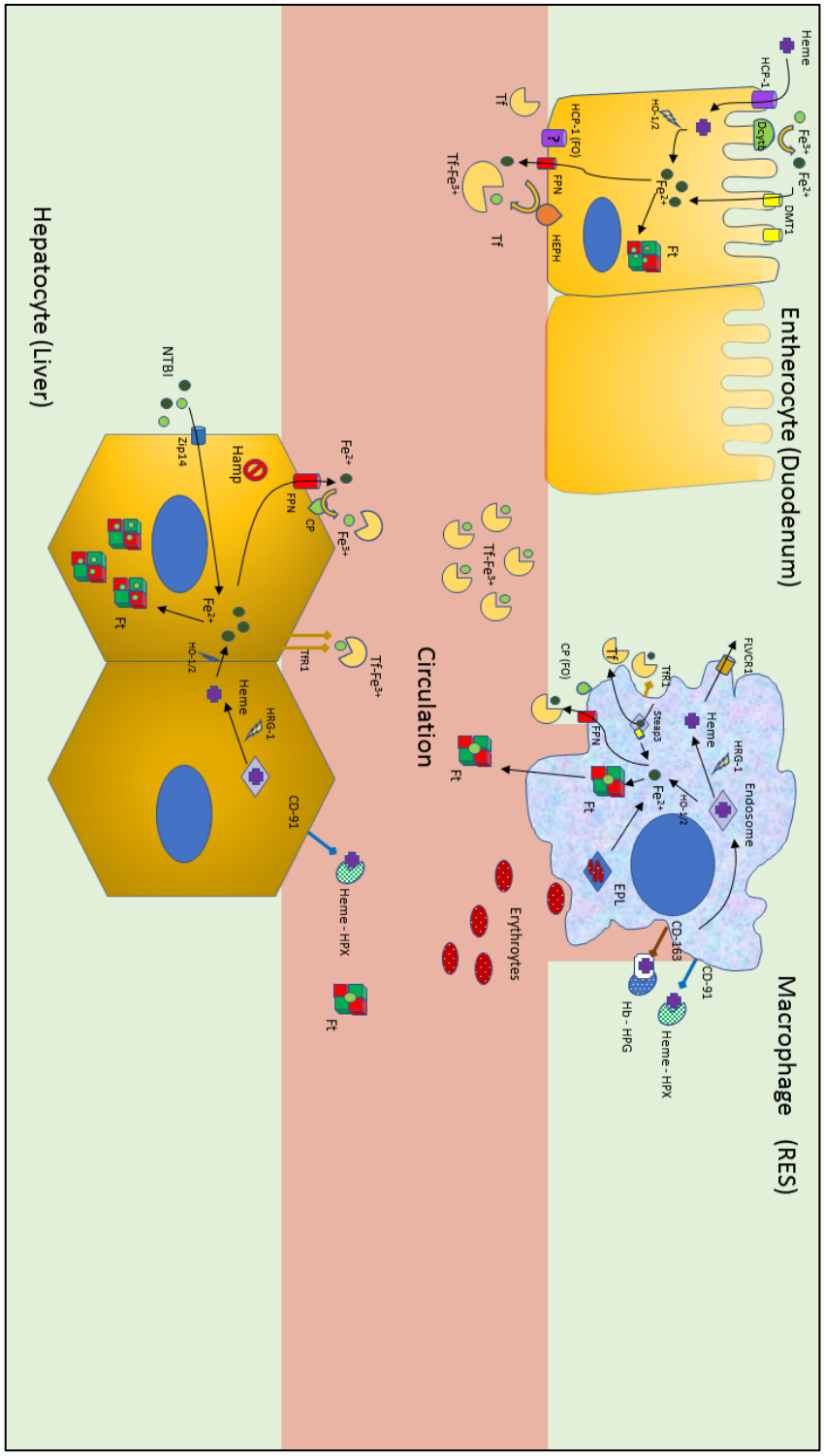

Abbreviations: DMT-1 (Divalent metal transporter 1); HO: heme Oxygenase; Ft, ferritin; FPN, ferroportin; HEPH, hephaestin; FO, ferroxidase activity; Tf, transferrin; EPL, erythrophagolysomes; HRG-1, Heme-responsive gene 1 protein homolog ; CP (FO), ceruloplasmin, ferroxidase activity; HPX, hemopexin; HPG, haptoglobin; NTBI, non-transferrin-bound iron; TfR1, transferrin receptor 1; FLVCR!, Feline leukaemia virus subgroup C receptor-related protein 1.

1.2.e Iron in the cell

Extracellular iron can be taken up by various routes: from transferrin, via its receptor mediated pathway or by the receptor independent pathway; from ferritin; from non-transferrin bound iron (NTBI), by importers such as ZIP14; from other sources (as heme, in one of its many forms) (77).

Inside the cell, iron enters a labile, cytosolic pool. This iron is available for heme synthesis and for iron incorporation into iron-dependent enzymes and ferritin. Enlargement of this pool promotes ferritin synthesis. Iron also enters this transit pool not only from outside the cell, but also as a result of the endogenous heme breakdown and the mobilization of ferritin iron.

Labile pool iron (LPI) represents approximately less than 5% of the total body iron and is composed by a pool of redox-active iron complexes. Such complexes consist of both Fe^{2+} and Fe^{3+} associated with a heterogeneous group of ligands, such as organic anions (phosphates and carboxylates), polypeptides and surface components of membranes (phospholipid head groups), that can change dynamically following biochemical stimuli and potentially participate in redox-cycling but can also be scavenged by permeant chelators (78). Changes in LPI levels are usually transitory and homeostatic in nature, however, in extreme cases of iron overload or deprivation, such changes might exceed the cell homeostatic capacity, with consequential toxicity and cell's integrity impairment.

1.3 IRON HOMEOASTASIS: IMPORTANCE OF THE HEPCIDIN-FERROPORTIN AXIS

1.3.a Regulation of ferroportin

Ferroportin is highly expressed by cells and tissues associated with iron transport, such as duodenal enterocytes, liver Kupffer cells and splenic red pulp macrophages, periportal hepatocytes, and the placental syncytiotrophoblast.

Early work demonstrated the fundamental role of ferroportin using a series of transgenic mice (24): if complete FPN-ko mice died at embryonal stage, a model with selective embryonic deletion (survived to birth but was rapidly affected by anemia, with iron load in erythrocytes, splenic macrophages, Kupffer cells, and in hepatocytes. When ferroportin was inducibly and exclusively deleted in intestinal cells in adult mice, they also rapidly became anemic, supporting that ferroportin is essential for intestinal absorption of iron. In further studies, inactivation of ferroportin in macrophages and in hepatocytes showed that ferroportin is essential for efficient mobilisation of stored iron in these cells: in fact, mice lacking ferroportin in these cells became anemic more rapidly than controls when fed iron-deficient diet (79). However, the same mice on standard diet maintained intact erythropoiesis, indicating that duodenal ferroportin upregulation and increased intestinal absorption can compensate for the decreased activity of ferroportin in recycling and storage compartments.

The regulation of ferroportin regulation is quite complex, and can happen at transcriptional, post-transcriptional, post-translational and cell-lineage levels. These different control phases allow multiple and diverse physiological inputs to influence ferroportin activity at its various sites of expression. Ferroportin regulation varies among different cell types, allowing increased flexibility in controlling systemic iron flow under different conditions.

For instance, in macrophages the total ratio of iron which is released by the cell is subject to systemic control; however, there is also a response to erythrophagocytosis directly regulated by

the cell, in which ferroportin expression is stimulated by heme and iron derived from destroyed erythrocytes (80). Ferroportin contains in its promoter sequence an antioxidant response element (ARE), which can be bound either by Bach1 (leading to gene repression) or Nrf2 (leading to gene activation): heme causes Bach1 degradation, with consequent Nrf2-mediated activated transcription of the FPN gene (with a similar effect on HO-1 and ferritin, in a coordinated cellular response) (81). It has indeed been seen that activators of Nrf2 increase Fpn1 mRNA in macrophages, and can counteract Fpn1 suppression induced by inflammation (82).

Iron itself influences ferroportin expression at the translational level. In fact, ferroportin mRNA contains a 5' iron response element (IRE), which under iron deficiency binds IRP proteins, causing translational repression (83). In macrophages phagocyting erythrocytes, iron liberated from heme inactivates IRPs, resulting in de-repression of Fpn1a mRNA translation. Moreover, the 3' untranslated region of ferroportin is targeted by miR-485-3p microRNA which is induced by cellular iron deficiency (84). As cellular iron levels rise, the downregulation of this miRNA may also contribute to increased ferroportin expression.

In enterocytes, ferroportin is highly regulated by iron and hypoxia, the main objective being the increased absorption of dietary iron during iron deficiency and anemia. As mentioned previously, hypoxia acts by stabilisation of factors (hypoxia inducible factors (HIFs)) that transcriptionally activate genes in order to respond to a low cellular oxygen state. Iron deficiency per se stabilises HIFs since their degradation is triggered by iron-dependent hydroxylation of proline residues and therefore HIFs may also function as sensors of iron scarcity. HIF activation in enterocytes results in the upregulation of both the apical importers and the basolateral exporter, DcytB,DMT1 and ferroportin respectively (85, 86). Ferroportin gene promoter contains HIF response elements (HREs) that are targets for HIF2α binding, which has a demonstrable role in increasing ferroportin transcription during hypoxia and iron deficiency. Interestingly, as HIF2α is also involved in

erythropoietin transcription regulation, it has been hypothesized that it may have a role as a coordinator between iron supply and erythropoiesis during hypoxia.

It is to be noticed that the IRP/IRE system in iron-deficient enterocytes does not impair ferroportin expression through translational repression by the 5'IRE: under conditions of iron deficiency, increased production of ferroportin, combined with its decreased hepcidin-mediated endocytosis and proteolysis, results in higher transfer of iron from the diet into plasma at the expense of iron depletion of enterocytes. In fact, if a different response would protect enterocytes from cellular iron deficiency, it would be detrimental to an iron-deficient organism as iron would be retained in enterocytes, decreasing iron transfer to plasma.

The lack of repression from the IRE/IRP system on ferroportin translation in duodenal enterocytes is only partially justified by the existence of a splicing variant of ferroportin mRNA, called Fpn1b, which does not have the 5' IRE but produces an identical protein (87). Other, possibly hypoxia-dependent, mechanisms may act to limit IRP1-mediated translational repression (88) .

In comparison to hypoxia and iron deficiency, inflammation down-regulate ferroportin expression: this was observed in the liver and spleen following the administration of bacterial LPS (89, 90) , as well in monocytes (91).

The mechanism for a hepcidin-independent reduction in Fpn mRNA decrease caused by inflammation, is not well understood and seems to involve TLR signalling: such downregulation of ferroportin could contribute to the hypoferremia of inflammation that, a protective mechanism against infection with extracellular pathogens. However, the degree and duration of hypoferremia caused by this inflammatory suppression of Fpn1 mRNA are relatively minor in the absence of hepcidin, as evidenced by the small effects on circulating iron after infection with extracellular bacteria in hepcidin knockout mice (92).

A further level of regulation of ferroportin activity occurs from macrophage differentiation and polarization. Macrophages are markedly phenotypically and functionally diverse depending on their source (yolk sac-derived precursors or circulating bone-marrow derived monocytes), tissue location (resident in various organs or recruited from the blood), and exposure to a variety of signals originating from other cells. Iron-recycling macrophages in the spleen's red pulp, which express high levels of ferroportin, depend on the transcription factor SpiC for their development (93). SpiC activity is normally repressed by Bach1; heme causes Bach1 degradation and therefore derepresses SpiC in monocytes, leading to their differentiation into red pulp macrophages which express ferroportin and heme-oxygenase-1 (94). As previously mentioned, the transcription of ferroportin and heme-oxygenase-1 increases after heme-mediated Bach1 degradation and Nrf2 activation. Thus, increased levels of potentially toxic heme drive both the development of the cell type and the specific molecular processes that are proposed to detoxify heme and recycle heme iron.

Macrophages can also be differentiated in multiple other directions, roughly ranging from the M1 pro-inflammatory phenotype induced by LPS or interferon-gamma, to the M2 alternative specializations characterised by anti-inflammatory and tissue remodelling function (95). Ferroportin expression by M1 macrophages is low, and this, coupled with increased ferritin levels, confers an iron sequestration phenotype, whereas macrophages exposed to M-CSF, IL-4 or glucocorticoids develop an iron recycling/exporting phenotype, therefore express hemoglobin processing machinery, and high levels of ferroportin (96-98)

Ferroportin gene transcription and translation can therefore be modulated by all these signals; however the protein activity on cell membranes is predominantly regulated post-translationally by hepcidin (99).

Hepcidin is a cysteine-rich, 25-amino acid, antimicrobial peptide which was first isolated from human blood ultrafiltrate in 2000 (100). It is mainly produced by hepatocytes and its general structure is a hairpin-shaped β-sheet with four disulphide bridges (made up by eight cysteine residues) with a vicinal bridge at the hairpin turn (101). Hepatocellular expression of hepcidin is modulated by three key pathways: iron sensing, hypoxia, erythropoiesis and inflammation (102). In the bloodstream, hepcidin binds to Fpn on the plasma membrane to induce its ubiquitination, internalization, and degradation, which reduces iron efflux from the cells. Although initially described as antimicrobial peptide, it is in fact now clear that the main role of hepcidin is the regulation of systemic iron homeostasis: its expression increases in conditions of liver iron accumulation (103); its genetic inactivation or overexpression in mice cause body iron overload (104) or iron deficiency anemia (105), respectively, while hepcidin mutations in humans are associated with hereditary hemochromatosis (7), a genetic disease that causes body iron accumulation and organ failure. Gene mutations that either disrupt hepcidin expression or change Fpn activity cause hereditary iron disorders, emphasizing the essential role of the hepcidin-Fpn axis in systemic iron homeostasis.

1.3.b Regulation of hepcidin

Hepcidin levels are predominantly determined through transcriptional regulation and, it has been understood that this happens mainly through two regulatory pathways: 1) bone morphogenetic protein (BMP)/Smad and 2) IL-6/signal transducer and activator of transcription (STAT)3 pathways (106). BMPs and IL-6 induce phosphorylation of Smad1/5/8 and STAT3, respectively. Phosphorylated Smad1/5/8 and phosphorylated STAT3 are recruited to two BMP response elements (BMP-RE1 and BMP-RE2) and a STAT-binding site (STAT-BS), respectively, on the hepcidin promoter, leading to the transcriptional stimulation of hepcidin (107). BMP6

regulates hepcidin expression in response to systemic iron level (108), whereas IL-6/STAT signalling controls inflammation-induced hepcidin induction (106).

1.3.b.1 The BMP6 pathway

In 2005 it was unexpectedly found that Smad4 conditional inactivation in hepatocytes, although did not impair liver development, caused systemic iron overload due to inhibition of hepcidin expression (109), suggesting that both Transforming Growth Factor β (TGF-β) and BMP signalling, that share SMAD4 as signalling component, are involved in hepcidin expression.

BMPs are dimeric ligands and more than 20 types are known. They can form both homo and heterodimers, therefore a huge number of combinations is theoretically possible (110) . BMPs bind to activin receptor-like kinases (ALKs), which are serine-threonine kinase receptors. They are classified into type 2 (ACVR2A, ACVR2B and BMPR2), which are constitutively active, and type 1 (ALK1, ALK2, ALK3, ALK6), which need to be activated by BMPR2s through the phosphorylation of their intracellular glycine/serine-rich (GS) domain (110).

Both receptor types, as well as the ligands, act as dimers. Therefore, the formation of a hexameric complex, made up of two BMP-R1s, two BMP-R2s and a dimer of ligands, is needed to activate the signalling.

It is currently known that the regulatory SMADs (R-SMADs) SMAD1, SMAD5 and SMAD8 (also named SMAD9) are mediators of BMP signalling (111). Once phosphorylated by activated BMPRs, pSMAD1/5/8 form complexes with SMAD4 and translocate to the nucleus, with consequent transcription of genes regulated by BMP responsive elements (BRE).

The inhibitory SMADs (SMAD6 and SMAD7) are BMP responsive genes, such that a negative feedback loop on R-SMADs is formed to self-limit the signalling.

Finally, BMPs can also activate non-canonical pathways, such as p38-MAPK, ERK, and PI3K/Akt signalling, but until now such complex crosstalk has not been well explained.

Many BMPs are expressed in the liver but only BMP2 and BMP6 have been so far demonstrated to be involved in hepcidin activation in vivo. Interestingly, although hepcidin is expressed exclusively in hepatocytes, Bmp2 (112) and Bmp6 (113) (114) are expressed almost exclusively in liver sinusoidal endothelial cells (LSECs), supporting a possible paracrine function for these ligands.

The amount of BMP2 and BMP6 produced by LSECs is crucial to determine hepcidin levels according to body iron concentration. Although in iron-sufficient conditions BMP2 is the prevalent ligand that maintains basal hepcidin (since about 12-fold more expressed than Bmp6), in iron overload BMP6 strongly contributes to hepcidin activation due to its iron-dependent upregulation (although also Bmp2 is slightly increased) (115).

Germinal Bmp6 KO mice, that are viable and with minor bone defects, display a hemochromatosis-like phenotype with decreased hepcidin and body iron overload (116) (117). Similarly, conditional inactivation of Bmp6 in LSECs but not in KCs and HCs, recapitulates the low hepcidin-iron overload phenotype of the total Bmp6 KO mice, demonstrating the essential role of these cells in iron-dependent hepcidin regulation and confirming the paracrine effect of BMP6 on hepatocytes for hepcidin activation (108). In addition, some residual Bmp6 expression was actually observed in the total liver of Bmp6 LSEC-KO animals and, in agreement, hepcidin was slightly higher in this model compared to germinal KO mice, suggesting that other cell types, as hepatocyte and stellate cells, may contribute to BMP6 production (108).

In conditions of increased body iron levels, Bmp6 is transcriptionally upregulated exclusively in the liver (118), in particular in LSECs (113) (114), and its expression levels correlate with liver iron content in mice, whereas it remains unchanged in other tissues (119). Although upregulated, BMP6 cannot however compensate for BMP2 absence: inhibiting BMP2 via neutralizing

antibodies worsens the iron overload phenotype of the Bmp6 KO mice, supporting that the two ligands signal through different ways (115).

How LSECs sense changes in body iron concentration and upregulate BMP2 and BMP6 is still unclear. It has been reported that the nuclear factor erythroid 2-related factor 2 (NRF2), essential in gene expression modulation by oxidative stress, plays a role in iron-dependent Bmp6 upregulation (120). In addition, Bmp2 in endothelial cells is transcriptionally activated by reactive oxygen species (121). Future studies are needed to better address these preliminary findings.

SMAD1, 5 and 8 (also named SMAD9) are regulatory SMADs (R-SMADs) phosphorylated in response to BMPs. Although ubiquitously expressed and characterized by similarities in their structure, SMADs may have redundant or non-redundant functions in different cell types and organs. SMAD8 is the only R-SMAD that is transcriptionally activated by BMPs, in analogy with the inhibitory SMADs (I-SMADs) SMAD6 and 7. At difference with SMAD1 and 5, that strongly activate BMP target gene expression, SMAD8 is a weak activator and recent findings suggest that it binds SMAD1 and reduces SMAD1 transcriptional activation strength, thus acting as dominant negative (122). In agreement, Smad8 total KO mice are viable and fertile, and inactivation of one copy of Smad1 or Smad5 in Smad8 KO does not affect the mouse phenotype. On the contrary, total genetic inactivation of Smad1 or Smad5, or double combined single allele inactivation, is embryo lethal, suggesting strong genetic interaction. In hepatocytes, conditional inactivation of Smad1 or Smad5 leads to strong hepcidin downregulation in young (12-day-old) mice, suggesting a non-redundant function for these two R-SMADs, but soon after liver iron increase due to weaning, hepcidin is efficiently increased in the absence of Smad1 or Smad5, suggesting overlapping functions (123). The double conditional inactivation of Smad1 and 5 leads to strong hepcidin downregulation and severe iron overload, whereas inactivation of one copy of Smad1 in Smad5 liver conditional (LC) KO mice mildly impairs hepcidin expression, that results

inappropriately low considering liver iron content (123). Overall, these findings suggest that the redundant or non-overlapping functions of R-SMADs are dependent on the cell type and the physiologic context. SMAD8, whose expression is limited in hepatocytes and in human hepatoma cell lines, seems irrelevant in hepcidin regulation.

The inhibitory SMAD6 and 7 (I-SMADs) are both induced by dietary iron overload (118) (124), but SMAD7 is the only one which has been well studied in the context of hepcidin regulation. SMAD7 is activated by both BMPs (BMP2, BMP6 and BMP7) and TGF-β1 ligands (125), and is also coregulated with hepcidin via SMAD4 in vivo when iron availability is modified and mediates a negative feedback response to both TGF-β and BMP signalling. In vitro, SMAD7 inhibits hepcidin by halting the binding of SMAD4-containing activator complexes to the SMAD-responsive sequences of the hepcidin promoter (125). In vivo, inactivation of Smad7 gene in hepatocytes causes hepcidin upregulation and consequential decreased iron stores and mild iron-deficient anemia. (126). On the contrary, its overexpression in hepatocytes increases body iron stores because of hepcidin inhibition due to impaired TGF-β/BMP-SMAD signalling.

1.3.b.2 The IL6-STAT pathway

Low iron stores as cause of anemia of inflammation is a common finding in patients with conditions of chronic infections/inflammation, characterized by increased hepcidin levels (127). In fact, hepcidin expression is strongly upregulated by lipopolysaccharide (LPS), the most abundant component of the Gram-negative bacteria outer membrane, which stimulates a strong inflammatory response, with the production of several cytokines, such as IL-6, IL-1β and TNF-α (128) (129) (130).

IL-6 is the primary cytokine involved in anemia of inflammation; it interacts with its receptor in hepatocytes to activate the JAK2-STAT3 pathway, which leads to pSTAT3 binding to STAT3

responsive element (STAT3-RE) in hepcidin promoter and therefore to hepcidin expression upregulation (131). Recent studies confirm the important role of IL6 in hepcidin induction by infections from many different microorganisms such as streptococcus pneumonia and influenza A virus, as well as most extracellular pathogen-associated molecular patterns, with IL6 knockout mice demonstrating impaired or absent hepcidin induction to such stimuli (132). IL-22, another interleukin which can induce hepcidin expression both in vitro and in vivo, has only a minor role in hepcidin induction by LPS, as proved by studies in IL-22 knockout mice (133), although a role for IL-22 in other infectious or inflammatory conditions in vivo remains to be determined.

IL-1 can also regulate hepcidin, either by directly inducing IL-6 or by IL6-independent mechanisms (129, 134). In has indeed been confirmed that IL-1β stimulates hepcidin and induces hypoferremia in mice, also by an alternate mechanism which involves the induction of SMAD1/5/8 signalling (135). Such pathway was implicated as a mechanism for hepcidin induction by bacteria from the intestinal microbiota with potential relevance to inflammatory bowel disease, although the in vivo importance is yet to be confirmed.

The inflammatory pathway functionally interacts with the SMAD1/5/8 pathway to regulate hepcidin transcription. On the hepcidin promoter, the proximal BRE is adjacent to the single STAT3 binding element, and cooperativity between SMAD and STAT3 transcription factors at this site was explored by mathematical modelling and experimental validation (136). This study confirmed that the proximal BRE and a certain basal level of BMP signalling activity are required for hepcidin promoter responsiveness to IL6. Moreover, inflammation reduces hepcidin promoter sensitivity to maximally respond to iron/BMP signals, which may contribute to the pathogenesis of anemia of inflammation. Notably, inflammation also induces SMAD1/5/8 signalling independent of BMP-6, likely by inducing hepatic expression of another TGF-β/BMP superfamily ligand, Activin B (137). Activin B has been classically described to utilize distinct type

I receptors and SMAD2/3 signalling, but it can also utilize BMP type I receptors to stimulate SMAD1/5/8 signalling and hepcidin selectively in hepatocytes (138). A role for this pathway in vivo was suggested by the capacity of follistatin-315 (activin inhibitor) to hinder hepcidin induction in mouse models of inflammation. IL-1β may be one of the systems by which inflammation upregulates Activin B expression in the liver (135).

Inflammation is also associated with ER stress, which can upregulate hepcidin transcription via CREB3L3 (also known as CREBH) both in vitro and in animals (139). This transcription factor is also linked to hepcidin regulation by gluconeogenic signals, together with the transcriptional co-activator PPARGC1A (140). Many other nutritional, hormonal, and growth factor stimuli have also been implicated in hepcidin regulation, including hepatocyte growth factor, epidermal growth factor, estrogen, testosterone, progesterone, platelet derived growth factor-BB, and the Ras/RAF and mTOR signalling pathways (141-144).

Therefore, several lines of evidence support the concept that modulation of hepcidin by iron and inflammation are strictly connected.

1.4 IRON IN METABOLIC SYNDROME

Metabolic syndrome (MetS) includes several metabolic abnormalities that typically identify subjects with increased risk of developing diabetes and cardiovascular disease. It is common to find alterations in iron status or serum iron-related parameters in patients with MetS, and it is a clinically important differential diagnosis in cases of hyperferritinemia, once inflammatory conditions or true iron overload syndromes have been excluded (145). In fact, a raised serum ferritin is the hallmark of dysregulated iron homeostasis in MetS, and transferrin saturation is usually slightly increased or ranges in the upper range of normal.

The term ‘dysmetabolic iron overload syndrome’ (DIOS) is used to describe the association of hepatic steatosis with mild to moderate iron deposition in the liver and increased serum ferritin in patients with insulin resistance (IR) (145, 146). Since body iron in obesity or IR is rarely increased, despite a disproportionate elevation of ferritin (147), it seems reasonable that hyperferritinemia in NAFLD patients could mirror both true iron excess as well as obesity-associated low-grade inflammation; thus, elevated ferritin may be found in the metabolic syndrome without evidence of iron excess (146).

The association of higher iron stores with diabetes, IR and NAFLD has been repeatedly confirmed in many investigations (148). Ferritin levels were found to predict a higher rate of diabetes and gestational diabetes in prospective investigations and case–control cohorts (149) (150). Serum ferritin was positively associated with BMI, visceral fat mass (151), serum glucose levels and insulin sensitivity (152), blood pressure, the MetS (153) and also related to cholesterol levels (154). Iron stores clustered with metabolic risk markers in a population of both obese (155) and apparently healthy, lean teenagers (156). These findings are clinically relevant due to the higher risk of developing cardiovascular or cerebrovascular disease in these patients with IR (157). Similarly, iron stores are also increased in the polycystic ovary syndrome (PCOS) (158). In such patients, increased iron stores were linked to IR and not explained by menstrual irregularities (159). In summary, these data reflect a relationship between elevated body iron stores and several clinical manifestations of IR or the MetS.

On the other hand, severe forms of obesity are frequently accompanied by iron deficiency and even anaemia. The association between adult obesity and low iron stores has been evaluated in a recent meta-analysis of all controlled studies (160). Although iron deficiency appears as a typical finding in severe obesity which has been documented in several investigations, the review concluded that most studies demonstrated higher haemoglobin and ferritin concentrations, and

transferrin saturation decreased as BMI increases, likely for the influence of obesity-related inflammation. Elevated serum hepcidin concentrations, which indicate the absence of true iron deficiency, have been reported in severe obesity. Expression of hepcidin was found in adipose tissue of morbidly obese patients (161). Markedly decreased duodenal iron absorption has been observed in obese subjects compared to healthy lean controls. These are hallmarks of iron homeostasis also reported in patients with DIOS, suggesting that DIOS and obesity-related iron deficiency may be the two sides of the same coin.

Studies investigating the expression of hepcidin in patients with DIOS found increased urinary, serum and liver hepcidin concentrations in such patients compared to controls, hemochromatosis patients and insulin-resistant subjects without excess iron (162, 163). Increased hepcidin correlates directly with liver iron concentration, indicating an intact physiological response to full iron stores (162, 163). Additionally, highly significant association was observed in vivo in patients with DIOS between hepcidin concentrations and TNF-alpha, suggesting that, besides the presence of iron, the low-grade inflammatory status also contributes to hepcidin production (163).

1.4.b Iron in NAFLD

Nonalcoholic fatty liver disease (NAFLD) is an increasingly prevalent disease affecting approximately 30% of unselected population in western countries (164). It is usually one of the key features of metabolic syndrome (MetS), but can also be found , although in a smaller percentage, in subjects with normal weight (7%) (165). NAFLD encompasses a wide spectrum of histological conditions, from simple steatosis with or without mild lobular inflammation (nonalcoholic fatty liver, NAFL) to steatohepatitis or NASH (characterized by ballooning and lobular inflammation) with subsequent development of fibrosis that could lead to cirrhosis. Despite its high prevalence, only a small proportion of subjects with NAFLD develop NASH and

face a higher risk of liver disease progression (166). On the other hand, there is increasing evidence of hepatocellular carcinoma (HCC) growth in patients with NAFLD without cirrhosis (167, 168).

A high serum ferritin (SF) is a common finding in NAFLD; in fact it is often the biochemical abnormality that leads to medical attention, involving up to 30% of affected subjects, but it is still unclear whether it simply reflects hepatic inflammation or represents true hepatic iron-overload (169, 170).

In this context, serum ferritin has been proposed as a marker of both NASH and liver fibrosis (171-173) and, although several studies have questioned its use as a biomarker on its own, serum ferritin is incorporated in serum marker panels for liver fibrosis assessment (174). More recently, serum ferritin has been proposed as an independent predictor of long-term mortality in NAFLD (175).

The contribution of increased iron stores for NAFLD disease severity and progression has been intensely investigated. Several investigations found an association of iron with more progressed stages or higher incidence of NAFLD (176-179); however, this association was not confirmed in subsequent studies (180, 181). Data about the role of excess iron in NAFLD disease progression are mainly undermined by the lack of prospective investigations with serial liver biopsies in cohorts of patients large enough to correct for known co-factors for disease progression (180),(182). An Italian group investigated the therapeutic role of iron depletion in patients with NAFLD, not evidencing improvement in terms of histological parameters but obtaining better insulin sensitivity (183).

Excess liver iron may also be involved in the progression of NASH-associated fibrosis to hepatocellular carcinoma (184).

From the pathophysiological point of view, the interaction between genetic, nutritional and environmental factors is of extreme importance. In a recent study three independent variants of genes involved in iron metabolism (rs1800562 [C282Y] and rs1799945 [H63D] in HFE and rs855791 [V736A] in TMPRSS6) were found to be associated with liver iron content, as well as the presence of central obesity (185).

Particularly, the interplay between hepcidin and fatty acids and other iron-metabolism effectors' regulation and action seems to be involved in a sort of 'hepcidin- resistance' (186).

In another study it was observed that, despite decreased uptake of dietary iron, rats fed with a high fat diet (HFD) accumulated more hepatic iron than those fed regular diet, which was associated with steatosis development and paralleled by induction of ferritin and upregulation of hepcidin. HFD was associated with increased expression of the major iron uptake protein Transferrin receptor-1 (TfR-1), consistently with upregulation of the intracellular iron sensor Iron regulated protein-1 (IRP1). In vitro, supplementation with fatty acids induced TfR-1 and IRP1 in HepG2 hepatocytes, inducing intracellular iron accumulation following exposure to iron salts. IRP1 silencing completely abrogated TfR-1 induction and the facilitation of intracellular iron accumulation induced by fatty acids. In humans, hepatic TfR-1 mRNA levels were upregulated in patients with fatty liver and DIOS, whereas they were not associated with liver fat nor with inflammation. In conclusion, it would seem that increased exposure to fatty acids could alter hepatic iron metabolism, favouring the induction of an iron uptake program despite hepatocellular iron accumulation (187).

In NAFLD subjects increased hepcidin and pro-inflammatory cytokines may be derived also from the expanding adipose tissue, over the liver (188). In response to glucose ingestion, serum iron concentrations have been proved to gradually decline along with an increase in serum hepcidin. Preliminary data show that the decline in serum iron is augmented in NAFLD patients, suggesting

that hepcidin secreted in response to nutrient ingestion may contribute to iron perturbations observed in NAFLD.

Hepcidin exerts its influence on iron metabolism via downregulation of FPN-mediated iron export. In duodenal biopsies from NAFLD patients without liver iron deposition, FPN expression was similar to healthy control subjects, whereas it was decreased in NAFLD patients with iron accumulation (163). In support of these molecular findings, dietary iron uptake was decreased in patients with the DIOS (189).

Aggregates of erythrocytes were documented in microscopic areas of increased inflammation in human NAFLD (190). Hence, heme iron uptake via hepatic erythrophagocytosis may also be involved in the deposition of iron in NAFLD, subsequently enhancing inflammation and oxidative stress.

Copper is another important modulator of iron homeostasis, and copper status is linked to iron perturbations in NAFLD. Copper is of extreme importance for hephaestin ferroxidase activity in the duodenal enterocytes where it facilitates the loading of iron to apo-Tf. In a similar manner, copper is required for ceruloplasmin ferroxidase activity to mobilize iron from storage sites like the liver or the RES, adequate copper supply induces FPN expression and membrane-bound ceruloplasmin expression is required for FPN expression and cell surface stability (191). Low liver and serum copper concentrations were found in NAFLD patients with iron accumulation (192). Low copper concentrations were linked to low serum activity of the ferroxidase ceruloplasmin. In addition, lower hepatic expression of FPN was detected in rats on a copper deficient diet. These observations demonstrate that besides low FPN expression, inadequate copper bioavailability can further impair iron export from liver cells in patients with NAFLD and likely also MetS.

1.4.c Iron and glucose metabolism

It has long been known that in hemochromatosis, iron overload may cause diabetes. In fact, hepatic and peripheral IR increase (with decreasing pancreatic insulin secretion) as body iron rises. On the other hand liver and muscle insulin sensitivity, as well as pancreatic insulin secretion, are re-established if iron is removed (193). As previously seen, iron is a potent catalyst for the formation of ROS, therefore it is assumed that augmentation of oxidative stress is the key mechanism underlying iron-induced IR. Oxidative stress is increased in T2DM and obesity and induces IR in adipose cells (194). In vitro analyses demonstrated that intracellular iron chelation enhances while iron excess decreases insulin receptor signalling. Intracellular iron depletion with deferoxamine leads to an increase in phosphorylation of Akt/protein kinase B (Akt/PKB), fork head transcription factor O1 (FoxO1) and glycogen synthase kinase 3b (GSK3b), which are mediators of the insulin effects on gluconeogenesis and glycogen synthesis. Likewise, genes involved in glucose utilization such as GLUT1 and hypoxia-inducible factor 1a (HIF1a) were up-regulated in hepatoma cells along with improved glucose clearance (195). Thus, iron overload may worsen IR by interfering with insulin receptor signalling and inhibiting the ability to burn carbohydrates in the liver and muscle. In isolated adipocytes, iron treatment induced an insulin resistant phenotype, characterized by increased lipolysis and impaired glucose uptake in response to insulin (196).

Associative links have been observed between iron metabolism and adipokines, a group of peptide hormones mediating the metabolic effects of adipose tissue to other tissues. Ferritin is inversely related to adiponectin serum concentrations in insulin-resistant and insulin-sensitive subjects (197). A positive association was found between iron stores and circulating retinol-

binding protein 4 (RBP4), which both decreased in response to iron depletion (198). A similar relationship was observed between serum visfatin and parameters of iron metabolism (199). These findings may reflect the correlation between increased iron stores and other surrogate IR markers and do not provide evidence of a causative link between these adipokines and regulation of iron homeostasis. Nevertheless, an interesting concept has been suggested that excess dietary iron may be re-routed to visceral adipose tissue and alter its adipokine secretion, as recorded for resistin (200). This may represent a mechanistic link between the observed associations of elevated ferritin concentrations with adipokines. Furthermore, the adipokine leptin, which is increased in the IR state, was found to up-regulate hepcidin transcription in hepatocyte cultures via JAK2/STAT3-dependent signalling pathways. Thus, leptin-induced hepcidin synthesis may contribute to iron perturbations in NAFLD (201).

2. SPECIFIC BACKGROUND AND AIM OF THE PROJECT

STUDY 1

IRON IN NONALCOHOLIC FATTY LIVER DISEASE (NAFLD), THE HEPATIC MANIFESTATION OF METABOLIC SYNDROME

CLINICAL STUDY - A high serum ferritin (SF) is a common finding in NAFLD, and hepatic iron accumulation of different degree can occur , particularly with three different patterns of main deposition (hepatocellular, in RES cells, in both); however, the link with progressive hepatic damage, is not clear.

We therefore planned to assess SF levels and its correlation with the presence and pattern of hepatic iron accumulation and disease severity in a cohort of patients with biopsy-proven NAFLD in a retrospective study.

Furthermore, we schemed to measure serum hepcidin in a subgroup of contemporary patients and determine its relationship with other serum iron parameters, presence of hepatic iron and stages of hepatic damage progression in NAFLD, from NASH to fibrosis.

EXPERIMENTAL STUDY - Since typical feature of NAFLD is the accumulation of fat in the liver (steatosis), we wondered if hepatic steatosis per se, could alter iron homeostasis in such patients, influencing hepcidin expression. Therefore, in a pilot study, we tried to create a simplified cellular model of NAFLD by administrating free fatty acids to hepatocyte cell lines and determine hepcidin expression in such cells.

STUDY 2

BASIC RESPONSE TO STARVATION AND ACTIVATED GLUCONEOGENESIS IN AN ANIMAL MODEL OF HEREDITARY HEMOCHROMATOSIS

Hepcidin has been found to be increased, correlating with hepatic iron stores, in conditions of insulin resistance such as NAFLD and MetS. Furthermore, our group has previously shown that, in condition of induced insulin resistance such as starvation (where gluconeogenesis is activated), hepcidin is up-regulated by glucogenic signals with consequent increased iron accumulation in the liver.

Patients with hereditary hemochromatosis (HH) have insufficient hepcidin activity and/or levels, and may present diabetes and metabolic alterations attributed to iron excess; on the other hand, *Hfe*-KO mice (with reduced/altered hepcidin function) exhibit enhanced glucose tolerance, likely derived from increased glucose disposal that does not result from increased insulin action.

Therefore, we wondered whether, in condition of starvation, which represents both a model of insulin resistance and a condition of reduced iron adsorption, hepcidin deficiency per se independently on iron might represent a factor influencing survival and metabolic adaptation/changes, using a murine model of HH based on *Hamp* gene ablation.

.

3. MATERIAL AND METHODS

3.1 STUDY 1

3.1.1 Clinical study

Patients population

We retrospectively evaluated all consecutive outpatients (aged ≥ 18 years) with a liver biopsy showing NAFLD, irrespective of fibrosis severity, seen at two large hepatology clinics in a time frame of 20 and 12 years respectively, and finally included 468 out of 477 patients. Histological and clinical criteria for NAFLD definition and inclusion in this study were: presence of steatosis in more than 5% of hepatocytes in the absence of features characteristic of other etiologies of liver disease(14); alcohol intake lower than 20/30 g/day in females/males; absence of chronic liver disease of other etiologies such as viral hepatitis, autoimmune hepatitis, primary biliary cholangitis, hereditary hemochromatosis (evidence of iron overload and relevant genetic testing showing C282Y homozygosity, C282Y/H63D compound heterozygosity, H63D homozygosity), Wilson's disease, alpha-1-antitrypsin deficiency based on appropriate testing. We excluded causes of secondary hepatic steatosis, such as use of fatty liver-inducing drugs or previous gastro-intestinal by-pass surgery. Clinical information including presence of hypertension (blood pressure ≥ 140/90 mm Hg measured in 2 different occasions and/or antihypertensive drug treatment), type 2 diabetes mellitus (DM) or impaired fasting glucose (IFG), dyslipidemia (elevated triglycerides [TG], low-density lipoprotein cholesterol [LDL-C], decreased high-density lipoprotein cholesterol [HDL-C] (15) or use of a lipid-lowering agent) and body mass index (BMI) were collected from clinical documentation recorded within 6 months from liver biopsy.

Metabolic syndrome was diagnosed according to the National Cholesterol Education Program Adult Treatment Panel III criteria (16), when at least 3 of the followings were present: enlarged waist circumference (≥102-88 cm, males-females), TG ≥ 1.7 mmol/L and/or medication use for elevated TG, reduced HDL cholesterol (<1.0-1.3 mmol/L, males-females) and/or medication use

for reduced HDL cholesterol, blood pressure ≥130/85 mm Hg and/or medication use for hypertension, fasting glucose ≥5.6 mmol/L and/or medication use for elevated glucose. Biochemical parameters included platelet count (PLT), aminotransferases (ALT, AST), bilirubin, serum albumin, gamma-glutamiltranspeptidase (GGT), fasting glucose, HOMA (homeostatic model assessment) index and glycosylated hemoglobin (HbA1c) when available.

Iron status

Serum iron, serum ferritin SF and total iron binding capacity (TIBC) and/or transferrin saturation (TSAT) were determined using automated biochemical methods. HFE genetic test had been performed in patients with hyperferritinemia (above 200 µg/L in females and 300 µg/L in males or menopause females) and an abnormal transferrin saturation (TSAT > 45%) and in selected patients with hyperferritinemia and normal TSAT according to the physicians' discretion, by PCR-based techniques.

Serum hepcidin measurement

Serum hepcidin determination was performed in a subgroup of patients who had undergone liver biopsy within 3 months around the time of patients' selection. All serum samples were obtained by centrifugation within two hours from blood sample collection and stored at -80°C. Hepcidin determination was performed by a high sensitive enzyme immunoassay kit (DRG Hepcidin 25 (bioactive) HS ELISA, DRG International, Inc, USA) and the results confronted to the values range provided by the manufacturer.

Histological assessment

All liver biopsy specimens were obtained by percutaneous or trans-jugular route, with a median length of 19 mm (6-58 mm). Specific criteria for liver biopsy were length of at least 10 mm, comprising at least six portal tracts or less if cirrhotic or considered of enough quality for a diagnosis and staging by the pathologist. We included 6 biopsies <10 mm (6, 7, 8, 9, 9 and 9 mm

respectively) presenting simple steatosis since the histopathologist was satisfied with the representativity of the sample and the results of the analysis were not changed by their removal. Liver sections were routinely stained with hematoxylin/eosin, silver reticulin, blue aniline or Sirius red for collagen, Perls' Prussian blue for iron. Liver biopsies were centrally reviewed by a single pathologist in each centre. NAFLD lesions were scored according to the NASH Clinical Research Network (CRN) NAS scoring system (17). NASH was diagnosed in the presence of the combination of any degree of hepatic steatosis, hepatocellular ballooning and lobular inflammation.18,19 Hepatic fibrosis was staged on a 5-point scale (0 = absence of fibrosis, 1 = zone 3 perisinusoidal/ perivenular fibrosis, 2 = zone 3 and periportal fibrosis, 3 = septal/ bridging fibrosis, 4 = cirrhosis17). Significant and advanced fibrosis was defined as stages ≥F2 and ≥F3, respectively. Advanced fibrosis

was chosen as one of the main variables of interest based on previous studies demonstrating that it is associated with long-term clinical outcomes and increased mortality in NAFLD patient (20,21).

Inter-observer agreement regarding histological evaluation by the 2 pathologists was tested on a set of 30 slides by weighted Cohen's kappa, with a resulting k value for fibrosis of 0.76, meaning excellent agreement. The presence of iron was assessed both in hepatocytes and reticuloendothelial cells and the degree of liver siderosis was classified according to a modified Scheuer's system.

Ethical approval

Blood tests and liver biopsies were performed as part of the standard or routine care. Both centres had the approval from the local ethical committee to use registered parameters and liver

biopsies for studies. The study was carried out in accordance with the principles of the Helsinki Declaration.

3.1.2 In vitro study

HepG2 cells were cultured in MEM (with Earle's salts) supplemented with 10 % fetal bovine serum, 100 U/ml penicillin and 10 µg/ml streptomycin and L-glutamine 2mM.

For sub culturing purposes, cells were detached by treatment with 0.25% trypsin/0.02% EDTA in PBS at 37 ◦C. Cells were used at 70% confluency.

Fat-overloading induction in HepG2 cells and hepatocytes

To induce fat-overloading of cells, HepG2 cells at 70% confluency were exposed to a long-chain mixture of FFAs (oleate and palmitate) and to oleate and palmitate alone at different ratios. Stock solutions of 100 mM oleate acid and 100 mM palmitate were prepared in culture medium containing 1% bovine serum albumin (BSA) were conveniently diluted in culture medium to obtain the desired final concentrations. The FFA mixture was added to HepG2 cells 24 hours after seeding.

Fluorimetric determination of fat content in intact cells by Nile Red staining

The lipid content in cultured cells was determined fluorimetrically and at fluorescence microscopy using Nile Red, a vital lipophilic dye used to label fat accumulation in the cytosol. Cell monolayers were washed twice with PBS and incubated for 15 min with Nile Red solution at a final concentration of 1 mg/ml in PBS at 37 ◦C. Monolayers were washed thereafter with PBS and read in a micro fluorimeter (excitation 488 nm and emission 550 nm).

Cytotoxicity assay

Cells were seeded in 96-well microtiter plates. After treatment with FFA mixtures, the cytotoxicity was assessed by MTT (3-(4,5-dimethylthiazol-2-yl)-2,5-diphenyl tetrazolium bromide).

Cellular RNA extraction, retrotranscription and RT qPCR

RNA was extracted by using the iScript™ RT-qPCR sample preparation reagent (Bio-Rad Laboratories, Inc). Complementary DNA was generated by reverse transcription of 1 µg RNA with iScript™ cDNA Syntesis Kit (Bio-Rad) following the manufacturer's instructions. Amplification was generated using SSO Advanced Universal SYBR Green Supermix (Bio-Rad) in CFX96 qPCR Detection System Bio-Rad). Gene expression was calculated by the software using the $2^{-\Delta\Delta Ct}$ method and normalized on *RPLP0 h*ousekeeping mRNA expression after validation using the target stability value obtained from the CFX Manager software (version 2.0; Bio-Rad).

3.2 STUDY 2

Animal study

All animal procedures were performed in a licensed establishment and in accordance with the D.Lvo 26/2014 of the Italian Ministry of Health, and were approved by the University of Modena and Reggio Emilia ethical review committee and by the Italian Ministry for Research (Authorization n° 256/2016-PR)

Animals

Mice were bred and housed in individually ventilated cages within the inter-departmental animal research facility, biology section, of the University of Modena and Reggio Emilia.

***Hamp*-KO and CTRL**

Hamp-KO mice were obtained by Prof. S. Vaulont. In these mice the first 2 exons and part of exon 3 were deleted by gene targeting as described by Lesbordes-Brion et al. (202). A breeding colony of homozygous knock-out mice is maintained within the animal facility of the University of Modena and Reggio Emilia.

i-*Hamp*-KO and i-CTRL

Tamoxifene-inducibile model of Hamp knock-out mice were obtained by concession from the Oxford University (of courtesy from Armitage, Drakesmith group). To create such iHamp1-KO model, floxed-hepcidin mice on a C57BL/6 background (Hamp fl/fl) generated by gene targeting in JM8F6 embryonic stem cells were used (Hamp tm1Wthg); in these mice, exons 2 and 3 of the Hamp1 gene are flanked by LoxP sites. These were crossed with B6.129-Gt(ROSA)2 6Sortm1(cre/ERT2)Tyj / J mice (referred to henceforth as Rosa-CreERT 2), which express Cre fused to a modified estrogen receptor (allowing nuclear translocation, and thus activation, in the presence of tamoxifen) under the control of the ubiquitous Gt(ROSA)26Sor promoter [14] .

A breeding colony of mice homozygous for the floxed- Hamp allele and either heterozygous or wild-type for Rosa-CreER T2 was generated in our facility and crossed to yield 50% Cre-positive

Hamp fl/fl (termed 'i-Hamp-KO' mice) and 50% Cre-negative Hamp fl/fl littermate control (termed 'i Hamp-Ctrl' or 'i-CTRL') offspring.

Induction of targeted disruption of *Hamp*1 in i-*Hamp*-KO

To stimulate targeted disruption of the Hamp1 gene, mice were given 1 mg of tamoxifen (Sigma, T5648) in 100 µl of 10% ethanol (Sigma)/90% corn oil (Sigma) vehicle intraperitoneally, once daily for two consecutive days at the beginning of the light cycle.

Genotyping

Genotyping was performed initially using DNA extracted from ear notches, with subsequent confirmation using DNA extracted from the liver; DNA was extracted using Easy-DNA purification kit (Thermo Fisher) or by alkaline lysis (50 mM NaOH) at 95 ° C followed by neutralization (100 mM Tris-HCl pH 8; ear notches only). Genotyping PCRs were performed using Taq DNA Polymerase (Sigma, Milan, Italy) to detect: (a) floxed or wild-type Hamp1 alleles, (b) deleted Hamp1, and (c) Cre. The primers and cycling conditions are described in the online supplementary materials.

Starvation experiments

Starvation experiments were carried as follows: 8 to 10-week-old male Hamp-KO and i-Hamp-KO mice and relative controls (CTRL and i-CTRL) were allowed free access to water and fed a standard, iron-balanced chow diet in pellets (VRF1(P), Charles River, Lecco, Italy); iron content, 280 mg/kg) or starved up to 6, 12, 24, 48 or 72 hours starting at the beginning of the light cycle and then sacrificed.

Ethical considerations

All animals received humane care according to the criteria outlined by the Federation of European Laboratory Animal Science Associations (FELASA). The study was approved by the

Ethics Committee for Animal Studies at the University of Modena and Reggio Emilia and by the Italian Ministry for Research (Authorization num. 256/2016-PR)

Blood Measurements

Biochemical parameters such as hemoglobin, circulating iron parameters (serum iron, serum ferritin), nutritional and metabolic parameters (serum glucose, triglycerides, cholesterol) were determined using an automated COBAS C501 counter (Roche, Milan, Italy) at the clinical-chemical laboratory of the University Hospital Policlinico of Modena.

Serum ketone bodies were quantified using a β-Hydroxybutyrate Assay Kit (Sigma-Aldrich, Milan, Italy) following the manufacturer's instructions.

Tissue Iron Content measurement

Non-heme iron content quantification in liver and spleen tissue specimens was performed according to the method of Torrance and Bothwell. Briefly, tissues were dehydrated at 100°C for several days and digested in 1 mL of acid solution containing 3M HCl and 0,61 M TCA for 20 hours at 65°C. After cooling at room temperature, 10 uL of sample was added to 200 uL of Chromogen Solution (169 µM Bathophenantroline Sulphonate, 13 mM Thioglycollic Acid in Saturated Sodium Acetate Solution) in a 96 multiwells plate. After 10 minutes incubation samples were read at 535 nm in a multiplate reader (Sinergy HTX, Biotek). Results were calculated against a standard curve obtained with stabilized Iron Standard (Sigma).

Tissue iron staining

Liver specimen were fixed over-night in 10% Formalin and, after dehydration, paraffin embedded. For histological analysis 5-6 µm sections have been cut, hydrated in alcohol-scale and processed for Hematoxylin-Eosin or Perls' Staining.

Hematoxylin-Eosin staining involved incubation of sections for 10 minutes in Carazzi's Hematoxylin (PanReach), followed by 5 minutes incubation in 1% Eosin solution (PanReach), After wash step in water sections were dehydrated in alcohol-scale and mounted in DPX Mounting Medium (Sigma)

For Perls' Staining sections were incubated in 1:1 solution of 2% Potassium Ferrocyanide and 2% HCl for 20 minutes and, after washing in water, counterstained with Nuclear Fast Red (PanReach) for 10 minutes.

Real-Time Quantitative Reverse-Transcription Polymerase Chain Reaction (RT-qPCR)

Total hepatic RNA was extracted by TRI Reagent (Sigma) using manufactured instruction. 50-100 mg of tissue sample was homogenized in 1 ml of TRI Reagent solution and samples with high content of fat, like liver, were centrifuged at 12.000 x g for 10 minutes at +4°C in order to remove insoluble material. The clear supernatant was removed in a fresh tube following an incubation of 5 minutes to ensure complete dissociation of nucleoprotein. After addition of 0,2 ml of chloroform, samples were mixed, allowed to stand 5 minutes at RT and then centrifuged at 12.000 x g for 15 minutes. The aqueous phase was transferred to a fresh tube, added 0,5 ml of 2-propanol and allowed to stand for 5 minutes before centrifugation at 12.000 x g for 10 minutes at +4°C. The pellet of RNA formed on the bottom of the tube was washed with 75% ethanol followed by centrifugation at 7500 x g for 5 minutes at +4°C. After discharged of supernatant, the pellet was dried by air and resuspended in DEPC-treated water followed by 10 minutes denaturation at 65°C.

Complementary DNA was generated by reverse transcription of 1 µg RNA with iScript™ cDNA Syntesis Kit (Bio-Rad) following the manufacturer's instructions. Amplification was generated using SSO Advanced Universal SYBR Green Supermix (Bio-Rad) in CFX96 qPCR Detection System Bio-Rad) with the following condition: 30 seconds at 95°C, followed by 40 cycles of 2 seconds at 98°C and 10 seconds at 60°C. After 40 amplification cycles, threshold cycle values were calculated automatically using the default settings of the CFX Manager software (version 2.0; Bio-Rad). At the end of the PCR run, melting curves of the amplified products were obtained and used to determine the specificity of the amplification reaction. Gene expression was calculated by the software using the $2^{-\Delta\Delta Ct}$ method and normalized on *RPLP0* housekeeping mRNA expression after validation using the target stability value obtained from the CFX Manager software (version 2.0; Bio-Rad). Primer sequences are listed in Table a.

Western Blot Analyses

In order to quantify proteins of interest, proteins were extracted by homogenizing mouse liver specimens in lysis buffer (150 mmol/L NaCl, 10 mmol/L Tris, pH 8, 1 mmol/L EDTA, 0.5% Triton X-100), adding 1:100 protease inhibitor cocktail 1 (Sigma-Aldrich) just before use.

After centrifugation at 13,000 × g at 4°C for 15 minutes, the supernatant was collected and the protein concentration was assayed in each sample by the Lawry method using a microplate reader (Sinergy HTX, Biotek). A total of 20 µg of liver extracts were loaded after or without boiling (according to the type of protein) on Mini-PROTEAN TGX Gel (Bio-Rad) with Laemmli loading buffer, and run in sodium dodecyl sulfate–polyacrylamide gel electrophoresis buffer at 150-200 V.

Transfer of proteins was performed using Tras-Blot Turbo System (Bio-Rad) using nitrocellulose membrane Transfer Pack (Bio-Rad)

Membranes were probed with specific antibodies: rabbit anti-FPN1 (1:3000; Alpha Diagnostic, Inc, San Antonio, TX), for a minimum of 12 hours, rabbit anti-Ft (1: 3000; Abcam), mouse anti-Tfr1 (1: 3000; Thermofisher), followed by appropriate horseradish-peroxidase–conjugated secondary antibodies.

Membranes were then probed with the following antibodies for housekeeping proteins: mouse anti-tubulin (1:2000; Sigma-Aldrich), mouse anti-Hsp90 (1:2000, Origene) Mouse anti-B actin (1:3000, Sigma-Aldrich).

Western blot analysis was performed by Western Lightning Ultra substrate (PerkinElmer, Waltham, MA) or Clarity and Clarity Max ECL Western Blotting Substrates (Bio-Rad) according to the manufacturer's instructions. Chemiluminescence was detected and quantified using the Molecular Imager ChemiDoc XRS+ with Image Lab Software (Bio-Rad).

Immunofluorescence analysis

Frozen liver specimens were cut and fixed in 4% paraformaldehyde for 20 minutes, incubate with 4% goat serum in PBS and then processed for multicolor immunostaining by sequential incubation with the following antibody: Rabbit anti-Ferroportin (Alpha Diagnostic) diluted 1: 100 in BPS+ 1% BSA and secondary antibody Goat anti-Rabbit Alexa Fluor 488 (Invitrogen) diluted 1:300 in PBS; Rat anti-F4/80 (Serotec) diluted 1:100 in PBS +1% BSA and secondary antibody Goat anti-Rat TRITC conjugated (eBioscience) diluted 1:200 in PBS. Samples were analyze using Confocal Microscope Sp8 (Leica) and relative LASx software.

Statistical Analyses

All data were controlled for normal distribution (Kolmogorov–Smirnov and Shapiro–Wilk tests).

Continuous data were presented as mean ± standard deviation (SD) or standard error of the mean (SEM) if parametric or median with interquartile range (IQR) if nonparametric.

Categorical data were presented as number and percentage. Comparisons between frequencies or percentages were performed by using the chi-square test or the Fisher's exact test.

Between group comparisons of continuous variables were performed using the Student's t test or Analysis of Variance for normally distributed variables (with the Tukey or Dunnett post hoc tests, depending on the presence or absence of homoscedasticity), and the Mann-Whitney or Kruskal-Wallis tests for non-normally distributed variables.

Multiple logistic regression analysis, stepwise approach, was used to examine the relationship between serum ferritin, presence and pattern of hepatic iron deposition and presence of NASH or fibrosis. All the variables that were associated with NASH at the univariate analysis with a statistical significance corresponding to a P value up to 0.1 were included in the multivariate analysis. Similarly, logistic regression analysis was performed to find variables associated to advanced fibrosis.

In all other analyses, a 2-sided P value less than 0.05 was considered significant.

All analyses were performed using IBM SPSS (22.0, IBM, New York, USA) or Prism 5 for mac OS X version 5.0a software (GraphPad Software, Inc, La Jolla, CA).

4. RESULTS

4.1 STUDY 1 - CLINICAL STUDY

Characteristics of the NAFLD population

Of the 477 patients initially considered, two were subsequently excluded because of suboptimal biopsy sample, three because of missing clinical and/or biochemical data and four because of compound C282Y/H63D heterozygosity at the HFE gene test. The demographic, clinical, biochemical, and histological details of the 468 patients included in the study are shown in Table 1: the mean age was 47 years, 76% of patients were of Caucasian ethnicity and 38% were females. The mean BMI was 30.4 kg/m2; a history of IFG was observed in 19% patients and DM in 29% of patients, of which 65% were on hypoglycemic agents, mainly metformin. There was a high percentage of patients affected by dyslipidemia (68%), of which only 25% were on statin treatment. Hypertension had already been diagnosed in 32% of subjects, and 62% were treated mainly with renin-angiotensin system inhibitors. Female subjects were more likely to have diabetes and hypertension (45% versus 29%, $p<0.001$, and 39% versus 27%, $p=0.009$, respectively). None of the included patients had radiological or histological evidence of HCC at the time of liver biopsy.

Histological criteria for NASH were fulfilled in 247 (53%) patients, while advanced fibrosis was prevalent in 89 (19%) patients (81 of which having NASH and 8 with likely 'burnt-out NASH').

The characteristics of the 247 patients with NASH are shown in Table 2. They were more likely to be older, have a higher BMI and be affected by diabetes when compared to patients without NASH. Interestingly, the prevalence of MetS was not different between the two groups. Diabetic patients with NASH had a higher probability of suboptimal glycemic control if compared to diabetic patients without NASH as shown by a significantly different distribution of HbA1c values (54(42-96) vs 44(38-55) mmol/mol, $p=0.02$), despite a similar proportion of patients on hypoglycemic treatment (data not shown); also, the HOMA index was higher in NASH patients (4.1 vs 1.7, $p=0.001$), reflecting higher insulin resistance. Serum transaminases were significantly

higher in patients with NASH, with a median value of 1.5-2xULN. When considering general markers of inflammation (CRP), no difference was found between patients with and without NASH.

Hepatic iron deposition

Stainable hepatic iron was found in 116 (25%) patients: the pattern of iron deposition was mainly HC in 42 patients (36%), mainly reticuloendothelial in 24 patients (21%) and mixed in 50 (43%) patients. An iron grade 2 was found in 11 (9%) patients and grade 3 in 3 (3%) patients; none had an iron grade 4.

Clinical and laboratory data of subjects according to the presence of stainable hepatic iron and to the pattern of iron deposition are shown in Table 3: subjects with stainable hepatic iron were more likely to be male and have a lower BMI, had increasingly higher levels of SF (particularly Mixed>RES>HC, $p<0.0001$), serum iron (23.4 vs. 17 µmol/L, $p<0.0001$) and TSAT (37 vs 27 %, $p=0.04$), with a higher proportion of patients with hyperferritinemia (60% vs 15%, $p<0.0001$) and TSAT >45% (27% vs 10%, $p=0.003$, data not shown). In addition, they had significantly higher levels of ALT ($p=0.007$).

Table 1. Characteristics of the 468 patients with nonalcoholic fatty liver disease.

	Total=468
Age, years	47±13
Caucasian ethnicity, n (%)	354 (76)
Females, n (%)	177 (38)
BMI, Kg/m²	30.4±5.8
Alcohol>10g/day, n (%)	27 (5.8)
Hypertension, n (%)	149 (32)
Dyslipidemia, n (%)	320 (68)
Diabetes, n (%)	133 (29)
IFG, n (%)	90 (19)
MetS, n (%)	143 (31)
Platelets, x 10^9/L	233 (192-277)
ALT, U/L	65 (37-93)
AST, U/L	40 (26-54)
GGT, U/L	73 (24-121)
Bilirubin, µmol/L	11 (7-14)
Albumin, g/dL	4.6 (4.4-4.8)
INR >1.2, n (%)	15 (3.3)
Cholesterol, mmol/L	5.2 (4.4-6)
HDL, mmol/L	1.2 (1-1.4)
TG, mmol/L	1.6 (1-2.2)

GLC, mmol/L	5.3 (4.6-6)
Ferritin, µg/L	188 (61-314)
Ferritin>ULN, n (%)	122 (32)
TSAT, %	29 (20-38)
NASH, n (%)	247 (53)
F0, n (%)	207 (44)
F1, n (%)	104 (22)
F2, n (%)	68 (15)
F3, n (%)	41 (9)
F4, n (%)	48 (10)
≥ F3, n (%)	89 (19)
Hepatic iron, n (%)	116 (25)
HC, n (%)	42 (9)
RES, n (%)	24 (5)
Mixed, n (%)	50 (11)

Data are reported as number and percentage (%), mean ± standard deviation, median and interquartile range (IQR). Abbreviations: BMI, body mass index; ALT, alanine aminotransferase; AST, aspartate aminotransferase; GGT, γ-glutamyl transpeptidase; INR, international normalised ratio; HDL, high density lipoprotein; TG, triglyceride; GLC, serum glucose; TSAT, transferrin saturation; NASH, non-alcoholic steatohepatitis; HC, hepatocellular iron deposition; RES, reticuloendothelial system cells iron deposition.

Table 2. Comparison of patients according to the presence of NASH.

	NASH (n=247)	No NASH (n=221)	*p*
Age, years	50 ±13	45±12	0.014
Females, n (%)	99 (40)	78 (35)	0.29
BMI, Kg/m²	31±6	29±6	0.014
Hypertension, n (%)	87 (35)	62 (29)	0.12
Dyslipidemia, n (%)	162 (66)	158 (72)	0.14
Diabetes, n (%)	114 (46)	49 (23)	<0.0001
IFG, n (%)	88 (39)	79 (40)	0.74
MetS, n (%)	81 (33)	62 (28)	0.26
Alcohol, g/day	1.3 ± 4	2.1 ± 5	0.055
Alcohol>10g/d, n (%)	11 (4.5)	16 (7)	0.19
HOMA	4.1 ± 3.7	1.7 ± 1.2	0.001
WCC, x10^9/L	6.56 (5.5-7.6)	6.8 (5.5-8.1)	0.63
ALT, U/L	74 (43-105)	58 (34-72)	<0.0001
GGT, U/L	68 (25-111)	81 (29-133)	0.13
Bilirubin, µmol/L	10 (7-13)	11 (8-14)	0.64
Cholesterol, mmol/l	5.2 (4.5-6)	5.2 (4.3-6.1)	0.75
HDL (mmol/L)	1.2 (1-1.4)	1.3 (1-1.6)	0.15
TG, mmol/L	1.5 (0.9-2.1)	1.7 1.1-2.3)	0.41
CRP, mg/L	4.5 (0.5-8.5)	3 (0.5-5.5)	0.24
Serum Iron, µmol/L	17.3 (12-22)	18.6 (13-23)	0.25
Ferritin, µg/L	198 (53-343)	181 (64-298)	0.42
Ferritin>ULN, n (%)	72 (26)	50 (23)	0.11

TSAT, %	24 (16-32)	33 (24-42)	0.001
Hepatic Iron, n (%)	66 (27)	50 (23)	0.31
HC	20 (8)	22 (10)	0.48
RES	11 (4)	13 (6)	0.49
Mixed	35 (14)	15 (7)	0.01

Data are reported as number and percentage (%), mean ± standard deviation, median and interquartile range (IQR). Abbreviations: BMI, body mass index; IFG, impaired fasting glucose; MetS, metabolic syndrome; ; HOMA IR, homeostatic model for assessment of insulin resistance; WCC, white cells count; A ALT, alanine aminotransferase; GGT, γ-glutamyl transpeptidase; HDL, high density lipoprotein; TG, triglyceride; CRP, C reactive protein; TSAT, transferrin saturation; HC, hepatocellular iron deposition; RES, reticuloendothelial system cells iron deposition.

Table 3. Demographic, clinical data and laboratory findings of the 468 patients with nonalcoholic fatty liver disease according to the presence of stainable iron in the liver and the pattern of iron deposition.

	Hepatic Iron (n=116)	**No hepatic Iron (n=352)**	***p***	**HC iron (n=42)**	**RES iron (n=24)**	**Mixed (n=50)**	***p***
Age, years	47±13	48±13	0.79	47 ±14	48±15	47±11	0.97
Females, n (%)	22 (19)	155 (44)	<0.001	8 (19)	5 (21)	9 (18)	0.95
BMI, Kg/m²	29 ± 5	31 ± 6	0.03	29±5	30.6±4	29±5	0.14
Alcohol, g/day	2.1±	1.5±4.5	0.23	2.2±5	1.6±4	2.3±5	0.61
Alcohol>10g/d,n(%)	9 (7)	18 (5)	0.28	4 (9)	1 (4)	4 (8)	0.58

HTN, n (%)	31 (27)	118 (33.8)	0.17	17 (40)	7 (30)	7 (14)	0.016
DM, n (%)	37 (32)	126 (36)	0.44	14 (33)	6 (26)	17 (34)	0.6
GLC, mmol/L	5.2(4.5-6)	5.3(2.5-6.1)	0.11	5.3 (4.6-6)	4.9(4.2-6)	5 (4.3-6)	0.6
HOMA-IR	3.2±2.9	4.4±3.8	0.14	3.5±3.1	3.8±3.2	4±2.7	0.35
PLT, x10^9/L	212 (78)	240 (76)	0.001	230 (116)	221 (53)	206 (58)	0.48
ALT, U/L	77(43-111)	64 (37-91)	0.007	77 (41-112)	70 (43-97)	76(40-111)	0.99
Albumin, g/dL	4.7 (4.4-5)	4.6(4.3-4.8)	0.05	4.7 (4.4-5)	4.7(4.5-5)	4.7(4.5-5)	0.67
Iron, µmol/L	22 (19-25)	17 (12-21)	<0.001	25 (21-28)	19 (15-23)	22 (17-27)	<0.001
SF, µg/L (IQR)	427(490)	146 (160)	<0.001	388 (372)	427 (517)	501 (453)	<0.001
SF>ULN,n (%)	70 (60)	52 (15)	<0.001	19 (45)	12 (50)	39 (78)	0.003
TSAT, %	37 (29-45)	27 (15-39)	0.01	47 (32-62)	33 (25-41)	31 (20-42)	0.04
≥ F1, n (%)	67 (58)	193 (55)	0.58	23 (55)	12 (50)	32 (64)	0.61
≥ F2, n (%)	41 (35)	115 (33)	0.6	16 (38)	7 (29)	18 (36)	0.84
≥ F3, n (%)	24 (21)	65 (19)	0.59	11 (26)	4 (17)	9 (18)	0.66
F4, n (%)	11 (9)	37 (10)	0.67	5 (11)	1 (5)	5 (10)	0.79
NASH, n (%)	66 (57)	181 (51)	0.31	20 (48)	11 (46)	35 (70)	0.05
NAS	3.5±1.8	3.4±1.7	0.49	3.4±1.9	3.1±1.9	3.9±1.8	0.24

Data are reported as number and percentage (%), mean ± standard deviation, median and interquartile range (IQR). Abbreviations: BMI, body mass index; HOMA IR, homeostatic model for assessment of insulin resistance; WCC, white cells count; ALT, alanine aminotransferase; GGT, γ-glutamyl transpeptidase, HDL, high density lipoprotein; TG, triglyceride; CRP, C reactive protein; TSAT, transferrin saturation; HC, hepatocellular iron deposition; RES, reticuloendothelial system cells iron deposition; NASH, nonalcoholic steatohepatitis; NAS, NASH activity score.

SF, serum hepcidin, iron deposition and liver disease severity

Hyperferritinemia was found in 122 (26%) patients.

Patients with hyperferritinemia had no difference in sex (p=0.23), ethnicity (p=0.64), cohort (0.17), age (0.39), BMI (p=0.83), prevalence of diabetes and or/IFG compared to non hyperferritinemics. When looking at mild alcohol consumption, an increasing trend in SF values was found for increasing alcohol intake; however, the prevalence of hyperferritinemia was not different between abstinent vs mild drinkers (p=0.1), even when considering subclasses of alcohol intake (p=0.097).

Looking at the single components of histological NASH, a positive association was found between SF and increasing degree of steatosis (p=0.008) but not with hepatocellular ballooning or lobular inflammation and overall SF did not associate with diagnosis of NASH (Table 2). Interestingly, SF showed a peculiar pattern throughout fibrosis stages, increasing from F0-F1 to F3, and subsequently decreasing in cirrhosis (Figure 1). When comparing the inter-group SF distribution, it was significantly higher for F3 compared to F0-F1 (p=0.024), with an average increase of 14% from F0-F1 to F2 and of 61% from F2 to F3 and a decrease of 43% from F3 to F4. The same pattern was observed in a recent study by Ryan et al (170).

Similarly, when determined in a subgroup of patients (n=23), serum hepcidin was higher in patients with stainable hepatic iron when compared to those without iron (46 versus 12 ng/ml, p=0.05), reaching the significance when taking into account the different patterns of deposition, particularly for mixed deposition, 66 vs 12 ng/ml, anova p=0.019) 11 ng/ml no iron, 14 ng/ml HC, 40 ng/ml RES, 66 mixed, anova p= 0.019) for patients with mixed hepatic iron (66 ng/ml), and also correlated with serum ferritin levels. No differences were found in hepcidin levels across fibrosis stages or according to the presence of NASH (p=0.74).

On the other hand, patients with a mixed pattern of iron deposition were more likely to have NASH if compared to patients with other patterns of iron deposition or to patients without hepatic iron. No difference was seen between patients with and without hepatic stainable iron when considering the individual components of histological NASH, NAS >3 or >5 (data not shown).

No association was found between presence of stainable hepatic iron and fibrosis (mild, significant, advanced), even after removing cases with cirrhosis.

At the multivariate analysis, BMI (OR 1.06, 95% CI 1.02-1.11, p=0.005), presence of diabetes (OR 2.13, 95% CI 1.31-3.45, p=0.01), ALT levels (OR 1.012, 95% CI 1.006-1.017, p<0.0001) and a mixed pattern of hepatic iron deposition, (OR 2.23, 95% CI 1.08-4.6, p=0.03) were independently associated with the presence of NASH (as reported by a previous study by the US NASH Clinical Research Network (203)) . Such variables remained the only significantly associated even after removing patients with TSAT higher than 45% and correcting for cohort and sex or when including alcohol as a categorical or continuous variable but not when considering each cohort separately (data not shown).

Advanced fibrosis was associated with advanced age (OR 1.04, 95% CI 1.01-1.06, p=0.01), presence of diabetes (OR 3.09, 95% CI 1.65-5.79, p<0.0001) and low platelet count (OR 0.987; 95% CI 0.982-0.992, p<0.0001) but not with serum ferritin.

4.2 STUDY 1 – IN VITRO STUDY

HepG2 cells were treated with FFA oleate or palmitate, at different concentration and for different time duration in order to find the appropriate protocol to induce hepatocyte fat accumulation. MTT analysis did not show reduced vitality in response to treatment with FFAs.

HepG2 cells treated for 24 hours developed lipid accumulation within the cytosol, increasingly according to the concentration of FFA, particularly for the mixture of mixed oleate/palmitate as evidenced by fluorescence microscopy (Figure 4 a, b, c) and microfluorimeter (Figure 4 d).

Figure 4. DAPI and Nile Red staining. Control (a), treatment with FFA 400 µM (b), treatment with FFA 600 µM (c).

a) **b)** **c)**

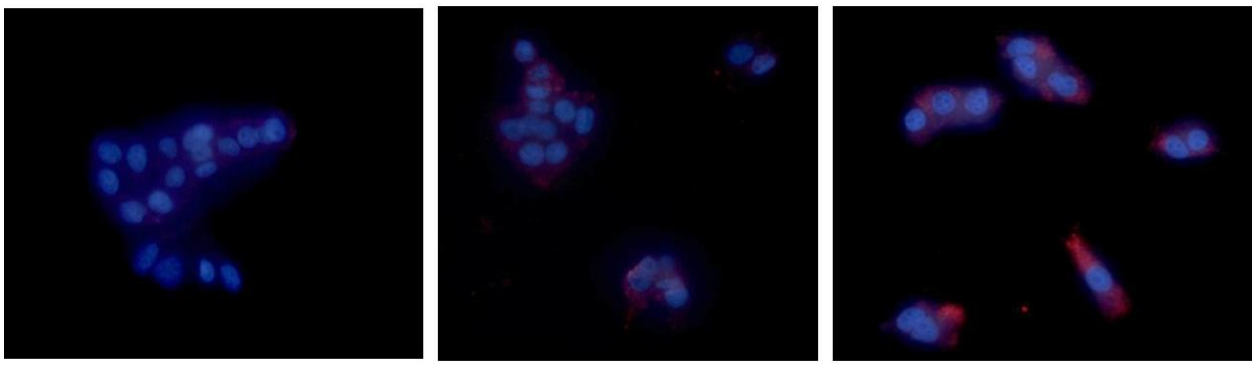

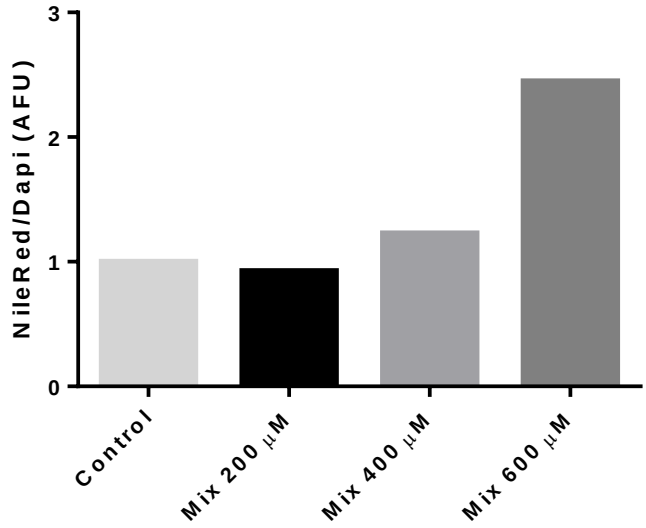

d)

After mRNA extraction and quantitation we found that HAMP mRNA levels tended to increase at higher concentration of FFA (600 µM) for all treatment (oleate, palmitate and both), reaching the highest peak after 3 hours from the beginning of the treatment (Figure 5), remaining activated after 6 hours of treatment with palmitate and mixed FFA and exhausting at 24 hours. In order to determine if such increase in HAMP expression was secondary to an inflammatory effect exerted by FFAs in hepatocytes we determined mRNA levels of TNF-alpha and IL-6, which did not show significant alterations after treatment (data not shown). Therefore, these preliminary data would support the hypothesis that lipid accumulation seems to influence HAMP expression in hepatocytes, and this could happen independently from the presence of inflammation, but further deepening is required.

Figure 5. Normalized hHAMP expression according to FFA treatment and time

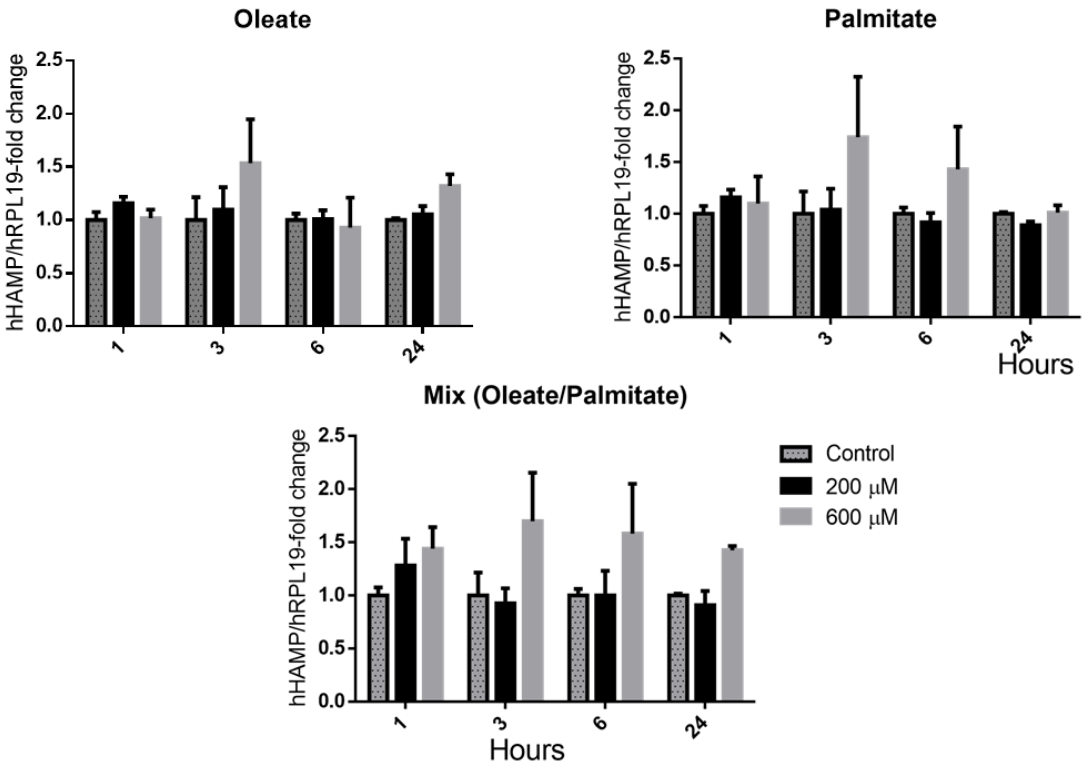

4.3 STUDY 2 – ANIMAL STUDY

Animal model and inducible gene deletion

Mice were divided in 6 treatment groups (ad libitum diet or starvation for 6, 12, 24, 48 or 72 hours, each group= 6 mice) for each strain and compared as follows: *Hamp*-KO vs CTRL, i-Hamp-KO vs i-CTRL

Genotyping showed complete ablation of the Hamp gene in *Hamp*-KO mice and in i-*Hamp*-KO mice after the injection protocol with tamoxifen. qRT-PCR also confirmed total absence of hepatic Hamp1 mRNA in both groups (Figure 6 a, b).

Figure 6. Hamp1 levels in CTRL vs Hamp-KO mice and i-CTRL vs i-*Hamp*-KO mice

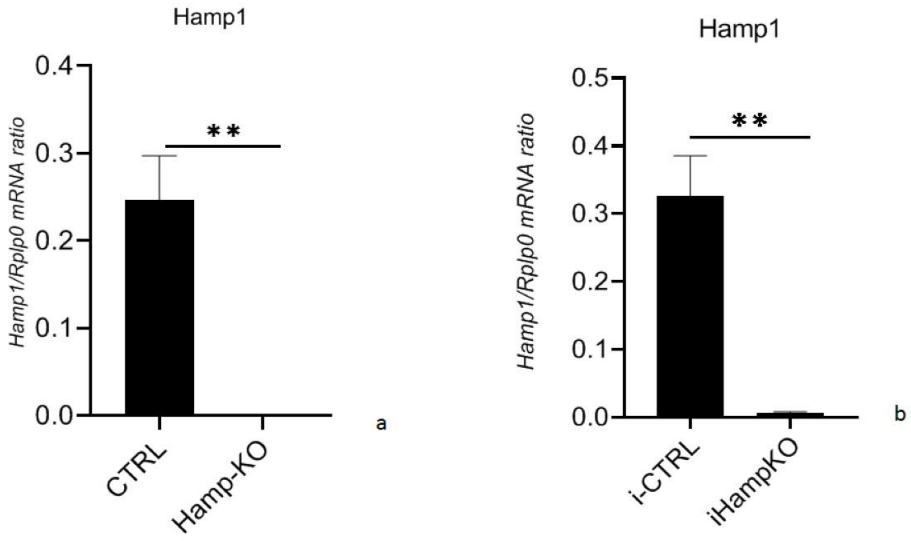

Response to starvation

Within all the starvation groups , *Hamp*-KO mice did not show a reduced survival compared to CTRLs.

On the contrary, 2 mice in the CTRL group died after 72 hours of starvation (mortality: 33% vs 0, CTRL vs *Hamp*-KO in the 72H group).

Similarly, 2 mice in the i-CTRL group died after 72 hours of starvation (vs none in the i-*Hamp*-KO group), confirming that neither iron overload nor absence of hepcidin per se seem to reduce the tolerance to food deprivation, even if prolonged.

Starting from similar weights at baseline (Figure 7 a and d), weight loss, proportional to the hours of starvation, was reported in all groups (Figure 7 b, c, e, f).

Figure 7. **Weight loss during starvation.**

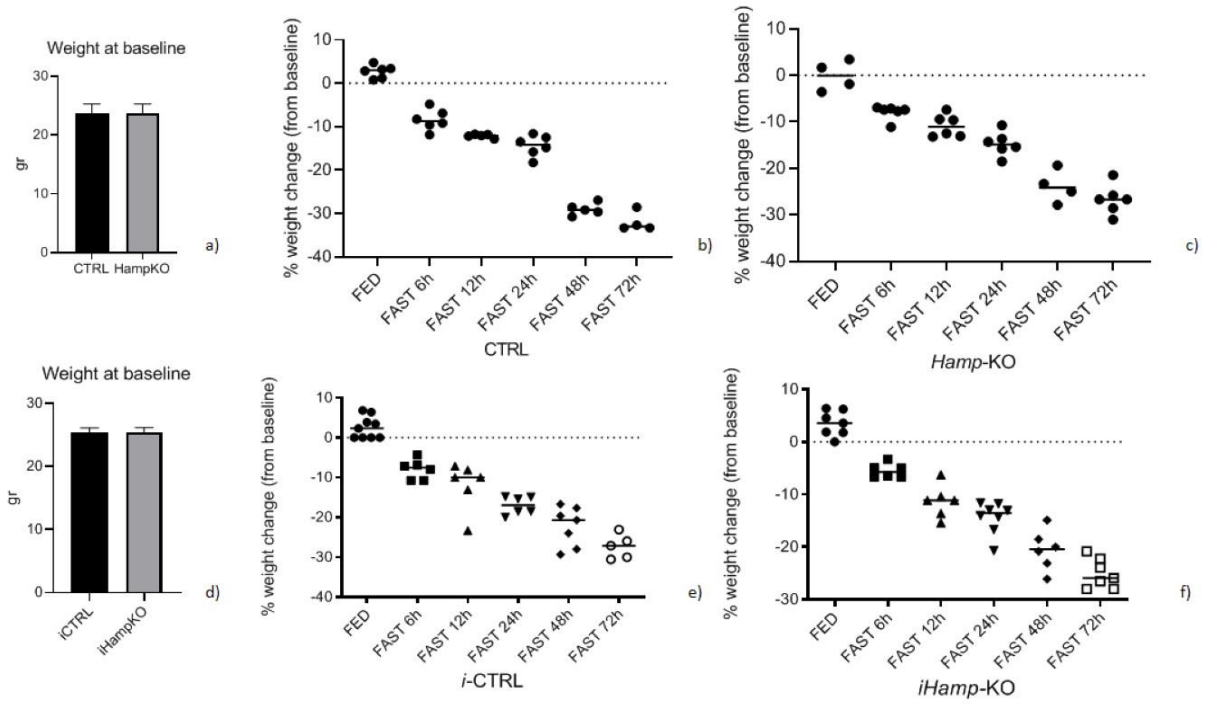

Of the measured serum biochemical parameters, glycaemia was similar at baseline in all groups compared to controls and diminished proportionally to the hours of starvation in both *Hamp*-KO and CTRLs; the drop was more rapid in *Hamp*-KO than in CTRLs (45 vs 16 % decrease after 6 hours), but reached a lower mean in CTRLs at 72 hours of starvation, suggesting a slower response of glycogenolysis and gluconeogenesis in *Hamp*-KO mice in response to starvation which, however, maintained higher glucose levels in prolonged starvation, despite not statistically significant (serum glucose at 48 hours: 153 vs 116 mg/dl, p = 0.23; serum glucose at 72 hours 203 vs 108 mg/dl, , p = 0.2) (Figures 8 a, b).

Activation of gluconeogenesis in response to food deprivation was confirmed by quantitative measurement of mRNA levels of phosphoenolpyruvate carboxykinase 1 (Pepck) mRNA, enzyme known to be readily responsive to gluconeogenic stimuli, which was induced after 6 hours of fasting and reached its peak at 12 hours, with a similar trend for both *Hamp*-KO and CTRL (Figure 8 d, e, f).

Also, the transcription factor Peroxisome Proliferator Activated Receptor Gamma Coactivator 1 alpha (Pgc1a), which regulates the hepatic expression of genes encoding for gluconeogenic enzymes and whose levels were lower at basal states (FED) in *Hamp*-KO compared to CTRL, increased at prolonged starvation in CTRL mice but such response was blunted in *Hamp*-KO mice (Figure 8 g, h, i).

Similarly to what was seen in *Hamp*-KO and CTRL, glucose serum levels decreased more rapidly in i-*Hamp*-KO than i-CTRL after 6 hours (39 vs 7%), reaching lower levels in i-CTRL after prolonged starvation (Figure 9 a, b, c), whereas Pgc1a expression in i-*Hamp*-KO was different at the basal (FED) state and attenuated and delayed in starvation as compared to i-CTRL mice (Figure 9 g, h, i), suggesting that hepcidin per se, while being a target of gluconeogenic stimuli, could be also involved in regulation of metabolic pathways involved in gluconeogenesis.

Figure 8. Serum glucose and expression of genes involved in gluconeogenesis in CTRL and *Hamp*-KO

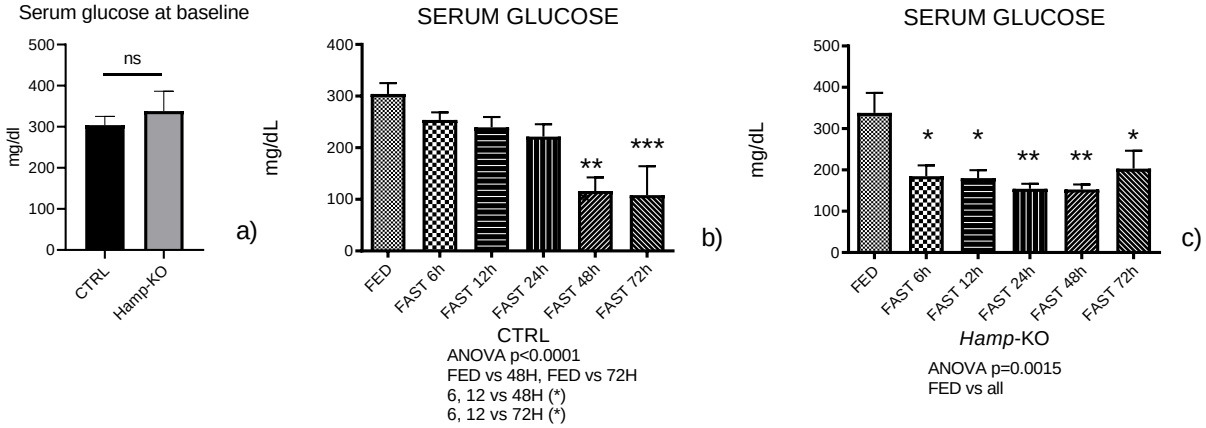
Serum glucose at baseline
mg/dl
ns
CTRL
Hamp-KO
a)
SERUM GLUCOSE
mg/dL
FED
FAST 6h
FAST 12h
FAST 24h
FAST 48h
FAST 72h
b)
CTRL
ANOVA p<0.0001
FED vs 48H, FED vs 72H
6, 12 vs 48H (*)
6, 12 vs 72H (*)
SERUM GLUCOSE
c)
Hamp-KO
ANOVA p=0.0015
FED vs all

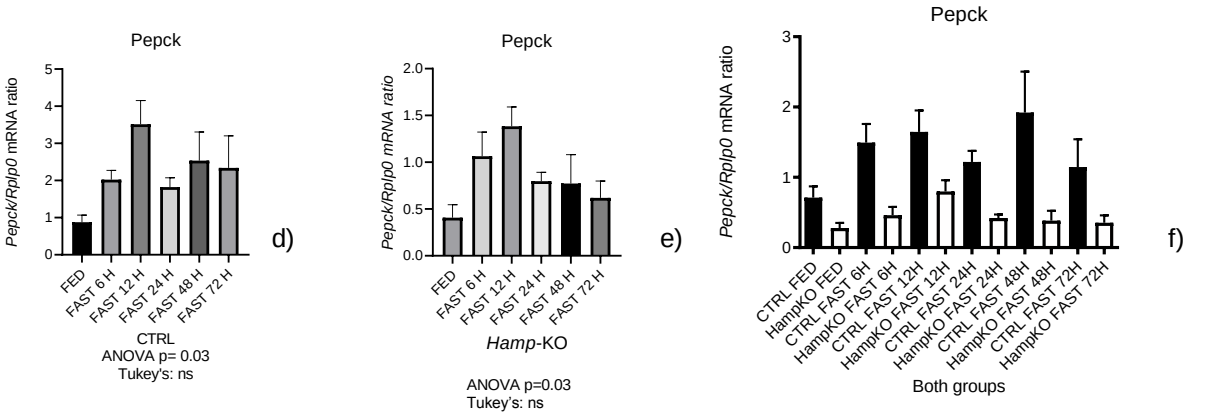
Pepck
Pepck/Rplp0 mRNA ratio
FED
FAST 6 H
FAST 12 H
FAST 24 H
FAST 48 H
FAST 72 H
d)
CTRL
ANOVA p= 0.03
Tukey's: ns
Pepck
e)
Hamp-KO
ANOVA p=0.03
Tukey's: ns
Pepck
f)
CTRL FED
HampKO FED
CTRL FAST 6H
HampKO FAST 6H
CTRL FAST 12H
HampKO FAST 12H
CTRL FAST 24H
HampKO FAST 24H
CTRL FAST 48H
HampKO FAST 48H
CTRL FAST 72H
HampKO FAST 72H
Both groups

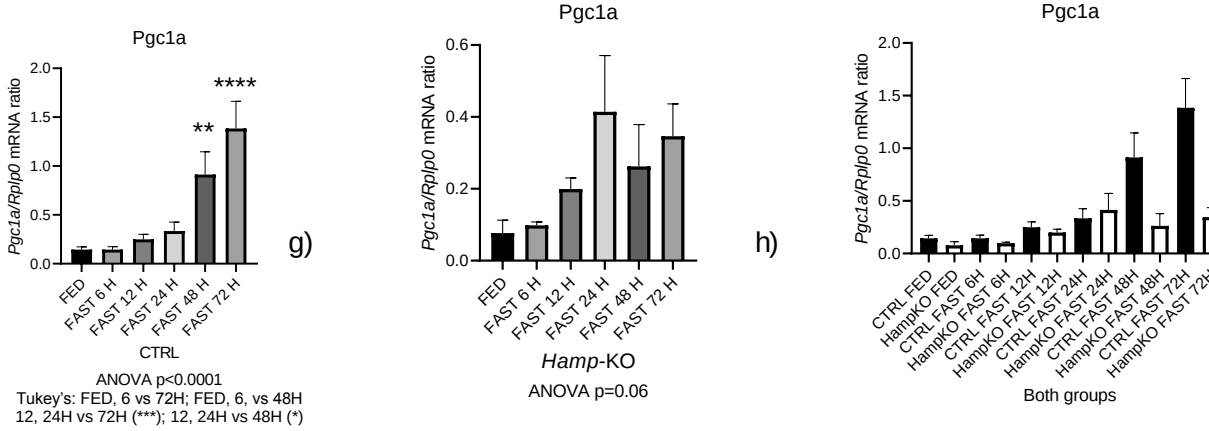
Pgc1a
Pgc1a/Rplp0 mRNA ratio
FED
FAST 6 H
FAST 12 H
FAST 24 H
FAST 48 H
FAST 72 H
g)
CTRL
ANOVA p<0.0001
Tukey's: FED, 6 vs 72H; FED, 6, vs 48H
12, 24H vs 72H (***); 12, 24H vs 48H (*)
Pgc1a
h)
Hamp-KO
ANOVA p=0.06
Pgc1a
i)
CTRL FED
HampKO FED
CTRL FAST 6H
HampKO FAST 6H
CTRL FAST 12H
HampKO FAST 12H
CTRL FAST 24H
HampKO FAST 24H
CTRL FAST 48H
HampKO FAST 48H
CTRL FAST 72H
HampKO FAST 72H
Both groups

Figure 9. **Serum glucose and expression of genes involved in gluconeogenesis in i-CTRL and i-*Hamp*-KO.**

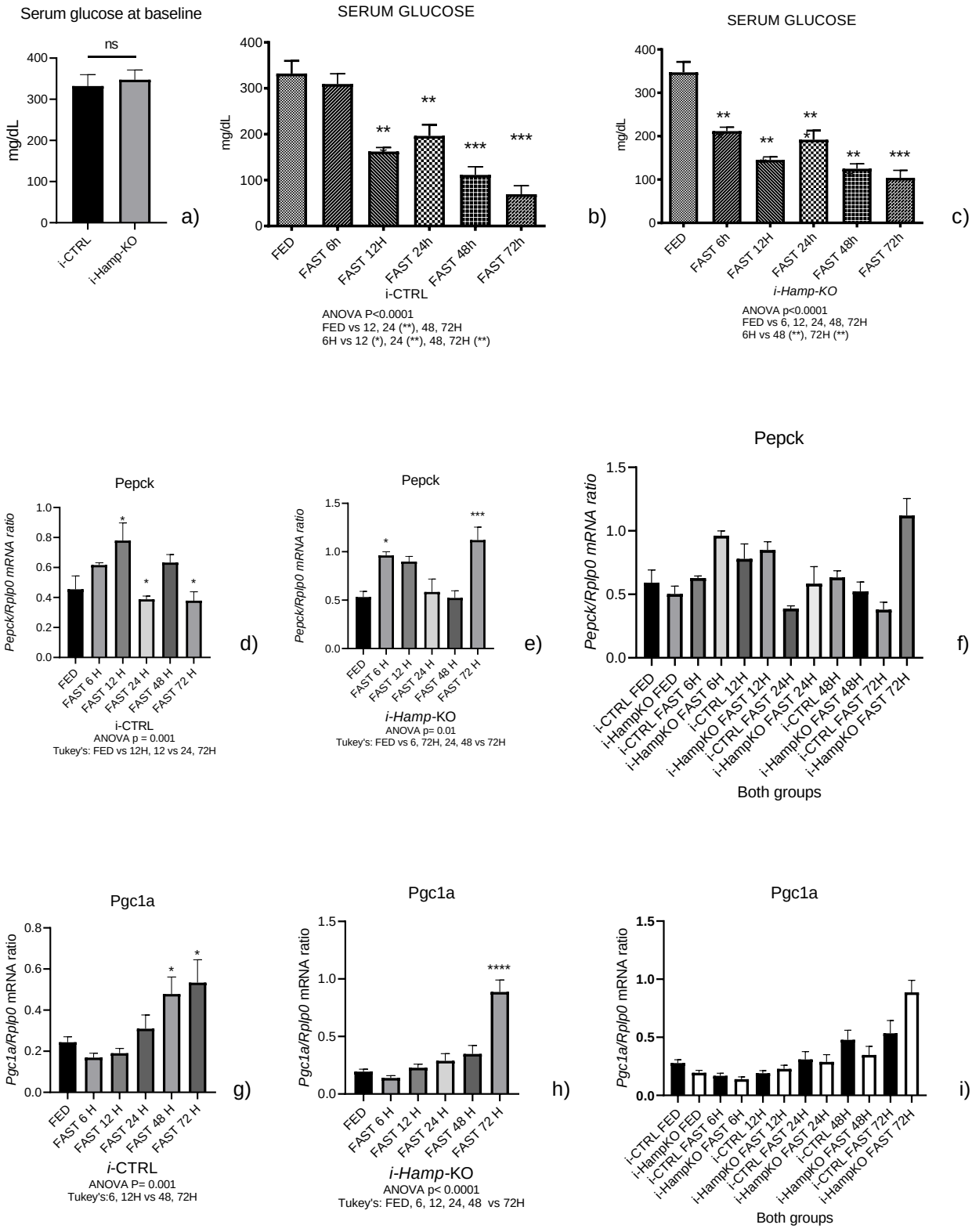

Mirroring the decline in triglycerides, ketone bodies raised during fasting, reaching a peak after 24 hours in CTRL and i-CTRL mice, while it was after 48 hours in i-*Hamp*-KO and at 72 hours in *Hamp*-KO mice (Figures 10 and 10 bis).

No meaningful alterations were seen in other nutritional parameters marking hepatic synthetic activity such as cholesterol, which was stable in all experimental groups, and albumin (which actually showed a small increase at 72 hours, likely due to hemoconcentration).

Aminotransferases serum levels increased after 7, 2 hours of starvation in both *Hamp*-KO and CTRL mice (figure 11 a-d) and i-*Hamp*-KO mice and i-CTRL (Figure 11 bis, a-d), and this could be partially ascribed to the hepatocellular injury seen in cases of severe malnutrition and sometimes called 'starvation hepatitis', caused by the combined effect of multiple mechanisms triggered by malnutrition including apoptosis/autophagy, hypoperfusion of the liver, hypoxia, oxidative stress, and iron deposition. Indeed, no macroscopic signs of hepatocyte necrosis were seen at histological evaluation.

Lastly, no alterations in haemochromocytometric parameters such as hemoglobin value and red blood cells number were seen at prolonged times of starvation, apparently excluding impairment of the bone marrow synthetic activity (Figure 12, data shown for *Hamp*-KO and CTRLs).

Figure 10: **Serum triglycerides and ketone bodies in CTRL mice and *Hamp*-KO mice.**

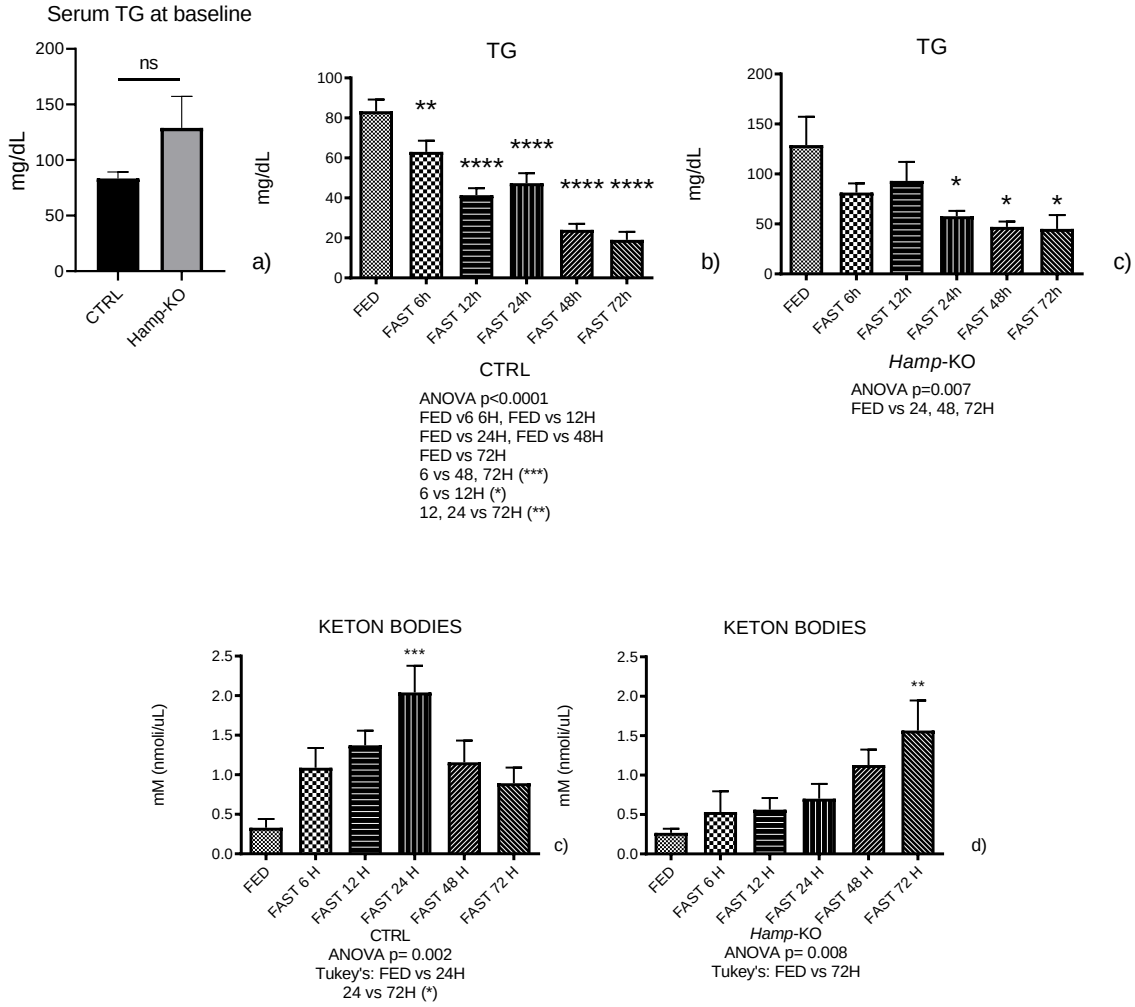

Figure 10 bis. Triglycerides and ketone bodies in i-CTRL mice and i-*Hamp*-KO mice

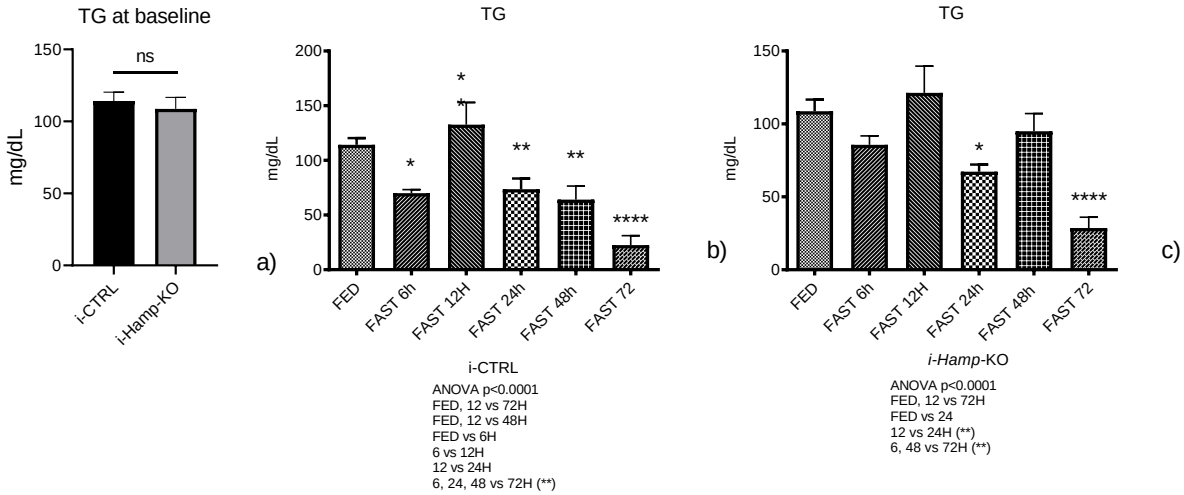

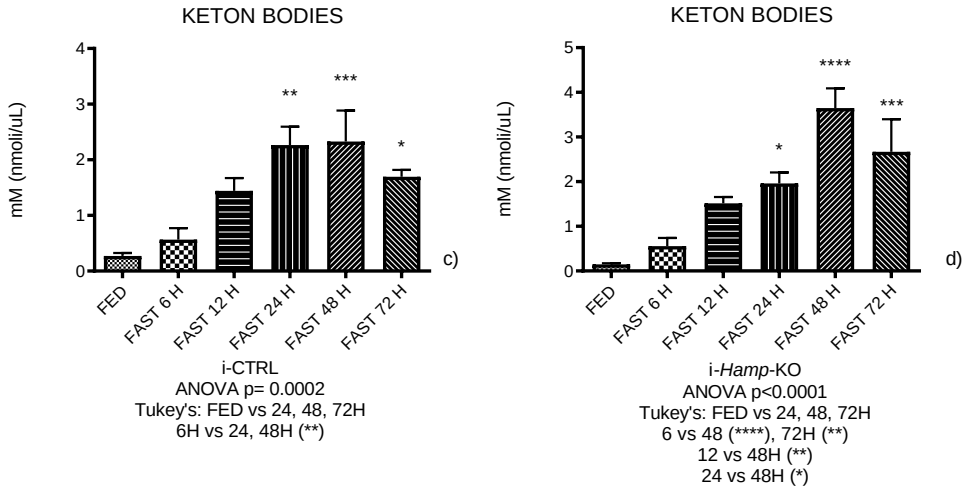

Figure 11. **Alanine aminotransferase and aspartate aminotransferase levels in CTRL and *Hamp*-KO mice.**

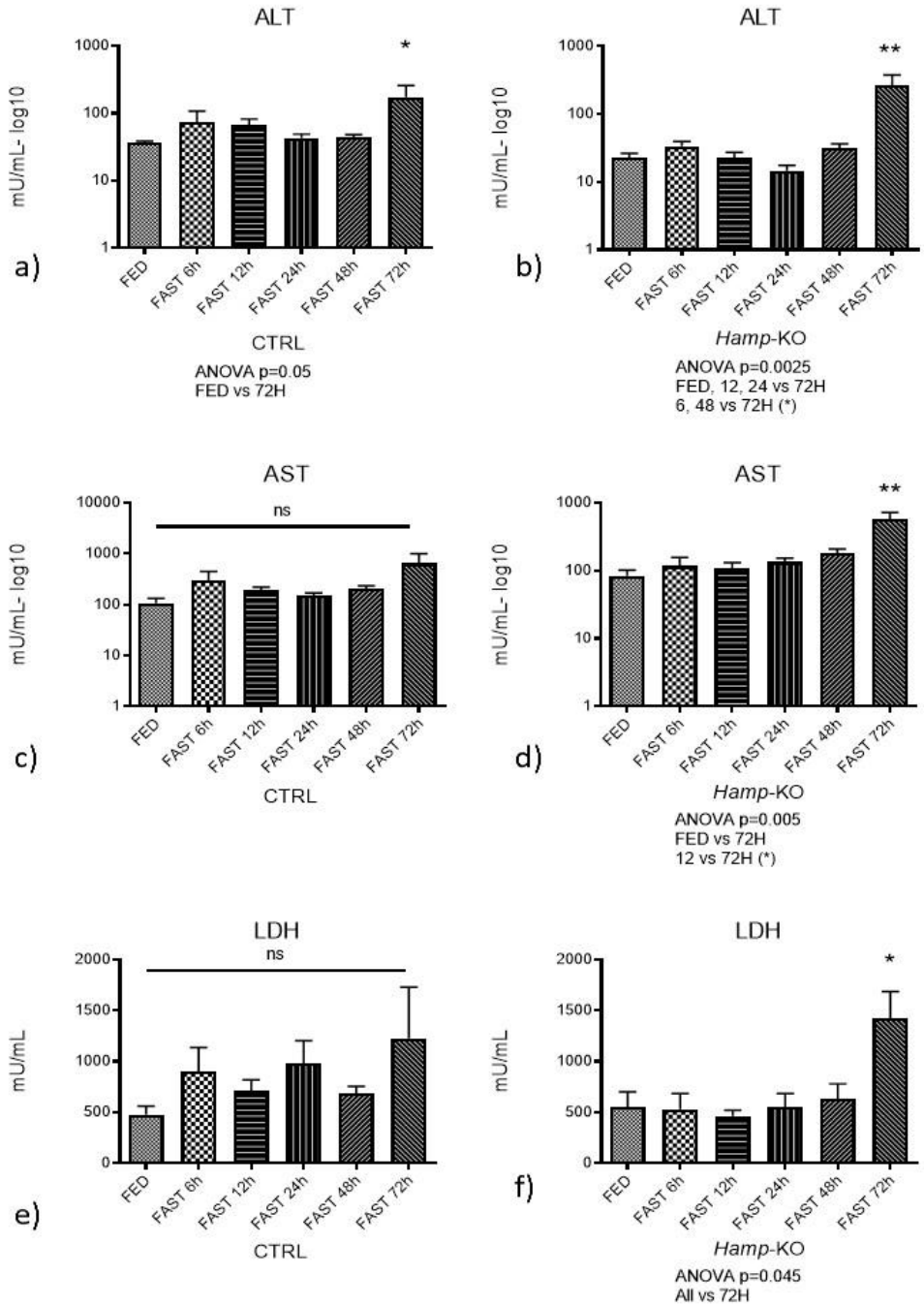

Figure 11 bis Alanine aminotransferase and aspartate aminotransferase levels in CTRL and *Hamp*-KO mice.

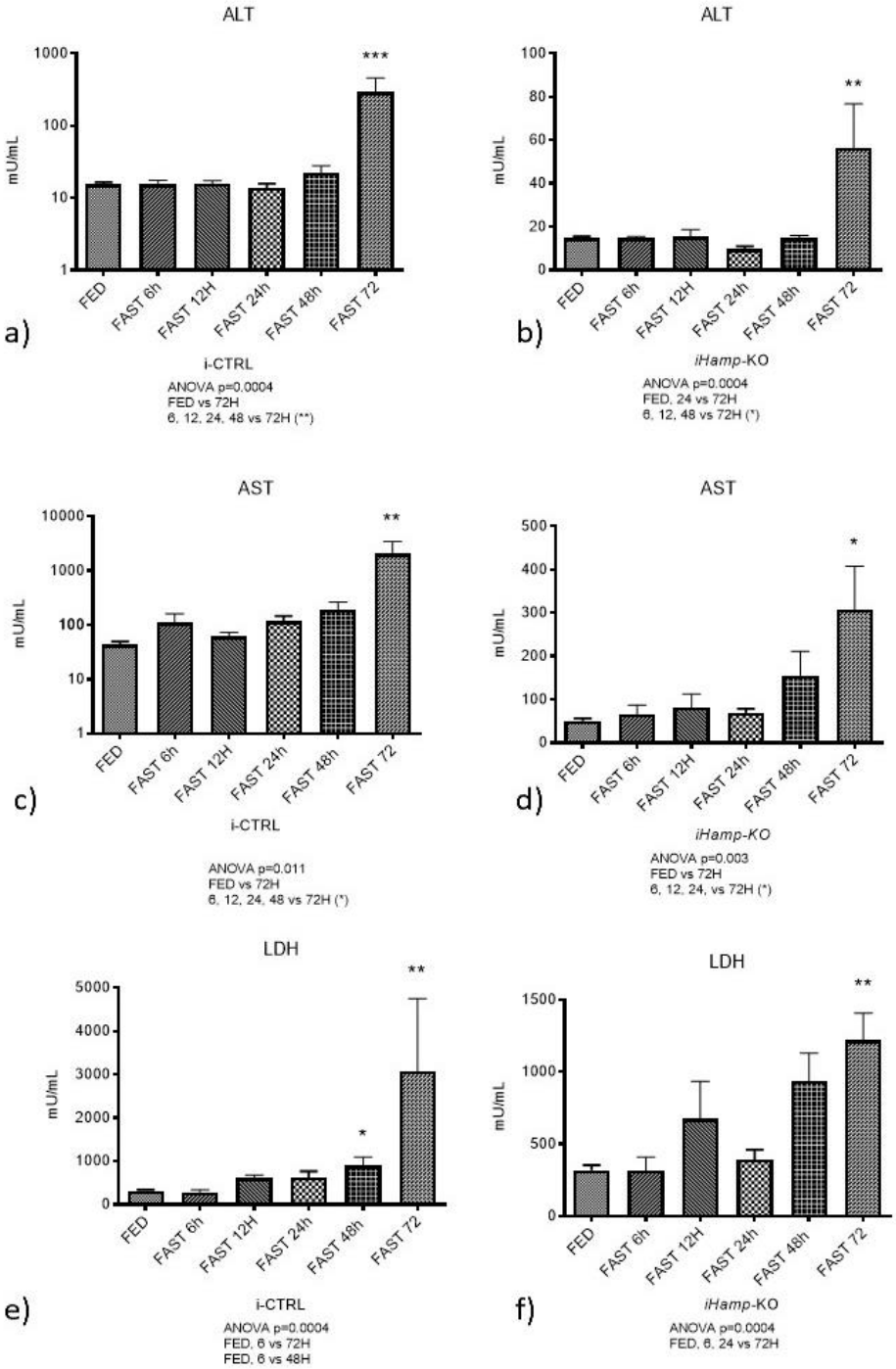

Figure 12: Red blood cell count, Hemoglobin and hematocrit

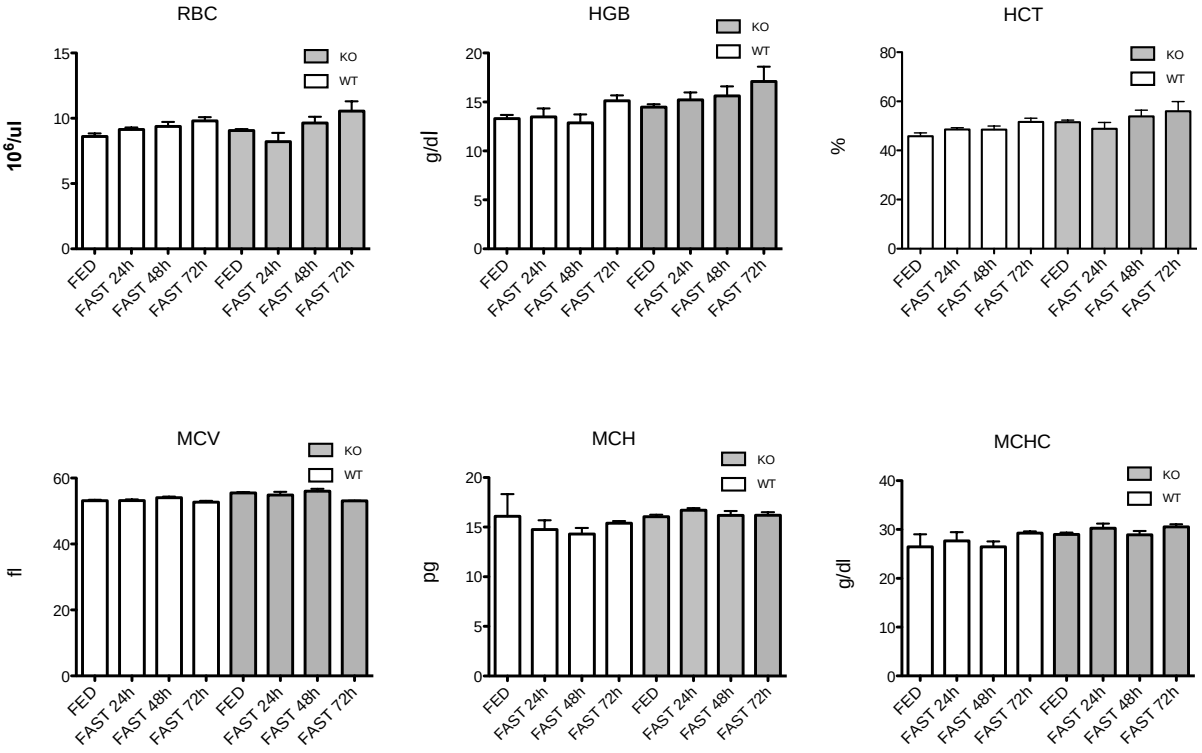

Serum and tissue iron parameters

As expected, serum iron at baseline was significantly higher (1.5 fold) in *Hamp*-KO compared to CTRL (Figure 13 a), while during food deprivation (Figure 13 c) remained relatively stable up to 24 hours (likely due to the higher basal transferrin saturation in this mouse model of hemochromatosis) and increased at 72 hrs. In CTRLs, serum iron fell at 6, 12 and 24 hours, while at 48 hours it started to increase (Figure 13 b). Such trend was confirmed also in i-CTRL mice (Figure 14 a), while in i-*Hamp*-KO mice (who had 1.5 fold more serum iron in the FED state than i-CTRLs, Figure 13 a), iron levels started to slightly decrease at 48 hours of starvation, indicating lower iron stores compared to congenic *Hamp*-KO mice (Figure 14 c). Serum ferritin increased in all groups with prolonged food deprivation (Figures 13 e, f; 14 c, d).

Figure 13: Serum iron parameters in CTRL and *Hamp*-KO mice

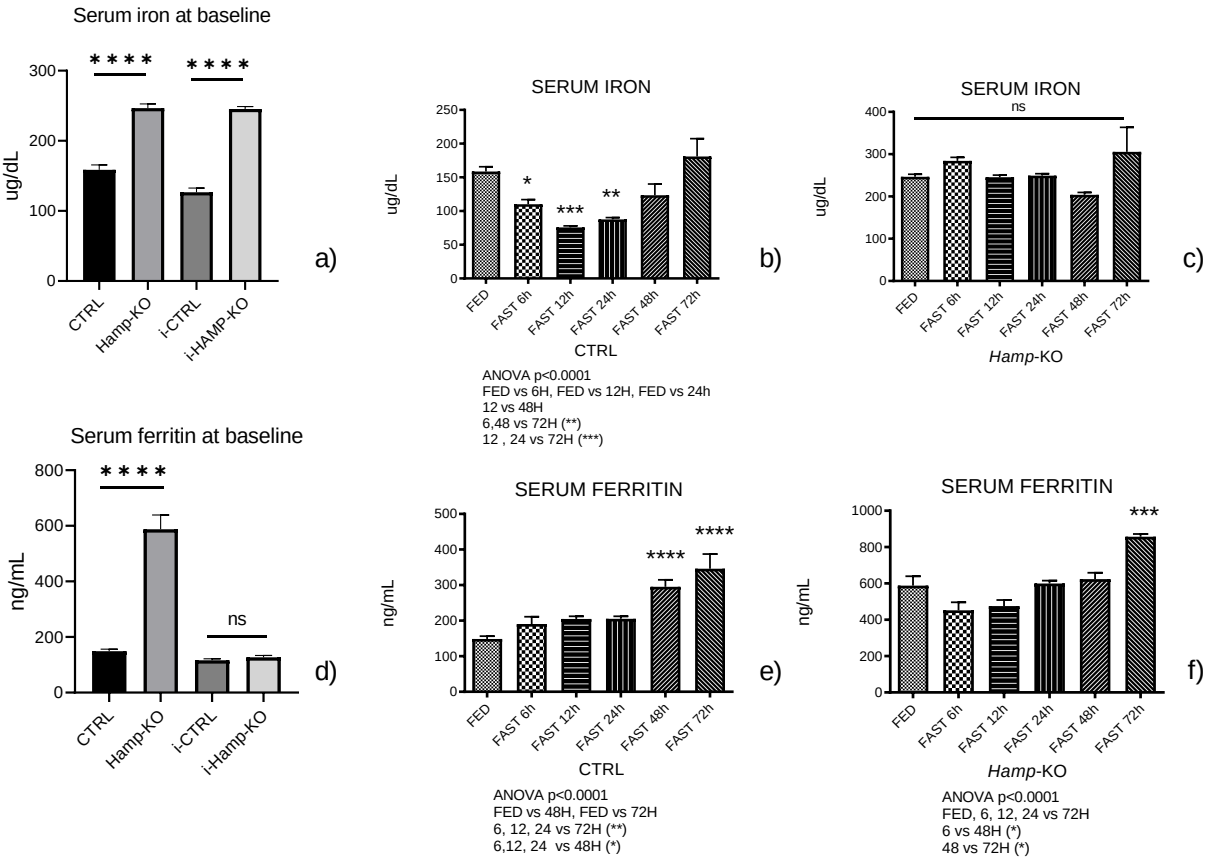

Figure 14: **Serum iron parameters in i-CTRL and i-*Hamp*-KO mice**

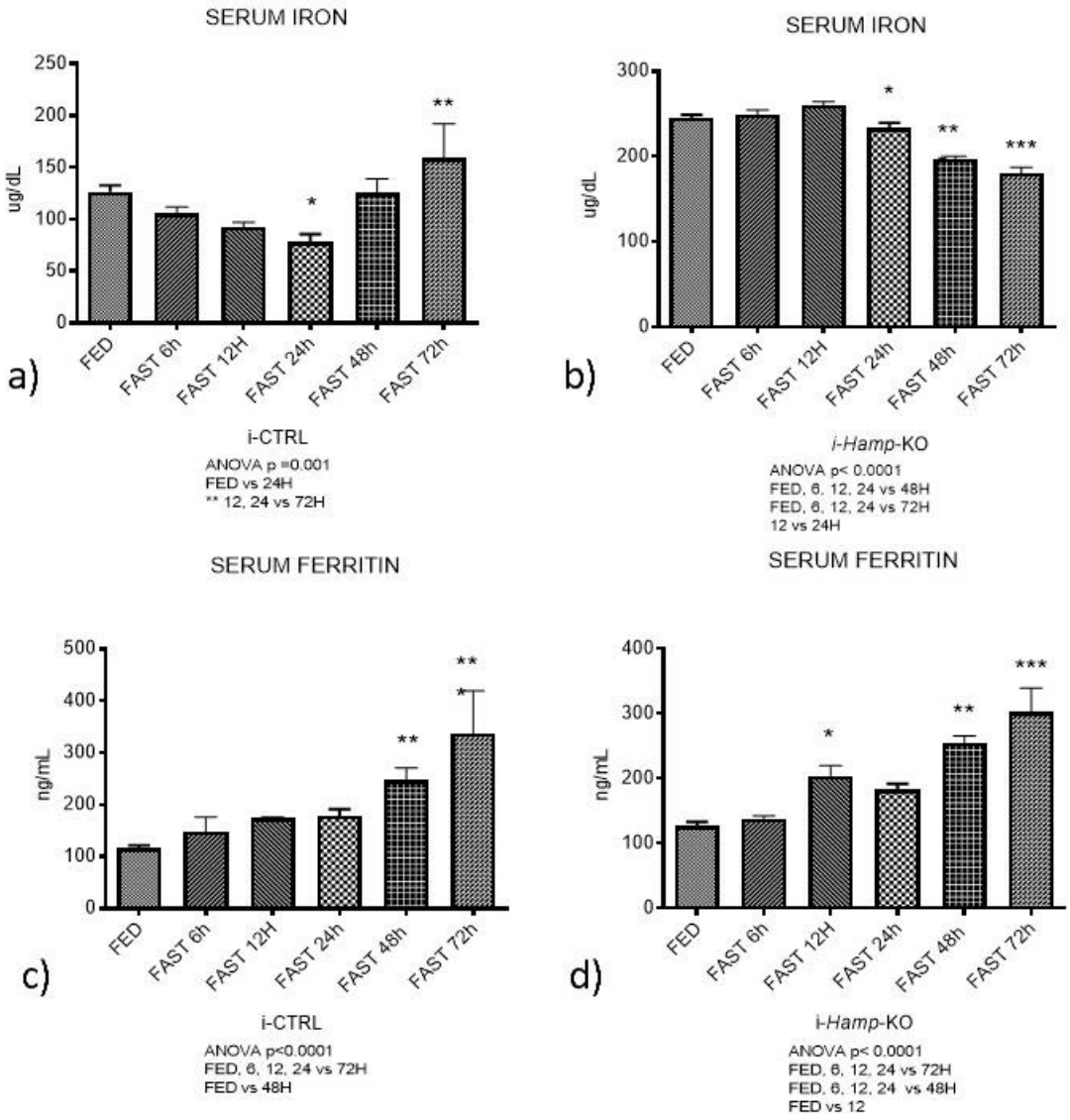

Hamp gene expression was induced in CTRL and i-CTRL mice at 6 hours and increased proportionally to the duration of fasting (Figure 15 a and 16 a), as previously reported.

Cyclic AMP-responsive element binding protein, hepatocyte specific (CREBH) is known to be induced by food deprivation and to bind to the Hamp1 promoter: *CrebH* mRNA was increased at all time points and showed maximal expression in mice that had been deprived of food for 12

and 24 hours (as previously reported). Food deprivation consistently induced *CrebH* expression compared with fed animals, similarly in *Hamp*-KO, i-*Hamp*-KO mice , CTRL and i-CTRL (Figure 15 c, d - 16, c, d; this indicates that the ability of fasting to induce *CrebH* is not affected by changes in iron homeostasis or hepcidin absence.

To dissect a possible contribution of the classic regulatory pathways, we measured *Bmp*6 and IL-6 mRNA levels.

*Bmp*6 expression in the liver, was more pronounced in *Ham*p-KO mice compared to CTRL at baseline (Figure 15 bis, a), reflecting the activation of the BMP pathways as sensor of high iron availability/load . The same was noticed also in i-*Hamp*-KO mice compared to controls (Figure 15 bis, a).

During starvation Bmp6 expression increased at 6-12 hours, then it remained increased compared to baseline (FED state) at prolonged starvation in controls (Figure 15 e, 16 e; 15 bis b, c) while in Hamp-KO and i-Hamp-KO it seemed to reduce/remain unchanged (Figure 15 f and 16 f; 15 bis b, c); this could reflect the different amount of circulating iron or a different sensitivity of the BMP6 system to iron in the hemochromatosis models compared to controls during starvation.

Despite not being fully indicative of systemic IL-6 levels, since hepatocytes can also produce IL-6 and be affected by it in a paracrine mode in response to inflammatory stimuli, we determined hepatic mRNA levels of IL-6: it seemed to be more expressed in Hamp-KO and i-Hamp-KO compared to CTRL and i-CTRL mice at baseline and during the whole experiment (Figure 15 bis, d, e, f): in Hamp-KO also significantly increased at 12 hours compared to CTRLs (Figure 15 g, h), as if absence of Hamp was associated with the activation, although minor, of hepatic inflammation, which would be maintained/worsen with starvation. However, our results do not allow to make definitive assumptions.

Figure 15. Hepatic expression of hepcidin and other genes involved in its regulation in CTRL and *Hamp*-KO mice during starvation

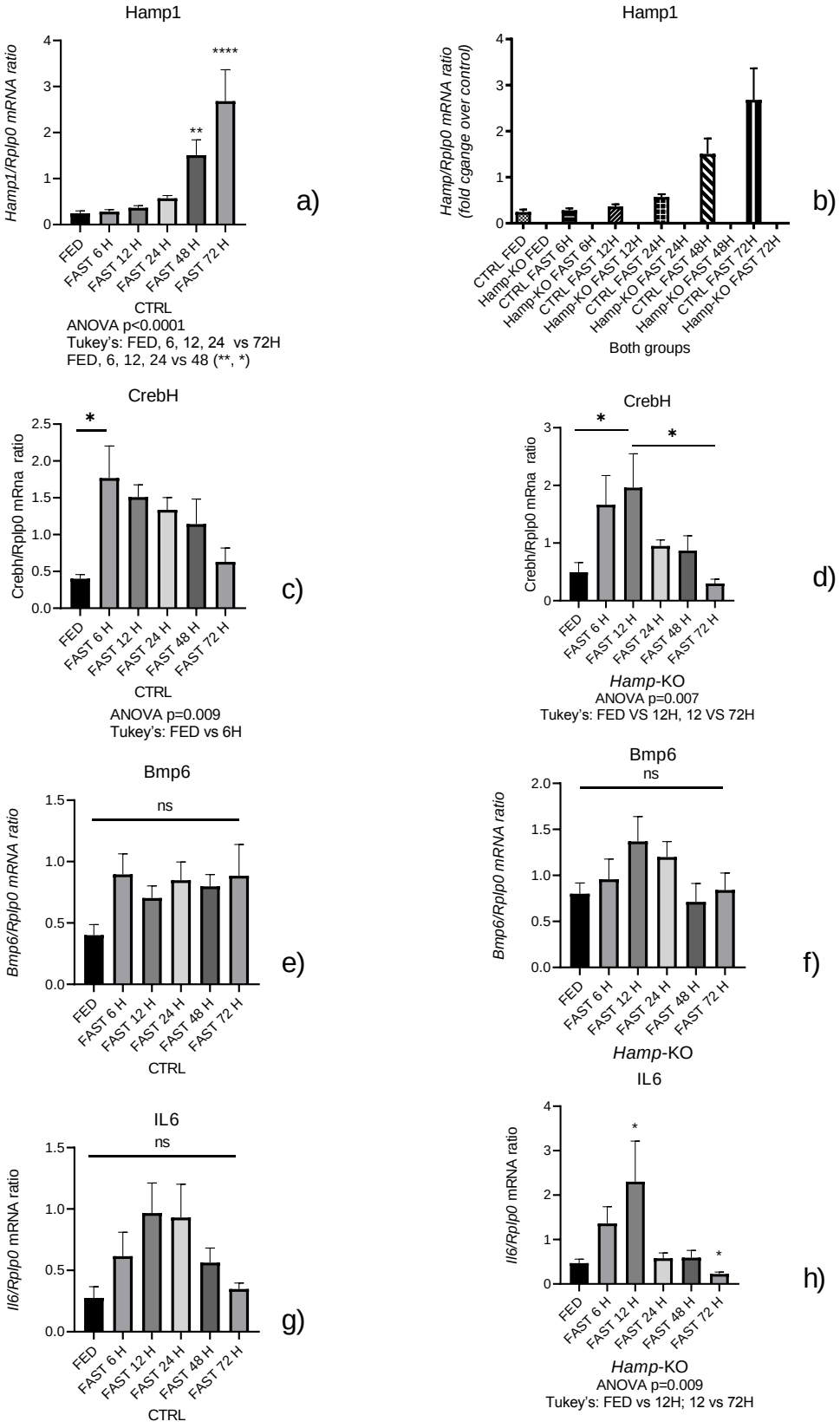

Figure 15 bis. Hepatic expression of BMP6 and IL6 in all groups at baseline and in the whole experiments

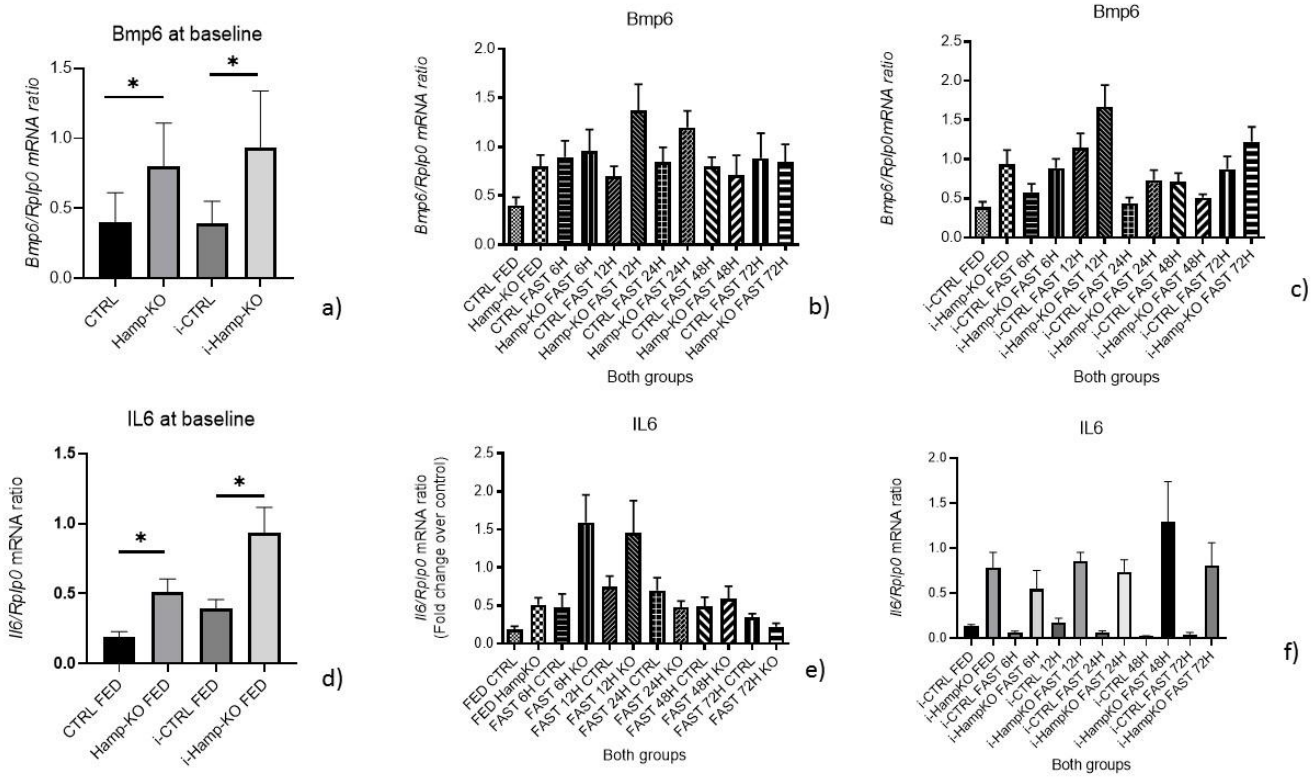

Figure 16 Hepatic expression of hepcidin and other genes involved in its regulation in CTRL and *Hamp*-KO mice during starvation

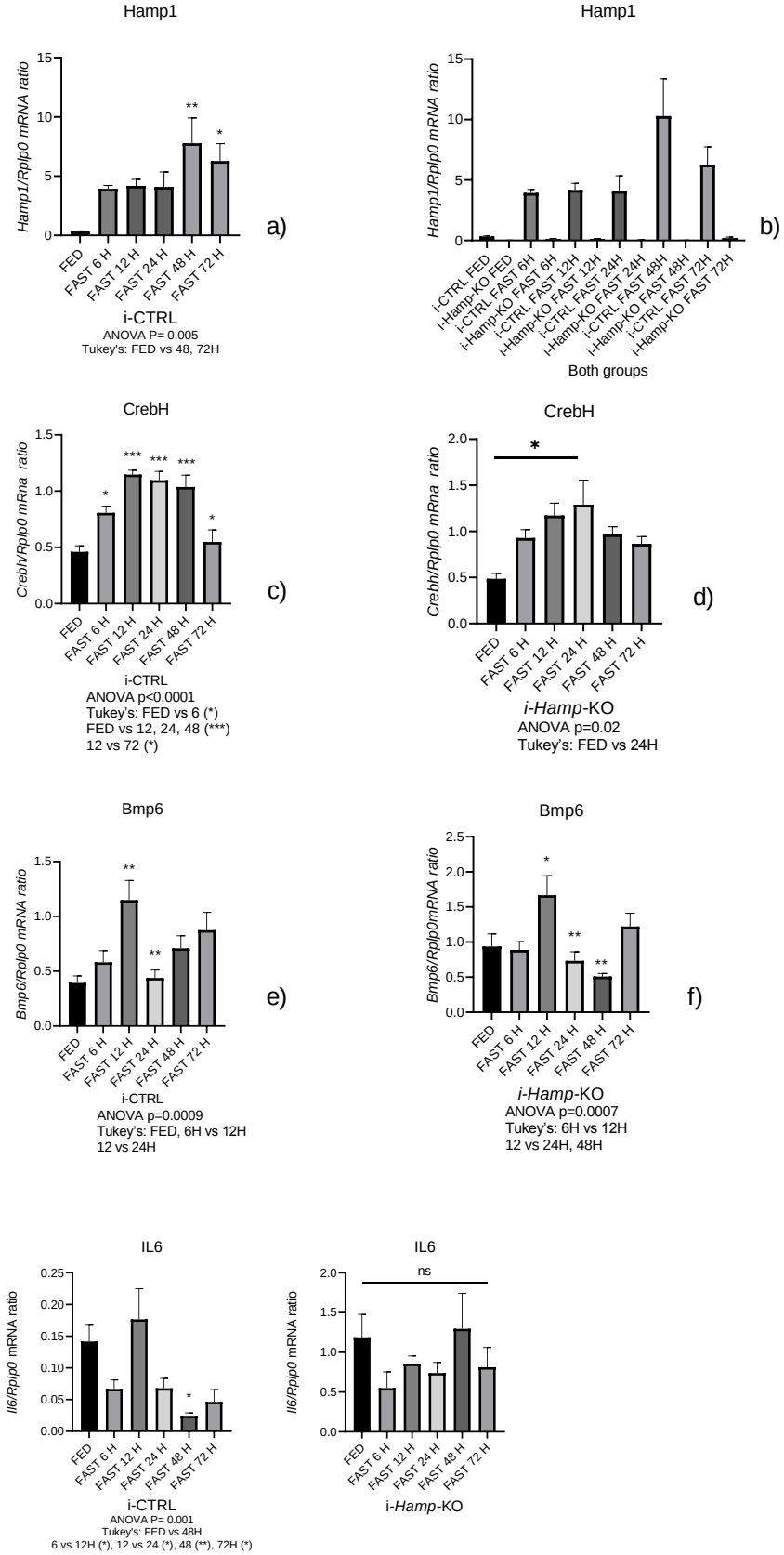

It was previously reported that, during starvation, hepatic iron levels increase and this was attributed to Hamp1 raised expression (140). In our experiment, hepatic iron increased in CTRL, wild-type mice as expected, but, surprisingly, it also increased in *Hamp*-KO mice (i.e. in the absence of hepcidin) (from 48 hours of starvation and although the iron content in the FED state was already 20 fold higher than the CTRL group) (Figure 17 a, b). This finding was maintained also when analysing i-*Hamp*-KO and i-CTRL groups (Figure 17 e, f). Such increase of iron levels, although less pronounced, was also observed in the spleen at 48 and 72 hours.

To exclude that the reported values of tissue iron might be falsely affected by the expected decrease of liver mass we corrected iron tissue levels for weight loss: excess hepatic iron, although not reaching the statistical significance, was still present in all groups at 72 hours of food deprivation. Moreover, tissue iron was measured in muscle, as a main target organ of catabolic activity during starvation: tissue iron concentration was stable in all experimental groups.

In order to explore the possible mechanism underlying tissue iron accumulation, we analysed the regulation of the main proteins and carriers responsible for cellular iron import and export.

The protein level of ferroportin, the target of hepcidin inhibitory activity, was expected to decrease on the contrary, it remained stable early during starvation and increased at 48 or 72 hours. Such stability/ increase was also found in *Hamp*-KO, i-*Hamp*-KO and i-CTRL, and is likely due to iron (Figures 18 a, b; 19 a, b). mRNA levels, on the contrary, decreased with prolonged starvation.

Figure 17. **Iron concentration in the liver and spleen in all experimental groups.**

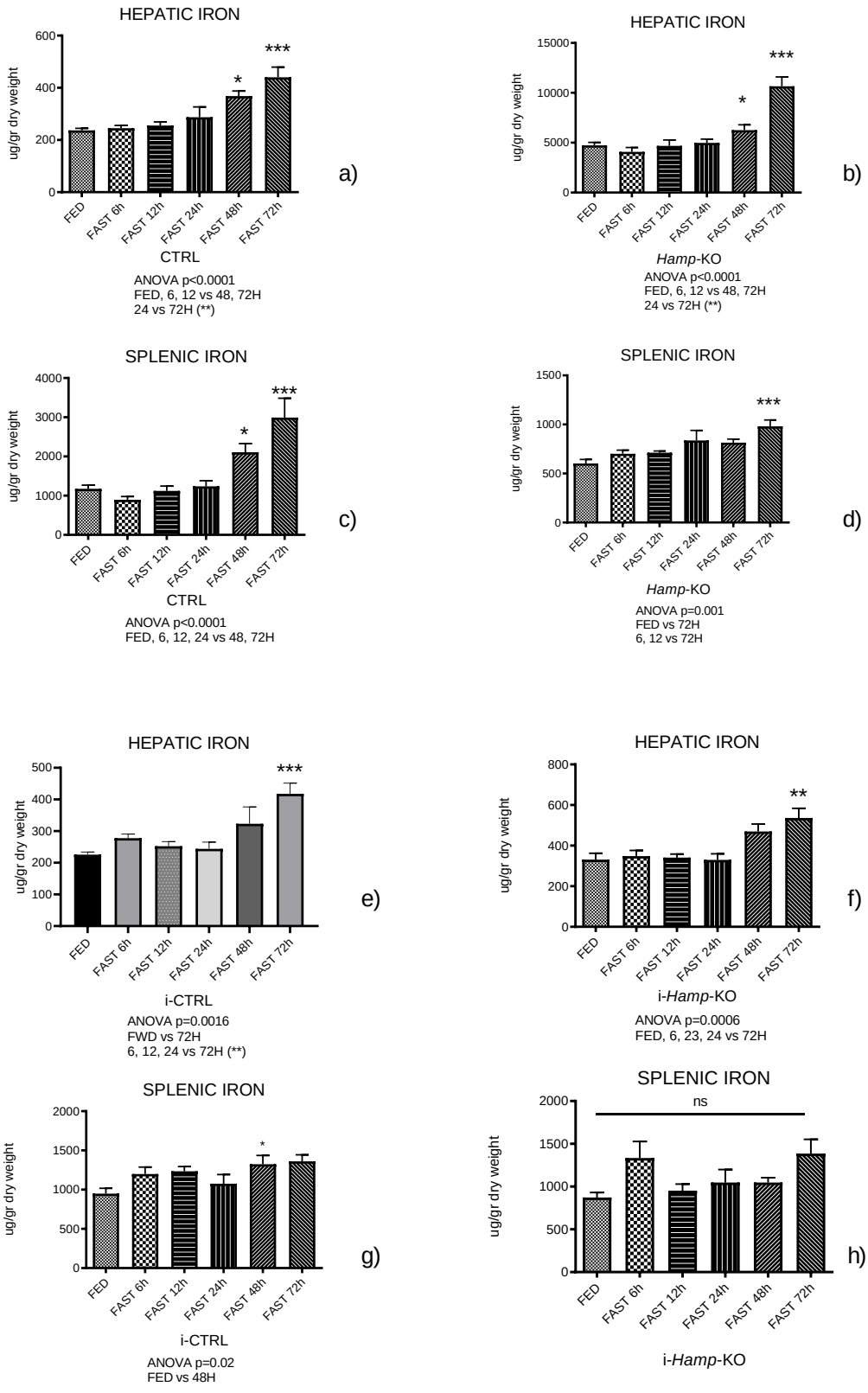

Figure 18. **Fpn in the liver of CTRL and *Hamp*-KO mice during starvation (protein, assessed at western blot and measured by densitometry, normalized by FED group) and mRNA levels**

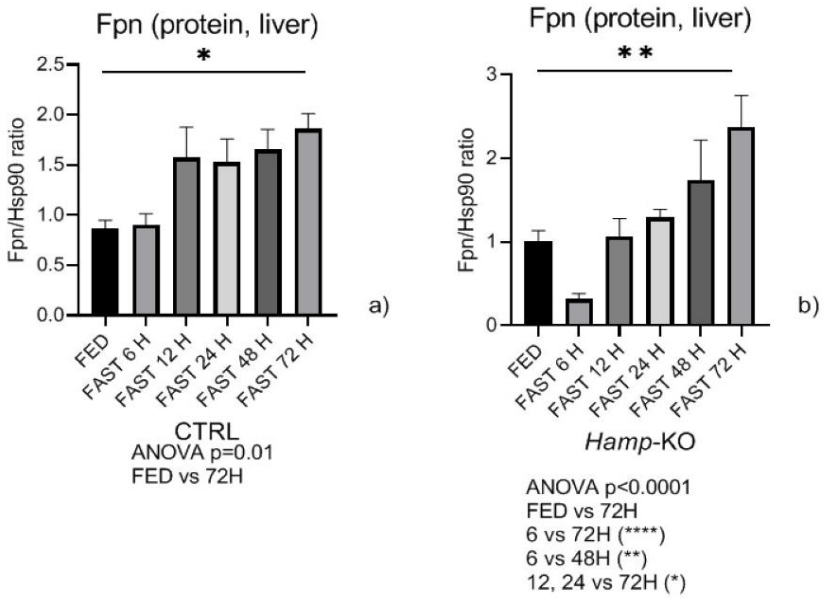

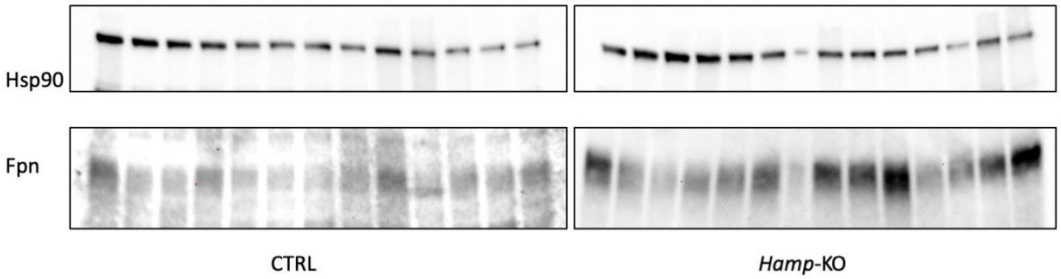

c, d)

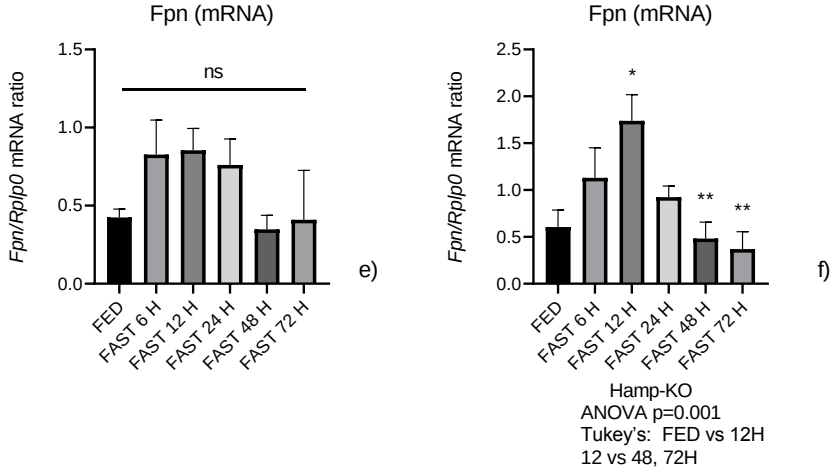

Figure 19. Fpn in the liver of i-CTRL and i-*Hamp*-KO mice during starvation (protein, assessed at western blot and measured by densitometry and normalized by FED group) and mRNA levels

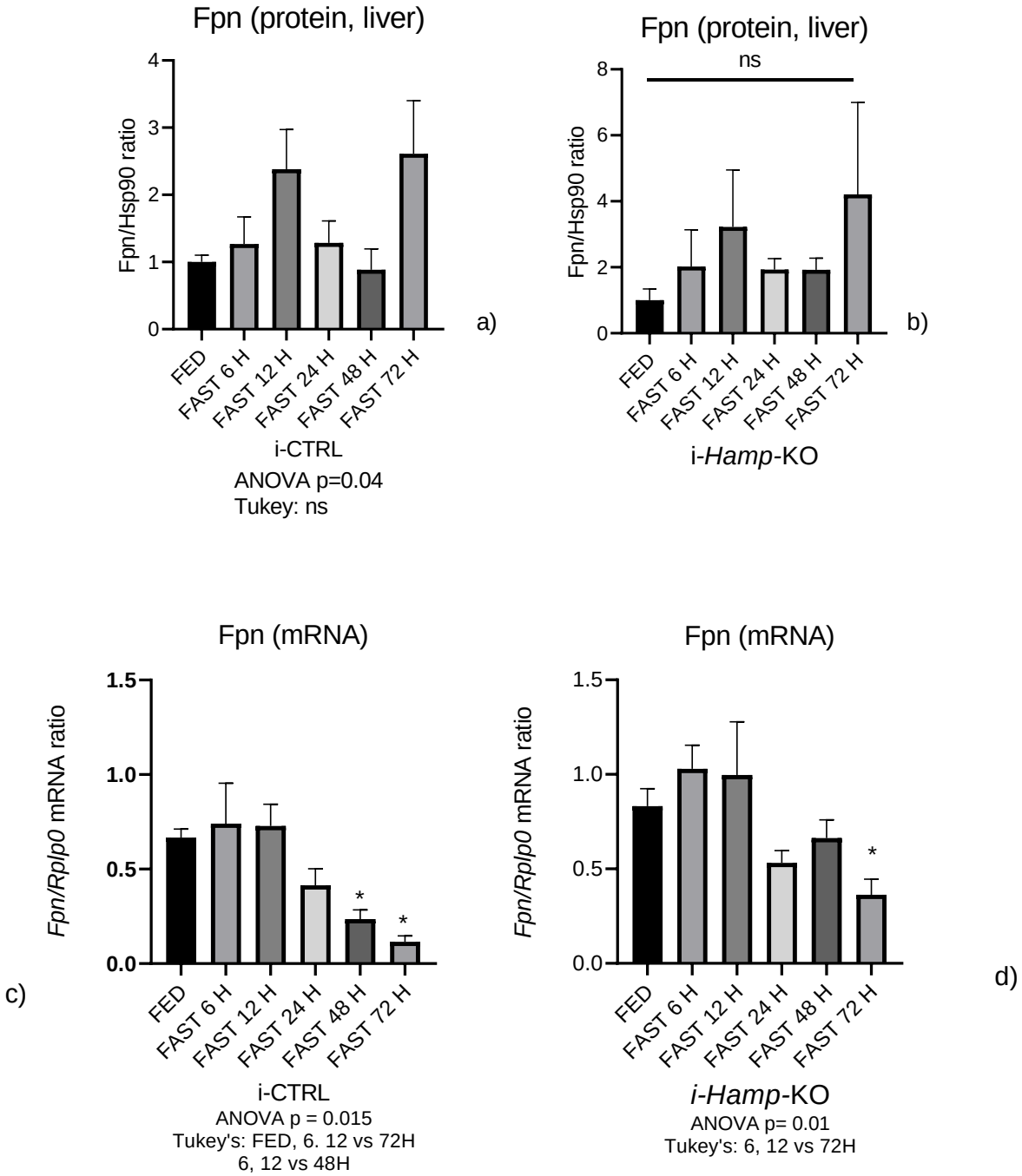

Figure 20: **Ferritin protein levels in CTRL and *Hamp*-KO, i-CTRL and i-Hamp-KO mice during starvation**

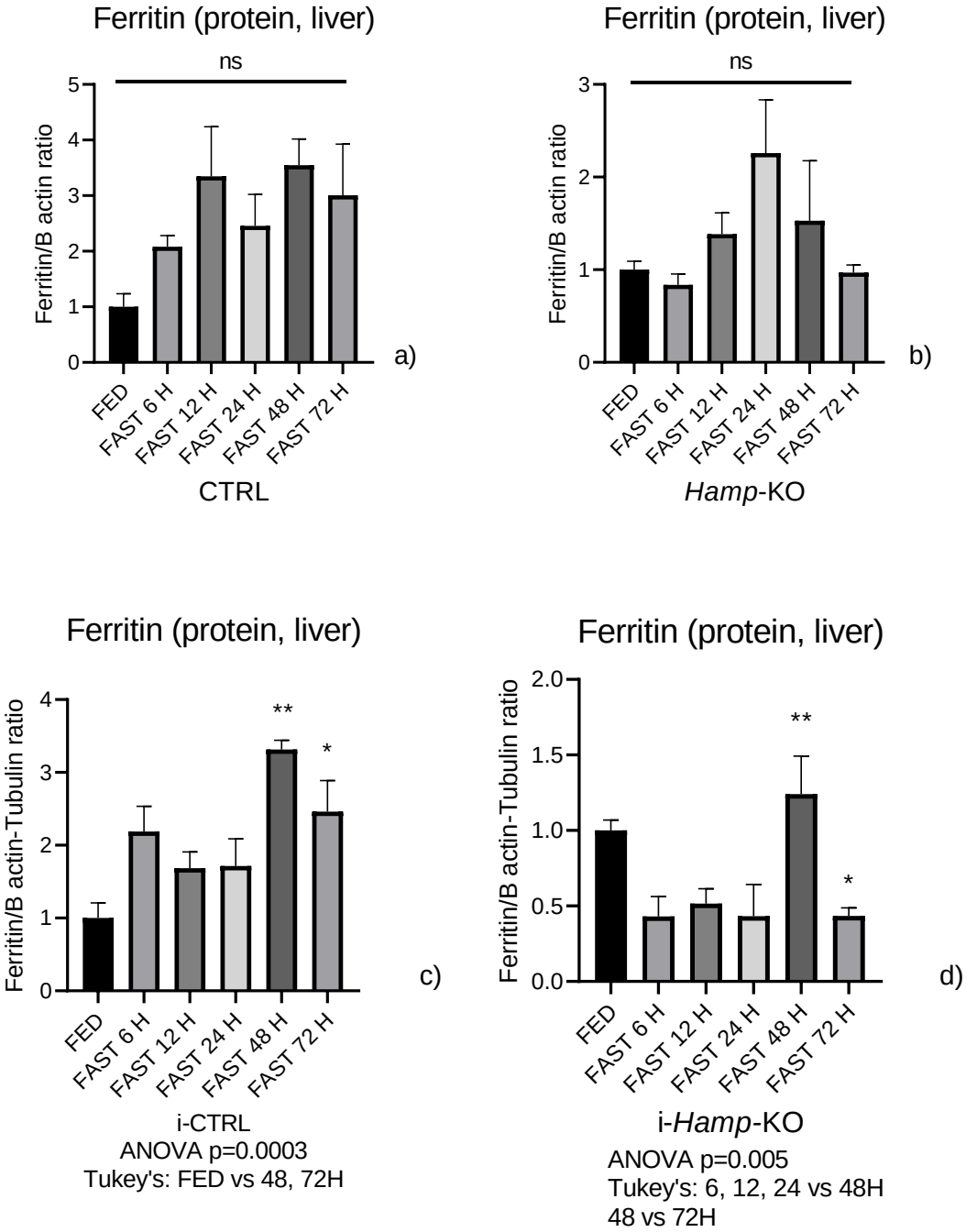

To explain the high hepatic iron concentration despite normal/increased levels of the ferroportin protein, we performed an immunofluorescence study in order to assess whether ferroportin was correctly localized at the membrane level.

In CTRL and i-CTRL FED mice ferroportin was mainly localized in the hepatocyte and Kupffer's cells cytoplasm (Figure 21 a and 22 a), and become just slightly more expressed after 24 and 48 hours starvation, respectively (Figure 21 b and 22 b), while in FED *Hamp*-KO mice it was definitively more expressed at the plasma membrane, with a slight increase after 48 hours of starvation (Figure 21 c and d).

In i-*Hamp*-KO mice, an intermediate picture was noticed in the FED state, with the ferroportin signal becoming more evident after 48 hours of starvation (Figure 22 c and d).

mRNA expression for ceruloplasmin (Cp), which is fundamental for iron export via ferroportin thanks to its ferroxidase activity, did not show appreciable alterations.

TfR1, which is in involved in cellular iron uptake and downregulated by increasing iron levels , was significantly suppressed in FED *Hamp*-KO mice compared to CTRLs (Figure 23 c); during starvation, although some discrepancies at different times, TfR1 increased progressively in CTRL ,from 6H to 72 hours in mRNA levels and from 24 to 72 hours in protein levels during starvation, particularly in CTRL mice both at the mRNA (from 6 to 72 hours, Figure 23 a) and protein level (from 24 to 72 hours, Figure 16 d). This was less apparent in *Hamp*-KO mice (Figure 23 b and e). No significant alterations were detected in i-*Hamp*-KO mice and their controls (Figure 24 a - e).

Zip14 has been described as the main hepatic importer for NTBI, a form of weakly bound iron which appears in the blood in cases of iron overload and over-saturation of transferrin capacity, such as post-transfusion hemolytic anemia). We wondered whether Zip14 modulation by starvation might explain the reported increased in liver iron accumulation. Zip14 mRNA was significantly lower in *Hamp*-KO compared to CTRLs at FED state ; it increased significantly at 72

hours in both CTRL (Figure 23 f) and i-Hamp-CTRL (Figure 24 f) mice but were not clearly indicative of a definite regulation during starvation in the other groups (Figure 23 g; Figure 24 g).

Figure 21: **IF of ferroportin in CTRL and *Hamp*-KO mice (green: Fpn in hepatocytes ; yellow: Fpn in Kupffer's cells)**

a, b

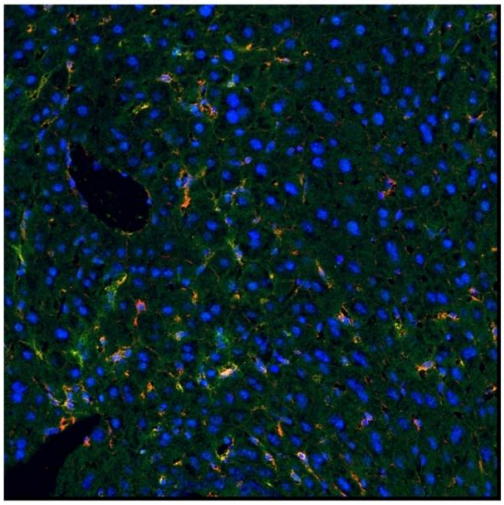

CTRL FED

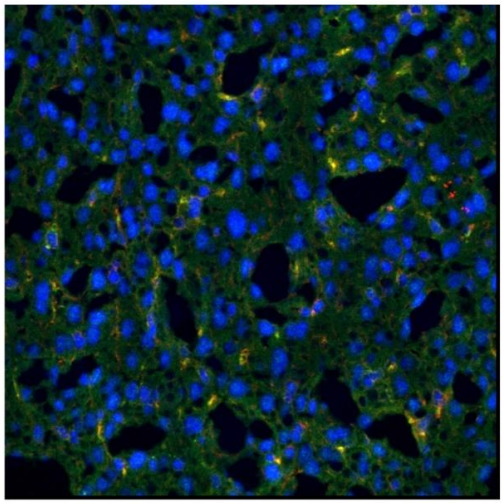

CTRL 24H

c, d

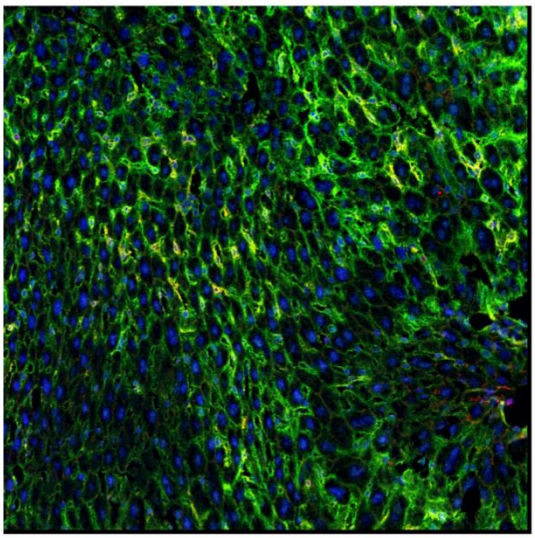

Hamp-KO FED

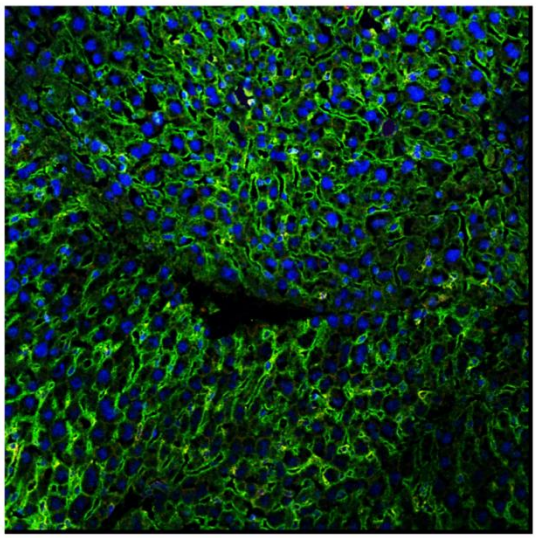

Hamp-KO FAST 48H

Figure 22: **IF of ferroportin in CTRL and *Hamp*-KO mice (green: Fpn in hepatocytes ; yellow: Fpn in Kupfer's cells)**
a, b

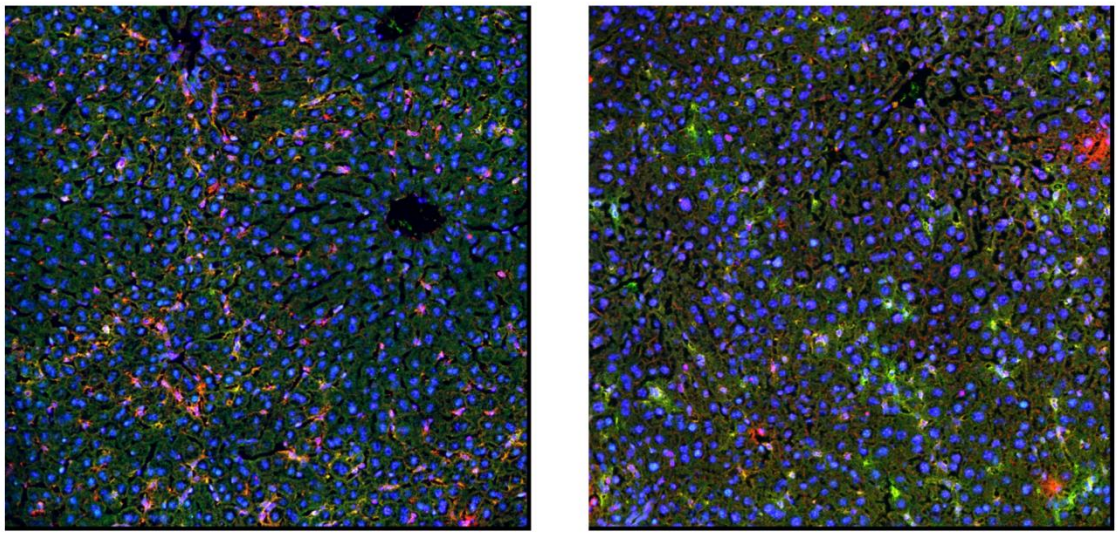

i*Hamp*-CTRL FED

i*Hamp*-CTRL FAST 48H

c, d, e

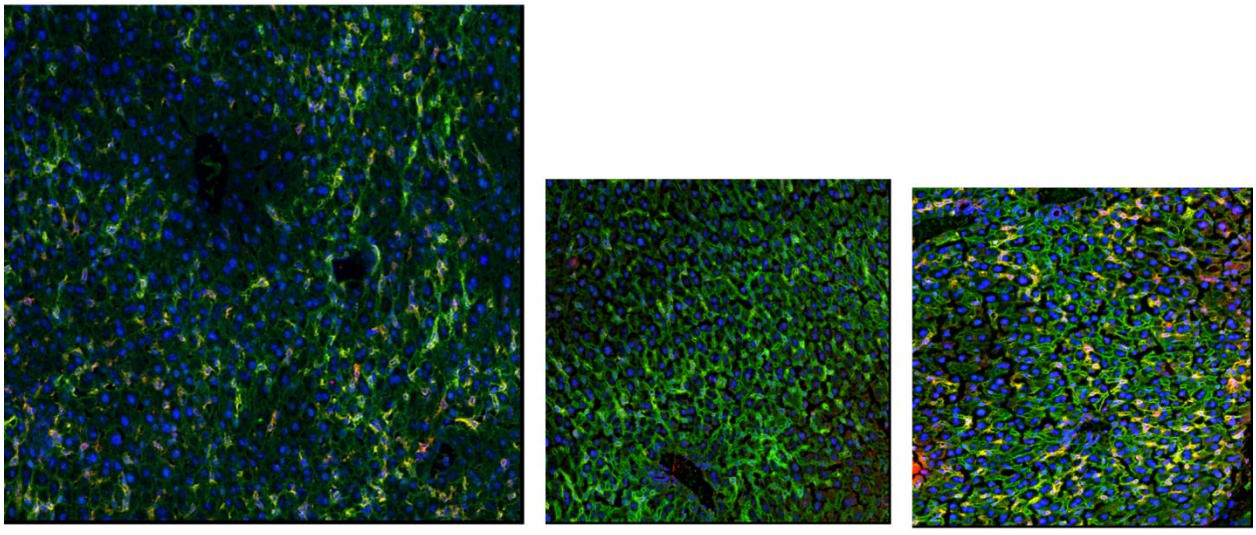

i*Hamp*-KO FED

i*Hamp*-KO FAST 48H

Figure 23. TfR1 mRNA and protein quantification and Zip14 mRNA levels in the liver of CTRL and *Hamp*-KO mice

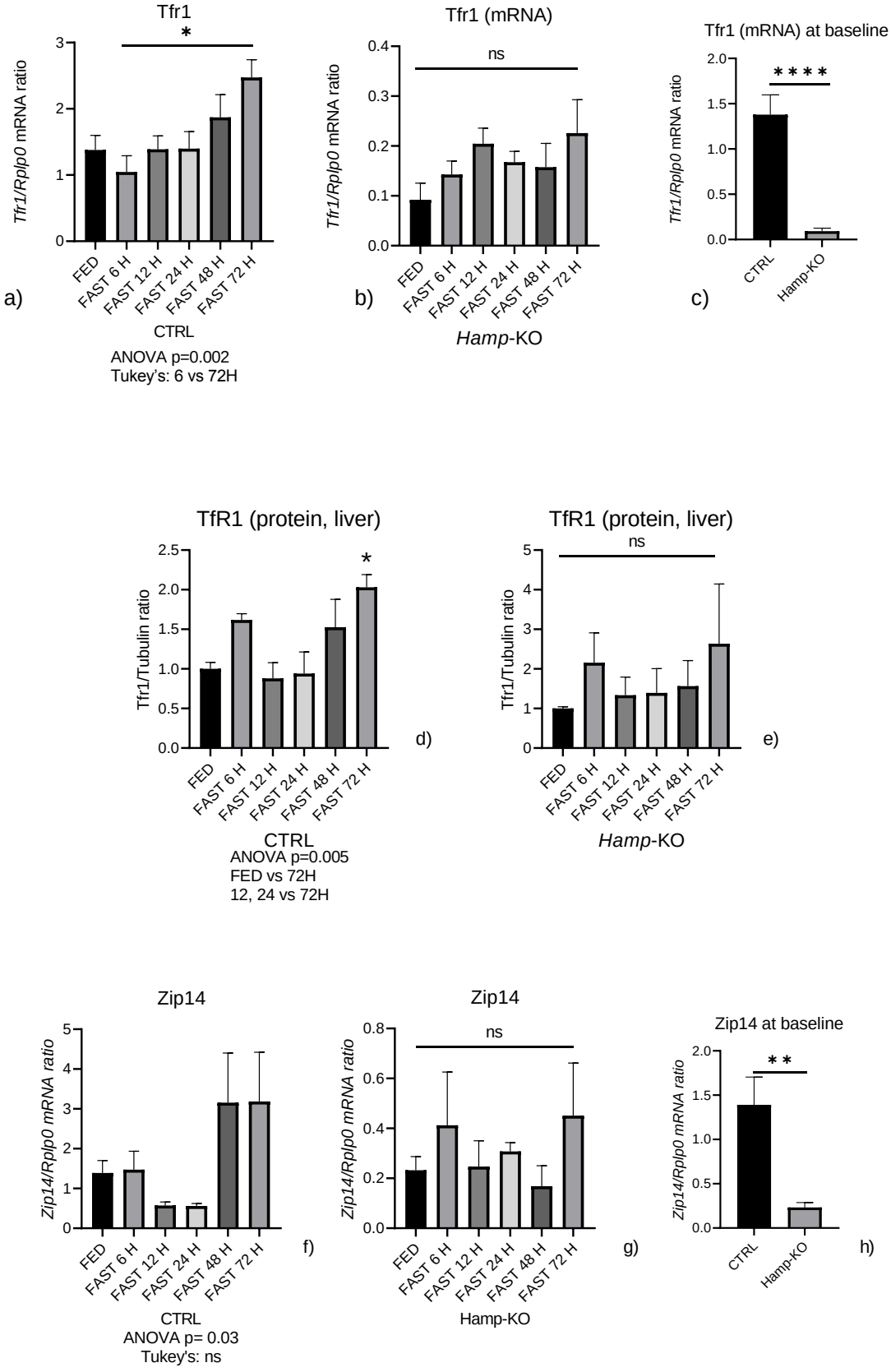

Figure 24. TfR1 mRNA and protein quantification and Zip14 mRNA levels in the liver of i-CTRL and i-*Hamp*-KO mice

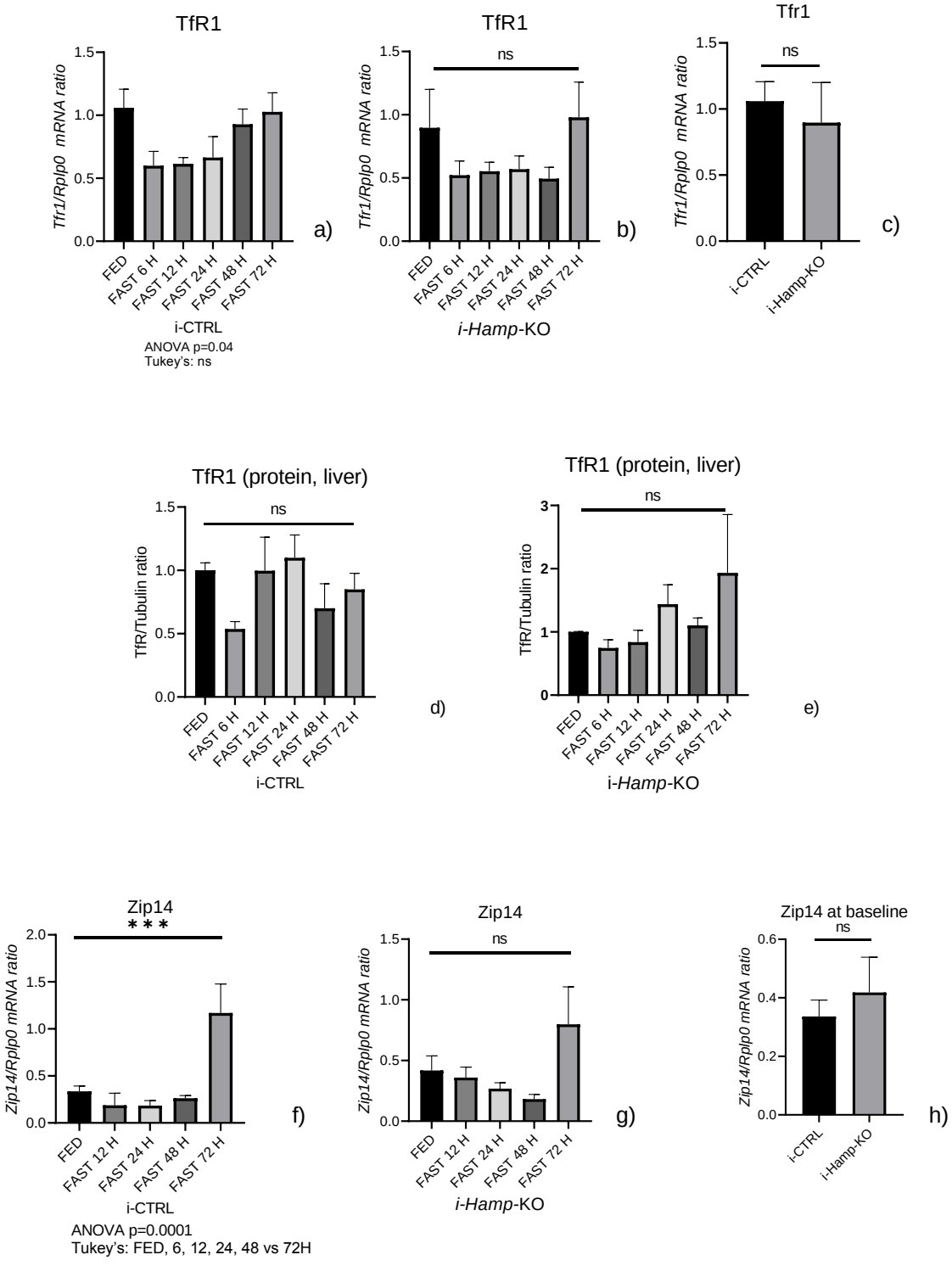

5. Discussion

It is currently well recognised that iron per se can be a co-risk factor that contributes to the progression of degenerative, chronic, inflammatory diseases (204, 205).

Moreover, the pathways which are involved in its homeostasis are actually interconnected with others which control nutritional, inflammatory, and stress-responsive mechanisms (128, 139, 152).

In this context, several studies have studied, or at least tried to unveil, the complex relationship between iron and alterations of glucose homeostasis, and more generally dysmetabolic conditions that represent the new epidemic in the western countries, such as metabolic syndrome and NAFLD (206, 207).

In NAFLD the role of iron, especially the effect hepatic iron deposit on resistance to insulin or progression of hepatic damage has been postulated (181, 193, 208), however, there is much controversy in determination of definite mechanism.

In the first part of this thesis, results of our clinical study on the role of iron in NAFLD including a population of almost 500 NAFLD patients are reported. We found that a mixed pattern of hepatic iron deposition (i.e. both in hepatocytes and RES cells) was associated with the presence of steatohepatitis, and hyperferritinemia with progressive fibrosis but not cirrhosis.

Excess iron in the liver was found in 25% of patients, in line to previous studies attesting a prevalence from 14% to 50% (203, 209, 210). Similarly, the grade of iron accumulation was always of a mild to moderate degree and never severe: this can be considered a typical characteristic of NAFLD patients with excess hepatic iron, and could possibly explain be why many studies of phlebotomy in NAFLD have failed to show a benefit or improvement in liver histology (211, 212).

An increased iron deposition in both hepatocytes and macrophages, which was the most common form (43% of patients with stainable hepatic iron, consistently with data from the

literature(209),(203),(170)), was indeed associated to the presence of NASH but not with fibrosis. This would support that NAFLD patients who display a mixed pattern of iron, which is caused by multiple factors such as genetics, local effect of inflammation on iron metabolism, leaking from dying hepatocytes and subsequent phagocytosis by liver macrophages(213), have higher probability to have a more active form of liver disease, but might still require a further stimulus to trigger and maintain fibrogenesis, as per the 'multiple hit' hypothesis (166).

When looking at markers of insulin resistance, HOMA index was significantly higher in patients with NASH, even after removing those with overt diabetes, while it was not different when considering presence and type of hepatic iron deposition (even if, consistently with their more frequent presence of NASH, patients with a mixed pattern of hepatic iron deposition tended to have higher HOMA index, although not significantly). This could suggest a positive correlation between worse insulin sensitivity, hepatic inflammation and iron deposition.

Our results are different from those previously presented by other groups. In 849 patients enrolled in the NASH CRN (203), despite similar rates of hepatic iron and mixed pattern deposition, it was only RES iron which was associated with advanced fibrosis. At variance to these data, in another study by Valenti et al (209) including 587 NAFLD patients, hepatocellular iron was associated with a 1.7-fold higher risk of fibrosis ≥F1. These discrepancies are indeed difficult to explain but could be partially due to the fact that differences linked to ethnicity and geographical provenience could play a role. In fact, preliminary data from next generation sequencing studies have shown how variants/polymorphisms of genes involved in iron metabolism, other than *HFE*, could have an impact on SF levels and hepatic iron in NAFLD patients(214, 215).

A serum ferritin (SF) higher than the upper level of normal was found in 26% of patients, and it correlated with presence of hepatic iron, particularly the mixed pattern. Similarly, in a study by Ryan et al.(216), SF correlated with liver iron determined by MRI in 51 NAFLD patients..

Interestingly, in our study SF was associated with increasing degree of steatosis but not with NASH and, more importantly, SF was not independently associated with fibrosis. Previous studies have indeed tried to understand the meaning of a raised SF in NAFLD, therefore dissecting its double role as both an acute phase protein and the protein responsible for iron storage real patients, particularly examining the role of SF as a noninvasive marker of NASH and/or fibrosis, some underlying its positive correlation with increasing fibrosis (172) (171) , others obtaining opposite results

Few studies have explored the role of diet and its influence on SF and iron levels: although there are not many solid data, the consumption of red meat or insufficient amount of vegetables, common in MetS patients, seems to be associated with higher SF levels(217). Unfortunately, we did not have such information from our cohort.

Considering our results, and the fact that ferritin levels in NAFLD patients tend to be higher than in hemochromatosis patients with the same amount of hepatic iron(218), hyperferritinemia in NAFLD might be due both to increased iron stores (without excluding the direct release by macrophage/hepatocytes in response to necrosis and inflammation-mediated mechanisms) and to the systemic inflammatory and metabolically altered status typical for these patients rather than reflect hepatic disease severity. This would be true in our NAFLD population even if raised SF was not associated with high CRP (a suboptimal marker of inflammatory activity) or single MetS components. Moreover, this would explain the reduction of SF seen in cirrhotic patients, where the extinguishing inflammation, the decrease in liver synthetic activity and the

development of portal hypertension, could concur in reducing iron adsorption and ferritin synthesis.

In conclusion, the findings presented in our clinical study would allow to identify two possible "iron signatures" in NAFLD patients: 1) hyperferritinemia is frequent, but in most cases does not associate to accumulation of iron in the liver, therefore SF likely reflects a systemic dysmetabolic/inflammatory state; 2) in a minority of patients, high SF associates with hepatic iron accumulation in RES cells and hepatocytes (mixed pattern) , who eventually develop NASH, and in such cases hepatic iron accumulation could likely be attributed to more pronounced intrahepatic necro-inflammatory events, which lead to an "iron retention phenomenon" possibly driven by hepcidin induction. Indeed, serum hepcidin was associated with serum ferritin levels but not with disease severity, but this could be due to the low number of hepcidin determinations.

The study was not built to demonstrate if increased iron and ferritin have a direct causative role in NASH, however, such hypothesis is corroborated by several studies establishing the damaging and pro-inflammatory activity of hepatocellular iron (219); and also ferritin per se could activate hepatic stellate cells involved in liver fibrosis (220). Moreover, a combined effect between iron and presence of lipid excess in the hepatocytes, which constitute steatosis hallmark, could contribute greatly to progression of the disease.

Recent research, using a myriad of model organisms, as well as data from clinical studies, has revealed links between lipid and iron metabolic pathways (221-223), but the mechanisms behind these interactions and the role these have in the progression of human diseases remains unclear.

It has recently been shown that triglycerides accumulation does not cause cellular injury in the liver; rather, FFAs or their metabolites are responsible for liver injury via increased oxidative stress (224).

In the second part of this thesis, we evaluated the possible effect of FFAs on iron homeostasis, particularly on hepcidin expression. After optimizing the protocol to induce intracellular lipid accumulation, we saw that the administration of both oleate (a monounsaturated FFA) and palmitate, a saturated fatty acid previously described as causative of lipotoxicity in NAFLD (225) , caused an increase in HAMP expression after 6 hours of treatment when at high concentration (600 microM). Moreover, such increase was more pronounced with palmitate administration but lasted more when the two FFAs were administered together. Levels of expression of inflammatory cytokines were not raised.

These data, although very preliminary, make us raise the question if certain type of FFAs could induce steatosis and upregulation of hepcidin in an inflammatory-independent way. To validate or confute such interrogative further studies are required.

Hepatic iron load in NAFLD has also been correlated to decreased insulin sensitivity (226) and its removal could potentially be beneficial in certain patients affected by obesity and NAFLD. Hepcidin has been found to be increased, correlating with hepatic iron stores, in conditions of insulin resistance such as NAFLD and MetS. Furthermore, our group has previously shown that, in condition of induced insulin resistance such as starvation (where gluconeogenesis is activated), hepcidin is up-regulated by glucogenic signals with consequent increased iron accumulation in the liver.

Patients with hereditary hemochromatosis (HH) have insufficient hepcidin activity and/or levels, and may present diabetes and metabolic alterations attributed to iron excess; on the other hand,

Hfe-KO mice (with reduced/altered hepcidin function) exhibit enhanced glucose tolerance, likely derived from increased glucose disposal that does not result from increased insulin action.

Therefore, we wondered whether, in condition of starvation, hepcidin deficiency per se independently on iron might represent a factor influencing survival and metabolic adaptation/changes.

In the final part of the thesis, a murine model of juvenile hemochromatosis (*Hamp*-KO), during short and prolonged starvation (i.e. a surrogate model of insulin resistance) was studied. In order to avoid the confounding effect of chronic iron overload associated with the classic *Hamp*-KO mouse mode, we also used an inducible *Hamp*-KO model in which the iron-loading phenotype is turned-on only during the starvation experiment (i-*Hamp*-KO).

Survival to prolonged starvation was not affected by iron overload or hepcidin deficiency; on the contrary, all registered deaths were in the control groups.

In this sense, there were no peculiar divergencies in serum nutritional parameters, although a different trend for glucose levels and gluconeogenic responsive genes was noticed: particularly, a delayed and initially blunted activation of gluconeogenesis was detected in both *Hamp*-KO and i-*Hamp*-KO mice.

Transaminases, which represent a marker, although sometimes unreliable, of hepatic injury, increased with prolonged starvation, particularly at 72 hours, without differences between the hemochromatosis murine models and their respective controls suggesting that progressive organ damage accompanies extreme starvation.

Serum iron had a different trend in *Hamp*-KO vs CTRL and in i-*Hamp*-KO vs i-CTRL mice but also in *Hamp*-KO vs *i-Hamp*-KO; this was likely due to the presence of larger amount of circulating iron in both models, much higher and stored (reaching the levels of real overload demonstrable by

Perl's staining) in the *Hamp*-KO model; both control groups showed an 'U' shaped trend, suggesting that, similarly to aminotransferases' trend, after prolonged starvation iron could be released by catabolic tissues or storage sites.

However, hepatic iron levels were actually increased in both control (CTRL and i-CTRL mice) and, quite unexpectedly, also in hepcidin-deficient mice (*Ham*p-KO and i-*Hamp*-KO), accompanied by an increase in ferritin protein and mRNA levels.

In order to study the underlying mechanisms, we studied the expression of main iron transporters in the liver. Ferroportin, which is internalised and degraded by hepcidin, was actually not decreased in control mice and remained manly localized in the cytoplasm, but was clearly increased and expressed at the cell plasma membrane in i-*Hamp*-KO and *Hamp*-KO mice during starvation, indicating that, in the absence of hepcidin, ferroportin is up-regulated, most-likely by the increasing tissue iron levels.

Based on TfR1 and Zip14 mRNA and protein expression, increased liver iron accumulation does not seem to be due to increased iron uptake.

Our findings suggest that mechanism(s), independent from hepcidin, could be involved in iron retention during starvation, as proved by hepatic iron accumulation also in hepcidin deficient murine models. Yet, in spite of its upregulation, ferroportin is apparently unable to deplete hepatocellular iron. Whether this depends on the fact that during starvation iron-retention in the liver occurs in cell compartments non-accessible to ferroportin traffic and cycling, remains to be determined.

In conclusion, such results would support that, similarly to what happens in infection and inflammation, when hepcidin induces tissue iron accumulation mainly in macrophages to limit iron availability for pathogens and support immune and anti-inflammatory response, during

starvation a similar mechanism driven by gluconeogenic signal in the liver could take place, even in the absence of hepcidin, to sustain mitochondrial activity and maintain energy balance.

BIBLIOGRAPHY

1. Abbaspour N, Hurrell R, Kelishadi R. Review on iron and its importance for human health. J Res Med Sci. 2014;19(2):164-74.

2. Dowden CW, McNeill C. A Clinical Study of Blood Iron and Hemoglobin. Trans Am Climatol Clin Assoc. 1932;48:1-21.

3. Pietrangelo A. Genetics, Genetic Testing, and Management of Hemochromatosis: 15 Years Since Hepcidin. Gastroenterology. 2015;149(5):1240-51 e4.

4. Pietrangelo A. Hereditary hemochromatosis: pathogenesis, diagnosis, and treatment. Gastroenterology. 2010;139(2):393-408, e1-2.

5. Feder JN, Gnirke A, Thomas W, Tsuchihashi Z, Ruddy DA, Basava A, et al. A novel MHC class I-like gene is mutated in patients with hereditary haemochromatosis. Nat Genet. 1996;13(4):399-408.

6. Camaschella C, Roetto A, Cali A, De Gobbi M, Garozzo G, Carella M, et al. The gene TFR2 is mutated in a new type of haemochromatosis mapping to 7q22. Nat Genet. 2000;25(1):14-5.

7. Roetto A, Papanikolaou G, Politou M, Alberti F, Girelli D, Christakis J, et al. Mutant antimicrobial peptide hepcidin is associated with severe juvenile hemochromatosis. Nat Genet. 2003;33(1):21-2.

8. Papanikolaou G, Samuels ME, Ludwig EH, MacDonald ML, Franchini PL, Dube MP, et al. Mutations in HFE2 cause iron overload in chromosome 1q-linked juvenile hemochromatosis. Nat Genet. 2004;36(1):77-82.

9. Montosi G, Donovan A, Totaro A, Garuti C, Pignatti E, Cassanelli S, et al. Autosomal-dominant hemochromatosis is associated with a mutation in the ferroportin (SLC11A3) gene. J Clin Invest. 2001;108(4):619-23.

10. Njajou OT, Vaessen N, Joosse M, Berghuis B, van Dongen JW, Breuning MH, et al. A mutation in SLC11A3 is associated with autosomal dominant hemochromatosis. Nat Genet. 2001;28(3):213-4.

11. Hentze MW, Muckenthaler MU, Andrews NC. Balancing acts: molecular control of mammalian iron metabolism. Cell. 2004;117(3):285-97.

12. Ems T, Huecker MR. Biochemistry, Iron Absorption. StatPearls. Treasure Island (FL)2019.

13. Fleming MD, Romano MA, Su MA, Garrick LM, Garrick MD, Andrews NC. Nramp2 is mutated in the anemic Belgrade (b) rat: evidence of a role for Nramp2 in endosomal iron transport. Proc Natl Acad Sci U S A. 1998;95(3):1148-53.

14. Mastrogiannaki M, Matak P, Peyssonnaux C. The gut in iron homeostasis: role of HIF-2 under normal and pathological conditions. Blood. 2013;122(6):885-92.

15. Waldvogel-Abramowski S, Waeber G, Gassner C, Buser A, Frey BM, Favrat B, et al. Physiology of iron metabolism. Transfus Med Hemother. 2014;41(3):213-21.

16. Gulec S, Anderson GJ, Collins JF. Mechanistic and regulatory aspects of intestinal iron absorption. Am J Physiol Gastrointest Liver Physiol. 2014;307(4):G397-409.

17. West AR, Oates PS. Mechanisms of heme iron absorption: current questions and controversies. World J Gastroenterol. 2008;14(26):4101-10.

18. West AR, Oates PS. Subcellular location of heme oxygenase 1 and 2 and divalent metal transporter 1 in relation to endocytotic markers during heme iron absorption. J Gastroenterol Hepatol. 2008;23(1):150-8.

19. Vanoaica L, Darshan D, Richman L, Schumann K, Kuhn LC. Intestinal ferritin H is required for an accurate control of iron absorption. Cell Metab. 2010;12(3):273-82.

20. Kovtunovych G, Ghosh MC, Ollivierre W, Weitzel RP, Eckhaus MA, Tisdale JF, et al. Wild-type macrophages reverse disease in heme oxygenase 1-deficient mice. Blood. 2014;124(9):1522-30.

21. Zhang DL, Senecal T, Ghosh MC, Ollivierre-Wilson H, Tu T, Rouault TA. Hepcidin regulates ferroportin expression and intracellular iron homeostasis of erythroblasts. Blood. 2011;118(10):2868-77.

22. de Back DZ, Kostova EB, van Kraaij M, van den Berg TK, van Bruggen R. Of macrophages and red blood cells; a complex love story. Front Physiol. 2014;5:9.

23. Theurl I, Hilgendorf I, Nairz M, Tymoszuk P, Haschka D, Asshoff M, et al. On-demand erythrocyte disposal and iron recycling requires transient macrophages in the liver. Nat Med. 2016;22(8):945-51.

24. Donovan A, Lima CA, Pinkus JL, Pinkus GS, Zon LI, Robine S, et al. The iron exporter ferroportin/Slc40a1 is essential for iron homeostasis. Cell Metab. 2005;1(3):191-200.

25. Ward DM, Kaplan J. Ferroportin-mediated iron transport: expression and regulation. Biochim Biophys Acta. 2012;1823(9):1426-33.

26. Taniguchi R, Kato HE, Font J, Deshpande CN, Wada M, Ito K, et al. Outward- and inward-facing structures of a putative bacterial transition-metal transporter with homology to ferroportin. Nat Commun. 2015;6:8545.

27. Nemeth E, Tuttle MS, Powelson J, Vaughn MB, Donovan A, Ward DM, et al. Hepcidin regulates cellular iron efflux by binding to ferroportin and inducing its internalization. Science. 2004;306(5704):2090-3.

28. Fuqua BK, Lu Y, Darshan D, Frazer DM, Wilkins SJ, Wolkow N, et al. The multicopper ferroxidase hephaestin enhances intestinal iron absorption in mice. PLoS One. 2014;9(6):e98792.

29. Harris ZL, Durley AP, Man TK, Gitlin JD. Targeted gene disruption reveals an essential role for ceruloplasmin in cellular iron efflux. Proc Natl Acad Sci U S A. 1999;96(19):10812-7.

30. Thorstensen K, Romslo I. The role of transferrin in the mechanism of cellular iron uptake. Biochem J. 1990;271(1):1-9.

31. Grossmann JG, Neu M, Evans RW, Lindley PF, Appel H, Hasnain SS. Metal-induced conformational changes in transferrins. J Mol Biol. 1993;229(3):585-90.

32. Grossmann JG, Neu M, Pantos E, Schwab FJ, Evans RW, Townes-Andrews E, et al. X-ray solution scattering reveals conformational changes upon iron uptake in lactoferrin, serum and ovo-transferrins. J Mol Biol. 1992;225(3):811-9.

33. Gerstein M, Anderson BF, Norris GE, Baker EN, Lesk AM, Chothia C. Domain closure in lactoferrin. Two hinges produce a see-saw motion between alternative close-packed interfaces. J Mol Biol. 1993;234(2):357-72.

34. Dubljevic V, Sali A, Goding JW. A conserved RGD (Arg-Gly-Asp) motif in the transferrin receptor is required for binding to transferrin. Biochem J. 1999;341 (Pt 1):11-4.

35. Cheng Y, Zak O, Aisen P, Harrison SC, Walz T. Structure of the human transferrin receptor-transferrin complex. Cell. 2004;116(4):565-76.

36. Kawabata H, Yang R, Hirama T, Vuong PT, Kawano S, Gombart AF, et al. Molecular cloning of transferrin receptor 2. A new member of the transferrin receptor-like family. J Biol Chem. 1999;274(30):20826-32.

37. Camaschella C, Roetto A, De Gobbi M. Genetic haemochromatosis: genes and mutations associated with iron loading. Best Pract Res Clin Haematol. 2002;15(2):261-76.

38. West AP, Jr., Bennett MJ, Sellers VM, Andrews NC, Enns CA, Bjorkman PJ. Comparison of the interactions of transferrin receptor and transferrin receptor 2 with transferrin and the hereditary hemochromatosis protein HFE. J Biol Chem. 2000;275(49):38135-8.

39. Levy JE, Jin O, Fujiwara Y, Kuo F, Andrews NC. Transferrin receptor is necessary for development of erythrocytes and the nervous system. Nat Genet. 1999;21(4):396-9.

40. Fleming RE, Ahmann JR, Migas MC, Waheed A, Koeffler HP, Kawabata H, et al. Targeted mutagenesis of the murine transferrin receptor-2 gene produces hemochromatosis. Proc Natl Acad Sci U S A. 2002;99(16):10653-8.

41. Casey JL, Hentze MW, Koeller DM, Caughman SW, Rouault TA, Klausner RD, et al. Iron-responsive elements: regulatory RNA sequences that control mRNA levels and translation. Science. 1988;240(4854):924-8.

42. Hentze MW, Kuhn LC. Molecular control of vertebrate iron metabolism: mRNA-based regulatory circuits operated by iron, nitric oxide, and oxidative stress. Proc Natl Acad Sci U S A. 1996;93(16):8175-82.

43. Wenger RH, Stiehl DP, Camenisch G. Integration of oxygen signaling at the consensus HRE. Sci STKE. 2005;2005(306):re12.

44. Fleming RE, Migas MC, Holden CC, Waheed A, Britton RS, Tomatsu S, et al. Transferrin receptor 2: continued expression in mouse liver in the face of iron overload and in hereditary hemochromatosis. Proc Natl Acad Sci U S A. 2000;97(5):2214-9.

45. Waheed A, Parkkila S, Saarnio J, Fleming RE, Zhou XY, Tomatsu S, et al. Association of HFE protein with transferrin receptor in crypt enterocytes of human duodenum. Proc Natl Acad Sci U S A. 1999;96(4):1579-84.

46. Johnson MB, Enns CA. Diferric transferrin regulates transferrin receptor 2 protein stability. Blood. 2004;104(13):4287-93.

47. Worwood M, Brook JD, Cragg SJ, Hellkuhl B, Jones BM, Perera P, et al. Assignment of human ferritin genes to chromosomes 11 and 19q13.3----19qter. Hum Genet. 1985;69(4):371-4.

48. Harrison PM, Arosio P. The ferritins: molecular properties, iron storage function and cellular regulation. Biochim Biophys Acta. 1996;1275(3):161-203.

49. Lawson DM, Treffry A, Artymiuk PJ, Harrison PM, Yewdall SJ, Luzzago A, et al. Identification of the ferroxidase centre in ferritin. FEBS Lett. 1989;254(1-2):207-10.

50. Arosio P, Levi S. Ferritin, iron homeostasis, and oxidative damage. Free Radic Biol Med. 2002;33(4):457-63.

51. Arosio P, Yokota M, Drysdale JW. Structural and immunological relationships of isoferritins in normal and malignant cells. Cancer Res. 1976;36(5):1735-9.

52. Cozzi A, Corsi B, Levi S, Santambrogio P, Albertini A, Arosio P. Overexpression of wild type and mutated human ferritin H-chain in HeLa cells: in vivo role of ferritin ferroxidase activity. J Biol Chem. 2000;275(33):25122-9.

53. Cozzi A, Corsi B, Levi S, Santambrogio P, Biasiotto G, Arosio P. Analysis of the biologic functions of H- and L-ferritins in HeLa cells by transfection with siRNAs and cDNAs: evidence for a proliferative role of L-ferritin. Blood. 2004;103(6):2377-83.

54. Epsztejn S, Glickstein H, Picard V, Slotki IN, Breuer W, Beaumont C, et al. H-ferritin subunit overexpression in erythroid cells reduces the oxidative stress response and induces multidrug resistance properties. Blood. 1999;94(10):3593-603.

55. Kaur D, Yantiri F, Rajagopalan S, Kumar J, Mo JQ, Boonplueang R, et al. Genetic or pharmacological iron chelation prevents MPTP-induced neurotoxicity in vivo: a novel therapy for Parkinson's disease. Neuron. 2003;37(6):899-909.

56. Orino K, Lehman L, Tsuji Y, Ayaki H, Torti SV, Torti FM. Ferritin and the response to oxidative stress. Biochem J. 2001;357(Pt 1):241-7.

57. Pham CG, Bubici C, Zazzeroni F, Papa S, Jones J, Alvarez K, et al. Ferritin heavy chain upregulation by NF-kappaB inhibits TNFalpha-induced apoptosis by suppressing reactive oxygen species. Cell. 2004;119(4):529-42.

58. Tsuji Y, Ayaki H, Whitman SP, Morrow CS, Torti SV, Torti FM. Coordinate transcriptional and translational regulation of ferritin in response to oxidative stress. Mol Cell Biol. 2000;20(16):5818-27.

59. Rushmore TH, Morton MR, Pickett CB. The antioxidant responsive element. Activation by oxidative stress and identification of the DNA consensus sequence required for functional activity. J Biol Chem. 1991;266(18):11632-9.

60. Larson JA, Howie HL, So M. Neisseria meningitidis accelerates ferritin degradation in host epithelial cells to yield an essential iron source. Mol Microbiol. 2004;53(3):807-20.

61. Ollinger K, Roberg K. Nutrient deprivation of cultured rat hepatocytes increases the desferrioxamine-available iron pool and augments the sensitivity to hydrogen peroxide. J Biol Chem. 1997;272(38):23707-11.

62. Konijn AM, Glickstein H, Vaisman B, Meyron-Holtz EG, Slotki IN, Cabantchik ZI. The cellular labile iron pool and intracellular ferritin in K562 cells. Blood. 1999;94(6):2128-34.

63. Goossen B, Caughman SW, Harford JB, Klausner RD, Hentze MW. Translational repression by a complex between the iron-responsive element of ferritin mRNA and its specific cytoplasmic binding protein is position-dependent in vivo. EMBO J. 1990;9(12):4127-33.

64. Hentze MW, Caughman SW, Rouault TA, Barriocanal JG, Dancis A, Harford JB, et al. Identification of the iron-responsive element for the translational regulation of human ferritin mRNA. Science. 1987;238(4833):1570-3.

65. Rouault TA, Hentze MW, Caughman SW, Harford JB, Klausner RD. Binding of a cytosolic protein to the iron-responsive element of human ferritin messenger RNA. Science. 1988;241(4870):1207-10.

66. De Domenico I, Vaughn MB, Li L, Bagley D, Musci G, Ward DM, et al. Ferroportin-mediated mobilization of ferritin iron precedes ferritin degradation by the proteasome. EMBO J. 2006;25(22):5396-404.

67. Worwood M, Dawkins S, Wagstaff M, Jacobs A. The purification and properties of ferritin from human serum. Biochem J. 1976;157(1):97-103.

68. Prieto J, Barry M, Sherlock S. Serum ferritin in patients with iron overload and with acute and chronic liver diseases. Gastroenterology. 1975;68(3):525-33.

69. Tran TN, Eubanks SK, Schaffer KJ, Zhou CY, Linder MC. Secretion of ferritin by rat hepatoma cells and its regulation by inflammatory cytokines and iron. Blood. 1997;90(12):4979-86.

70. Arranz Caso JA, Garcia Tena J, Llorens MM, Moreno R. High serum ferritin concentration in an AIDS patient with miliary tuberculosis. Clin Infect Dis. 1997;25(5):1263-4.

71. Shalitin S, Carmi D, Weintrob N, Phillip M, Miskin H, Kornreich L, et al. Serum ferritin level as a predictor of impaired growth and puberty in thalassemia major patients. Eur J Haematol. 2005;74(2):93-100.

72. Vahdat Shariatpanaahi M, Vahdat Shariatpanaahi Z, Moshtaaghi M, Shahbaazi SH, Abadi A. The relationship between depression and serum ferritin level. Eur J Clin Nutr. 2007;61(4):532-5.

73. Gray CP, Arosio P, Hersey P. Association of increased levels of heavy-chain ferritin with increased CD4+ CD25+ regulatory T-cell levels in patients with melanoma. Clin Cancer Res. 2003;9(7):2551-9.

74. Gray CP, Arosio P, Hersey P. Heavy chain ferritin activates regulatory T cells by induction of changes in dendritic cells. Blood. 2002;99(9):3326-34.

75. Adams PC, Powell LW, Halliday JW. Isolation of a human hepatic ferritin receptor. Hepatology. 1988;8(4):719-21.

76. Mack U, Powell LW, Halliday JW. Detection and isolation of a hepatic membrane receptor for ferritin. J Biol Chem. 1983;258(8):4672-5.

77. Crichton R. Inorganic Biochemistry of Iron Metabolism: From Molecular Mechanisms to Clinical Consequences. Second ed. New York: John Wiley & Sons Ltd; 2001 2001. 325 p.

78. Kakhlon O, Cabantchik ZI. The labile iron pool: characterization, measurement, and participation in cellular processes(1). Free Radic Biol Med. 2002;33(8):1037-46.

79. Zhang Z, Zhang F, Guo X, An P, Tao Y, Wang F. Ferroportin1 in hepatocytes and macrophages is required for the efficient mobilization of body iron stores in mice. Hepatology. 2012;56(3):961-71.

80. Delaby C, Pilard N, Puy H, Canonne-Hergaux F. Sequential regulation of ferroportin expression after erythrophagocytosis in murine macrophages: early mRNA induction by haem, followed by iron-dependent protein expression. Biochem J. 2008;411(1):123-31.

81. Marro S, Chiabrando D, Messana E, Stolte J, Turco E, Tolosano E, et al. Heme controls ferroportin1 (FPN1) transcription involving Bach1, Nrf2 and a MARE/ARE sequence motif at position -7007 of the FPN1 promoter. Haematologica. 2010;95(8):1261-8.

82. Harada N, Kanayama M, Maruyama A, Yoshida A, Tazumi K, Hosoya T, et al. Nrf2 regulates ferroportin 1-mediated iron efflux and counteracts lipopolysaccharide-induced ferroportin 1 mRNA suppression in macrophages. Arch Biochem Biophys. 2011;508(1):101-9.

83. Lymboussaki A, Pignatti E, Montosi G, Garuti C, Haile DJ, Pietrangelo A. The role of the iron responsive element in the control of ferroportin1/IREG1/MTP1 gene expression. J Hepatol. 2003;39(5):710-5.

84. Sangokoya C, Doss JF, Chi JT. Iron-responsive miR-485-3p regulates cellular iron homeostasis by targeting ferroportin. PLoS Genet. 2013;9(4):e1003408.

85. Taylor M, Qu A, Anderson ER, Matsubara T, Martin A, Gonzalez FJ, et al. Hypoxia-inducible factor-2alpha mediates the adaptive increase of intestinal ferroportin during iron deficiency in mice. Gastroenterology. 2011;140(7):2044-55.

86. Shah YM, Matsubara T, Ito S, Yim SH, Gonzalez FJ. Intestinal hypoxia-inducible transcription factors are essential for iron absorption following iron deficiency. Cell Metab. 2009;9(2):152-64.

87. Zhang DL, Hughes RM, Ollivierre-Wilson H, Ghosh MC, Rouault TA. A ferroportin transcript that lacks an iron-responsive element enables duodenal and erythroid precursor cells to evade translational repression. Cell Metab. 2009;9(5):461-73.

88. Anderson ER, Taylor M, Xue X, Ramakrishnan SK, Martin A, Xie L, et al. Intestinal HIF2alpha promotes tissue-iron accumulation in disorders of iron overload with anemia. Proc Natl Acad Sci U S A. 2013;110(50):E4922-30.

89. Liu XB, Nguyen NB, Marquess KD, Yang F, Haile DJ. Regulation of hepcidin and ferroportin expression by lipopolysaccharide in splenic macrophages. Blood Cells Mol Dis. 2005;35(1):47-56.

90. Yang F, Liu XB, Quinones M, Melby PC, Ghio A, Haile DJ. Regulation of reticuloendothelial iron transporter MTP1 (Slc11a3) by inflammation. J Biol Chem. 2002;277(42):39786-91.

91. Ludwiczek S, Aigner E, Theurl I, Weiss G. Cytokine-mediated regulation of iron transport in human monocytic cells. Blood. 2003;101(10):4148-54.

92. Arezes J, Jung G, Gabayan V, Valore E, Ruchala P, Gulig PA, et al. Hepcidin-induced hypoferremia is a critical host defense mechanism against the siderophilic bacterium Vibrio vulnificus. Cell Host Microbe. 2015;17(1):47-57.

93. Kohyama M, Ise W, Edelson BT, Wilker PR, Hildner K, Mejia C, et al. Role for Spi-C in the development of red pulp macrophages and splenic iron homeostasis. Nature. 2009;457(7227):318-21.

94. Haldar M, Kohyama M, So AY, Kc W, Wu X, Briseno CG, et al. Heme-mediated SPI-C induction promotes monocyte differentiation into iron-recycling macrophages. Cell. 2014;156(6):1223-34.

95. Mosser DM, Edwards JP. Exploring the full spectrum of macrophage activation. Nat Rev Immunol. 2008;8(12):958-69.

96. Corna G, Campana L, Pignatti E, Castiglioni A, Tagliafico E, Bosurgi L, et al. Polarization dictates iron handling by inflammatory and alternatively activated macrophages. Haematologica. 2010;95(11):1814-22.

97. Recalcati S, Locati M, Marini A, Santambrogio P, Zaninotto F, De Pizzol M, et al. Differential regulation of iron homeostasis during human macrophage polarized activation. Eur J Immunol. 2010;40(3):824-35.

98. Vallelian F, Schaer CA, Kaempfer T, Gehrig P, Duerst E, Schoedon G, et al. Glucocorticoid treatment skews human monocyte differentiation into a hemoglobin-clearance phenotype with enhanced heme-iron recycling and antioxidant capacity. Blood. 2010;116(24):5347-56.

99. Drakesmith H, Nemeth E, Ganz T. Ironing out Ferroportin. Cell Metab. 2015;22(5):777-87.

100. Krause A, Sillard R, Kleemeier B, Kluver E, Maronde E, Conejo-Garcia JR, et al. Isolation and biochemical characterization of LEAP-2, a novel blood peptide expressed in the liver. Protein Sci. 2003;12(1):143-52.

101. Hunter HN, Fulton DB, Ganz T, Vogel HJ. The solution structure of human hepcidin, a peptide hormone with antimicrobial activity that is involved in iron uptake and hereditary hemochromatosis. J Biol Chem. 2002;277(40):37597-603.

102. Nairz M, Dichtl S, Schroll A, Haschka D, Tymoszuk P, Theurl I, et al. Iron and innate antimicrobial immunity-Depriving the pathogen, defending the host. J Trace Elem Med Biol. 2018;48:118-33.

103. Pigeon C, Ilyin G, Courselaud B, Leroyer P, Turlin B, Brissot P, et al. A new mouse liver-specific gene, encoding a protein homologous to human antimicrobial peptide hepcidin, is overexpressed during iron overload. J Biol Chem. 2001;276(11):7811-9.

104. Nicolas G, Bennoun M, Devaux I, Beaumont C, Grandchamp B, Kahn A, et al. Lack of hepcidin gene expression and severe tissue iron overload in upstream stimulatory factor 2 (USF2) knockout mice. Proc Natl Acad Sci U S A. 2001;98(15):8780-5.

105. Nicolas G, Chauvet C, Viatte L, Danan JL, Bigard X, Devaux I, et al. The gene encoding the iron regulatory peptide hepcidin is regulated by anemia, hypoxia, and inflammation. J Clin Invest. 2002;110(7):1037-44.

106. Meynard D, Babitt JL, Lin HY. The liver: conductor of systemic iron balance. Blood. 2014;123(2):168-76.

107. Casanovas G, Mleczko-Sanecka K, Altamura S, Hentze MW, Muckenthaler MU. Bone morphogenetic protein (BMP)-responsive elements located in the proximal and distal hepcidin promoter are critical for its response to HJV/BMP/SMAD. J Mol Med (Berl). 2009;87(5):471-80.

108. Canali S, Zumbrennen-Bullough KB, Core AB, Wang CY, Nairz M, Bouley R, et al. Endothelial cells produce bone morphogenetic protein 6 required for iron homeostasis in mice. Blood. 2017;129(4):405-14.

109. Wang RH, Li C, Xu X, Zheng Y, Xiao C, Zerfas P, et al. A role of SMAD4 in iron metabolism through the positive regulation of hepcidin expression. Cell Metab. 2005;2(6):399-409.

110. Miyazono K, Kamiya Y, Morikawa M. Bone morphogenetic protein receptors and signal transduction. J Biochem. 2010;147(1):35-51.

111. Nishimura R, Hata K, Ikeda F, Matsubara T, Yamashita K, Ichida F, et al. The role of Smads in BMP signaling. Front Biosci. 2003;8:s275-84.

112. Zhang AS, Anderson SA, Wang J, Yang F, DeMaster K, Ahmed R, et al. Suppression of hepatic hepcidin expression in response to acute iron deprivation is associated with an increase of matriptase-2 protein. Blood. 2011;117(5):1687-99.

113. Enns CA, Ahmed R, Wang J, Ueno A, Worthen C, Tsukamoto H, et al. Increased iron loading induces Bmp6 expression in the non-parenchymal cells of the liver independent of the BMP-signaling pathway. PLoS One. 2013;8(4):e60534.

114. Rausa M, Pagani A, Nai A, Campanella A, Gilberti ME, Apostoli P, et al. Bmp6 expression in murine liver non parenchymal cells: a mechanism to control their high iron exporter activity and protect hepatocytes from iron overload? PLoS One. 2015;10(4):e0122696.

115. Canali S, Wang CY, Zumbrennen-Bullough KB, Bayer A, Babitt JL. Bone morphogenetic protein 2 controls iron homeostasis in mice independent of Bmp6. Am J Hematol. 2017;92(11):1204-13.

116. Andriopoulos B, Jr., Corradini E, Xia Y, Faasse SA, Chen S, Grgurevic L, et al. BMP6 is a key endogenous regulator of hepcidin expression and iron metabolism. Nat Genet. 2009;41(4):482-7.

117. Meynard D, Kautz L, Darnaud V, Canonne-Hergaux F, Coppin H, Roth MP. Lack of the bone morphogenetic protein BMP6 induces massive iron overload. Nat Genet. 2009;41(4):478-81.

118. Kautz L, Meynard D, Monnier A, Darnaud V, Bouvet R, Wang RH, et al. Iron regulates phosphorylation of Smad1/5/8 and gene expression of Bmp6, Smad7, Id1, and Atoh8 in the mouse liver. Blood. 2008;112(4):1503-9.

119. Kautz L, Besson-Fournier C, Meynard D, Latour C, Roth MP, Coppin H. Iron overload induces BMP6 expression in the liver but not in the duodenum. Haematologica. 2011;96(2):199-203.

120. Lin S, Wei L, Ping Y, Xia L, Xiao S. Upregulated BMP6 pathway involved in the pathogenesis of Abeta toxicity in vivo. Neurosci Lett. 2018;664:152-9.

121. Csiszar A, Ahmad M, Smith KE, Labinskyy N, Gao Q, Kaley G, et al. Bone morphogenetic protein-2 induces proinflammatory endothelial phenotype. Am J Pathol. 2006;168(2):629-38.

122. Tsukamoto S, Mizuta T, Fujimoto M, Ohte S, Osawa K, Miyamoto A, et al. Smad9 is a new type of transcriptional regulator in bone morphogenetic protein signaling. Sci Rep. 2014;4:7596.

123. Wang CY, Core AB, Canali S, Zumbrennen-Bullough KB, Ozer S, Umans L, et al. Smad1/5 is required for erythropoietin-mediated suppression of hepcidin in mice. Blood. 2017;130(1):73-83.

124. Vujic Spasic M, Sparla R, Mleczko-Sanecka K, Migas MC, Breitkopf-Heinlein K, Dooley S, et al. Smad6 and Smad7 are co-regulated with hepcidin in mouse models of iron overload. Biochim Biophys Acta. 2013;1832(1):76-84.

125. Mleczko-Sanecka K, Casanovas G, Ragab A, Breitkopf K, Muller A, Boutros M, et al. SMAD7 controls iron metabolism as a potent inhibitor of hepcidin expression. Blood. 2010;115(13):2657-65.

126. An P, Wang H, Wu Q, Wang J, Xia Z, He X, et al. Smad7 deficiency decreases iron and haemoglobin through hepcidin up-regulation by multilayer compensatory mechanisms. J Cell Mol Med. 2018;22(6):3035-44.

127. Nemeth E, Rivera S, Gabayan V, Keller C, Taudorf S, Pedersen BK, et al. IL-6 mediates hypoferremia of inflammation by inducing the synthesis of the iron regulatory hormone hepcidin. J Clin Invest. 2004;113(9):1271-6.

128. Kanamori Y, Murakami M, Sugiyama M, Hashimoto O, Matsui T, Funaba M. Interleukin-1beta (IL-1beta) transcriptionally activates hepcidin by inducing CCAAT enhancer-binding protein delta (C/EBPdelta) expression in hepatocytes. J Biol Chem. 2017;292(24):10275-87.

129. Lee P, Peng H, Gelbart T, Wang L, Beutler E. Regulation of hepcidin transcription by interleukin-1 and interleukin-6. Proc Natl Acad Sci U S A. 2005;102(6):1906-10.

130. Nemeth E, Valore EV, Territo M, Schiller G, Lichtenstein A, Ganz T. Hepcidin, a putative mediator of anemia of inflammation, is a type II acute-phase protein. Blood. 2003;101(7):2461-3.

131. Verga Falzacappa MV, Vujic Spasic M, Kessler R, Stolte J, Hentze MW, Muckenthaler MU. STAT3 mediates hepatic hepcidin expression and its inflammatory stimulation. Blood. 2007;109(1):353-8.

132. Rodriguez R, Jung CL, Gabayan V, Deng JC, Ganz T, Nemeth E, et al. Hepcidin induction by pathogens and pathogen-derived molecules is strongly dependent on interleukin-6. Infect Immun. 2014;82(2):745-52.

133. Wallace DF, Subramaniam VN. Analysis of IL-22 contribution to hepcidin induction and hypoferremia during the response to LPS in vivo. Int Immunol. 2015;27(6):281-7.

134. Kramer F, Torzewski J, Kamenz J, Veit K, Hombach V, Dedio J, et al. Interleukin-1beta stimulates acute phase response and C-reactive protein synthesis by inducing an NFkappaB- and C/EBPbeta-dependent autocrine interleukin-6 loop. Mol Immunol. 2008;45(9):2678-89.

135. Shanmugam NK, Chen K, Cherayil BJ. Commensal Bacteria-induced Interleukin 1beta (IL-1beta) Secreted by Macrophages Up-regulates Hepcidin Expression in Hepatocytes by Activating the Bone Morphogenetic Protein Signaling Pathway. J Biol Chem. 2015;290(51):30637-47.

136. Casanovas G, Banerji A, d'Alessio F, Muckenthaler MU, Legewie S. A multi-scale model of hepcidin promoter regulation reveals factors controlling systemic iron homeostasis. PLoS Comput Biol. 2014;10(1):e1003421.

137. Besson-Fournier C, Latour C, Kautz L, Bertrand J, Ganz T, Roth MP, et al. Induction of activin B by inflammatory stimuli up-regulates expression of the iron-regulatory peptide hepcidin through Smad1/5/8 signaling. Blood. 2012;120(2):431-9.

138. Canali S, Core AB, Zumbrennen-Bullough KB, Merkulova M, Wang CY, Schneyer AL, et al. Activin B Induces Noncanonical SMAD1/5/8 Signaling via BMP Type I Receptors in Hepatocytes: Evidence for a Role in Hepcidin Induction by Inflammation in Male Mice. Endocrinology. 2016;157(3):1146-62.

139. Vecchi C, Montosi G, Zhang K, Lamberti I, Duncan SA, Kaufman RJ, et al. ER stress controls iron metabolism through induction of hepcidin. Science. 2009;325(5942):877-80.

140. Vecchi C, Montosi G, Garuti C, Corradini E, Sabelli M, Canali S, et al. Gluconeogenic signals regulate iron homeostasis via hepcidin in mice. Gastroenterology. 2014;146(4):1060-9.

141. Latour C, Kautz L, Besson-Fournier C, Island ML, Canonne-Hergaux F, Loreal O, et al. Testosterone perturbs systemic iron balance through activation of epidermal growth factor receptor signaling in the liver and repression of hepcidin. Hepatology. 2014;59(2):683-94.

142. Li X, Rhee DK, Malhotra R, Mayeur C, Hurst LA, Ager E, et al. Progesterone receptor membrane component-1 regulates hepcidin biosynthesis. J Clin Invest. 2016;126(1):389-401.

143. Sonnweber T, Nachbaur D, Schroll A, Nairz M, Seifert M, Demetz E, et al. Hypoxia induced downregulation of hepcidin is mediated by platelet derived growth factor BB. Gut. 2014;63(12):1951-9.

144. Mleczko-Sanecka K, Roche F, da Silva AR, Call D, D'Alessio F, Ragab A, et al. Unbiased RNAi screen for hepcidin regulators links hepcidin suppression to proliferative Ras/RAF and nutrient-dependent mTOR signaling. Blood. 2014;123(10):1574-85.

145. Mendler MH, Turlin B, Moirand R, Jouanolle AM, Sapey T, Guyader D, et al. Insulin resistance-associated hepatic iron overload. Gastroenterology. 1999;117(5):1155-63.

146. Turlin B, Mendler MH, Moirand R, Guyader D, Guillygomarc'h A, Deugnier Y. Histologic features of the liver in insulin resistance-associated iron overload. A study of 139 patients. Am J Clin Pathol. 2001;116(2):263-70.

147. Guillygomarc'h A, Mendler MH, Moirand R, Laine F, Quentin V, David V, et al. Venesection therapy of insulin resistance-associated hepatic iron overload. J Hepatol. 2001;35(3):344-9.

148. Wood RJ. The iron-heart disease connection: is it dead or just hiding? Ageing Res Rev. 2004;3(3):355-67.

149. Ford ES, Cogswell ME. Diabetes and serum ferritin concentration among U.S. adults. Diabetes Care. 1999;22(12):1978-83.

150. Jiang R, Manson JE, Meigs JB, Ma J, Rifai N, Hu FB. Body iron stores in relation to risk of type 2 diabetes in apparently healthy women. JAMA. 2004;291(6):711-7.

151. Iwasaki T, Nakajima A, Yoneda M, Yamada Y, Mukasa K, Fujita K, et al. Serum ferritin is associated with visceral fat area and subcutaneous fat area. Diabetes Care. 2005;28(10):2486-91.

152. Fernandez-Real JM, Lopez-Bermejo A, Ricart W. Iron stores, blood donation, and insulin sensitivity and secretion. Clin Chem. 2005;51(7):1201-5.

153. Wrede CE, Buettner R, Bollheimer LC, Scholmerich J, Palitzsch KD, Hellerbrand C. Association between serum ferritin and the insulin resistance syndrome in a representative population. Eur J Endocrinol. 2006;154(2):333-40.

154. Galan P, Noisette N, Estaquio C, Czernichow S, Mennen L, Renversez JC, et al. Serum ferritin, cardiovascular risk factors and ischaemic heart diseases: a prospective analysis in the SU.VI.MAX (SUpplementation en VItamines et Mineraux AntioXydants) cohort. Public Health Nutr. 2006;9(1):70-4.

155. Bougle D, Brouard J. Iron in child obesity. Relationships with inflammation and metabolic risk factors. Nutrients. 2013;5(6):2222-30.

156. Aigner E, Hinz C, Steiner K, Rossmann B, Pfleger J, Hohla F, et al. Iron stores, liver transaminase levels and metabolic risk in healthy teenagers. Eur J Clin Invest. 2010;40(2):155-63.

157. Ramakrishnan U, Kuklina E, Stein AD. Iron stores and cardiovascular disease risk factors in women of reproductive age in the United States. Am J Clin Nutr. 2002;76(6):1256-60.

158. Martinez-Garcia MA, Luque-Ramirez M, San-Millan JL, Escobar-Morreale HF. Body iron stores and glucose intolerance in premenopausal women: role of hyperandrogenism, insulin resistance, and genomic variants related to inflammation, oxidative stress, and iron metabolism. Diabetes Care. 2009;32(8):1525-30.

159. Luque-Ramirez M, Alvarez-Blasco F, Botella-Carretero JI, Sanchon R, San Millan JL, Escobar-Morreale HF. Increased body iron stores of obese women with polycystic ovary syndrome are a consequence of insulin resistance and hyperinsulinism and are not a result of reduced menstrual losses. Diabetes Care. 2007;30(9):2309-13.

160. Cheng HL, Bryant C, Cook R, O'Connor H, Rooney K, Steinbeck K. The relationship between obesity and hypoferraemia in adults: a systematic review. Obes Rev. 2012;13(2):150-61.

161. Bekri S, Gual P, Anty R, Luciani N, Dahman M, Ramesh B, et al. Increased adipose tissue expression of hepcidin in severe obesity is independent from diabetes and NASH. Gastroenterology. 2006;131(3):788-96.

162. Barisani D, Pelucchi S, Mariani R, Galimberti S, Trombini P, Fumagalli D, et al. Hepcidin and iron-related gene expression in subjects with Dysmetabolic Hepatic Iron Overload. J Hepatol. 2008;49(1):123-33.

163. Aigner E, Theurl I, Theurl M, Lederer D, Haufe H, Dietze O, et al. Pathways underlying iron accumulation in human nonalcoholic fatty liver disease. Am J Clin Nutr. 2008;87(5):1374-83.

164. Ratziu V, Bellentani S, Cortez-Pinto H, Day C, Marchesini G. A position statement on NAFLD/NASH based on the EASL 2009 special conference. J Hepatol. 2010;53(2):372-84.

165. Younossi ZM, Stepanova M, Negro F, Hallaji S, Younossi Y, Lam B, et al. Nonalcoholic fatty liver disease in lean individuals in the United States. Medicine (Baltimore). 2012;91(6):319-27.

166. Buzzetti E, Pinzani M, Tsochatzis EA. The multiple-hit pathogenesis of non-alcoholic fatty liver disease (NAFLD). Metabolism. 2016.

167. Ertle J, Dechene A, Sowa JP, Penndorf V, Herzer K, Kaiser G, et al. Non-alcoholic fatty liver disease progresses to hepatocellular carcinoma in the absence of apparent cirrhosis. Int J Cancer. 2011;128(10):2436-43.

168. Piscaglia F, Svegliati-Baroni G, Barchetti A, Pecorelli A, Marinelli S, Tiribelli C, et al. Clinical patterns of hepatocellular carcinoma in nonalcoholic fatty liver disease: A multicenter prospective study. Hepatology. 2016;63(3):827-38.

169. Trombini P, Piperno A. Ferritin, metabolic syndrome and NAFLD: elective attractions and dangerous liaisons. J Hepatol. 2007;46(4):549-52.

170. Ryan JD, Armitage AE, Cobbold JF, Banerjee R, Borsani O, Dongiovanni P, et al. Hepatic iron is the major determinant of serum ferritin in NAFLD patients. Liver Int. 2018;38(1):164-73.

171. Manousou P, Kalambokis G, Grillo F, Watkins J, Xirouchakis E, Pleguezuelo M, et al. Serum ferritin is a discriminant marker for both fibrosis and inflammation in histologically proven non-alcoholic fatty liver disease patients. Liver Int. 2011;31(5):730-9.

172. Kowdley KV, Belt P, Wilson LA, Yeh MM, Neuschwander-Tetri BA, Chalasani N, et al. Serum ferritin is an independent predictor of histologic severity and advanced fibrosis in patients with nonalcoholic fatty liver disease. Hepatology. 2012;55(1):77-85.

173. Yoneda M, Thomas E, Sumida Y, Imajo K, Eguchi Y, Hyogo H, et al. Clinical usage of serum ferritin to assess liver fibrosis in patients with non-alcoholic fatty liver disease: Proceed with caution. Hepatol Res. 2014;44(14):E499-502.

174. Buzzetti E, Lombardi R, De Luca L, Tsochatzis EA. Noninvasive Assessment of Fibrosis in Patients with Nonalcoholic Fatty Liver Disease. Int J Endocrinol. 2015;2015:343828.

175. Hagstrom H, Nasr P, Bottai M, Ekstedt M, Kechagias S, Hultcrantz R, et al. Elevated serum ferritin is associated with increased mortality in non-alcoholic fatty liver disease after 16 years of follow-up. Liver Int. 2016;36(11):1688-95.

176. Fargion S, Mattioli M, Fracanzani AL, Sampietro M, Tavazzi D, Fociani P, et al. Hyperferritinemia, iron overload, and multiple metabolic alterations identify patients at risk for nonalcoholic steatohepatitis. Am J Gastroenterol. 2001;96(8):2448-55.

177. George DK, Goldwurm S, MacDonald GA, Cowley LL, Walker NI, Ward PJ, et al. Increased hepatic iron concentration in nonalcoholic steatohepatitis is associated with increased fibrosis. Gastroenterology. 1998;114(2):311-8.

178. Fierbinteanu-Braticevici C, Bengus A, Neamtu M, Usvat R. The risk factors of fibrosis in nonalcoholic steatohepatitis. Rom J Intern Med. 2002;40(1-4):81-8.

179. Valenti L, Dongiovanni P, Fracanzani AL, Santorelli G, Fatta E, Bertelli C, et al. Increased susceptibility to nonalcoholic fatty liver disease in heterozygotes for the mutation responsible for hereditary hemochromatosis. Dig Liver Dis. 2003;35(3):172-8.

180. Chitturi S, Weltman M, Farrell GC, McDonald D, Kench J, Liddle C, et al. HFE mutations, hepatic iron, and fibrosis: ethnic-specific association of NASH with C282Y but not with fibrotic severity. Hepatology. 2002;36(1):142-9.

181. Bugianesi E, Manzini P, D'Antico S, Vanni E, Longo F, Leone N, et al. Relative contribution of iron burden, HFE mutations, and insulin resistance to fibrosis in nonalcoholic fatty liver. Hepatology. 2004;39(1):179-87.

182. Adams LA, Lymp JF, St Sauver J, Sanderson SO, Lindor KD, Feldstein A, et al. The natural history of nonalcoholic fatty liver disease: a population-based cohort study. Gastroenterology. 2005;129(1):113-21.

183. Valenti L, Fracanzani AL, Dongiovanni P, Bugianesi E, Marchesini G, Manzini P, et al. Iron depletion by phlebotomy improves insulin resistance in patients with nonalcoholic fatty liver disease and hyperferritinemia: evidence from a case-control study. Am J Gastroenterol. 2007;102(6):1251-8.

184. Sorrentino P, D'Angelo S, Ferbo U, Micheli P, Bracigliano A, Vecchione R. Liver iron excess in patients with hepatocellular carcinoma developed on non-alcoholic steato-hepatitis. J Hepatol. 2009;50(2):351-7.

185. Wilman HR, Parisinos CA, Atabaki-Pasdar N, Kelly M, Thomas EL, Neubauer S, et al. Genetic studies of abdominal MRI data identify genes regulating hepcidin as major determinants of liver iron concentration. J Hepatol. 2019;71(3):594-602.

186. Rametta R, Dongiovanni P, Pelusi S, Francione P, Iuculano F, Borroni V, et al. Hepcidin resistance in dysmetabolic iron overload. Liver Int. 2016;36(10):1540-8.

187. Dongiovanni P, Lanti C, Gatti S, Rametta R, Recalcati S, Maggioni M, et al. High fat diet subverts hepatocellular iron uptake determining dysmetabolic iron overload. PLoS One. 2015;10(2):e0116855.

188. Dallalio G, Law E, Means RT, Jr. Hepcidin inhibits in vitro erythroid colony formation at reduced erythropoietin concentrations. Blood. 2006;107(7):2702-4.

189. Ruivard M, Laine F, Ganz T, Olbina G, Westerman M, Nemeth E, et al. Iron absorption in dysmetabolic iron overload syndrome is decreased and correlates with increased plasma hepcidin. J Hepatol. 2009;50(6):1219-25.

190. Otogawa K, Kinoshita K, Fujii H, Sakabe M, Shiga R, Nakatani K, et al. Erythrophagocytosis by liver macrophages (Kupffer cells) promotes oxidative stress, inflammation, and fibrosis in a rabbit model of steatohepatitis: implications for the pathogenesis of human nonalcoholic steatohepatitis. Am J Pathol. 2007;170(3):967-80.

191. De Domenico I, Ward DM, di Patti MC, Jeong SY, David S, Musci G, et al. Ferroxidase activity is required for the stability of cell surface ferroportin in cells expressing GPI-ceruloplasmin. EMBO J. 2007;26(12):2823-31.

192. Aigner E, Theurl I, Haufe H, Seifert M, Hohla F, Scharinger L, et al. Copper availability contributes to iron perturbations in human nonalcoholic fatty liver disease. Gastroenterology. 2008;135(2):680-8.

193. Abraham D, Rogers J, Gault P, Kushner JP, McClain DA. Increased insulin secretory capacity but decreased insulin sensitivity after correction of iron overload by phlebotomy in hereditary haemochromatosis. Diabetologia. 2006;49(11):2546-51.

194. Furukawa S, Fujita T, Shimabukuro M, Iwaki M, Yamada Y, Nakajima Y, et al. Increased oxidative stress in obesity and its impact on metabolic syndrome. J Clin Invest. 2004;114(12):1752-61.

195. Dongiovanni P, Valenti L, Ludovica Fracanzani A, Gatti S, Cairo G, Fargion S. Iron depletion by deferoxamine up-regulates glucose uptake and insulin signaling in hepatoma cells and in rat liver. Am J Pathol. 2008;172(3):738-47.

196. Green A, Basile R, Rumberger JM. Transferrin and iron induce insulin resistance of glucose transport in adipocytes. Metabolism. 2006;55(8):1042-5.

197. Ku BJ, Kim SY, Lee TY, Park KS. Serum ferritin is inversely correlated with serum adiponectin level: population-based cross-sectional study. Dis Markers. 2009;27(6):303-10.

198. Fernandez-Real JM, Moreno JM, Ricart W. Circulating retinol-binding protein-4 concentration might reflect insulin resistance-associated iron overload. Diabetes. 2008;57(7):1918-25.

199. Fernandez-Real JM, Moreno JM, Chico B, Lopez-Bermejo A, Ricart W. Circulating visfatin is associated with parameters of iron metabolism in subjects with altered glucose tolerance. Diabetes Care. 2007;30(3):616-21.

200. Dongiovanni P, Fracanzani AL, Fargion S, Valenti L. Iron in fatty liver and in the metabolic syndrome: a promising therapeutic target. J Hepatol. 2011;55(4):920-32.

201. Chung B, Matak P, McKie AT, Sharp P. Leptin increases the expression of the iron regulatory hormone hepcidin in HuH7 human hepatoma cells. J Nutr. 2007;137(11):2366-70.

202. Lesbordes-Brion JC, Viatte L, Bennoun M, Lou DQ, Ramey G, Houbron C, et al. Targeted disruption of the hepcidin 1 gene results in severe hemochromatosis. Blood. 2006;108(4):1402-5.

203. Nelson JE, Wilson L, Brunt EM, Yeh MM, Kleiner DE, Unalp-Arida A, et al. Relationship between the pattern of hepatic iron deposition and histological severity in nonalcoholic fatty liver disease. Hepatology. 2011;53(2):448-57.

204. Wang JY, Zhuang QQ, Zhu LB, Zhu H, Li T, Li R, et al. Meta-analysis of brain iron levels of Parkinson's disease patients determined by postmortem and MRI measurements. Sci Rep. 2016;6:36669.

205. Milic S, Mikolasevic I, Orlic L, Devcic E, Starcevic-Cizmarevic N, Stimac D, et al. The Role of Iron and Iron Overload in Chronic Liver Disease. Med Sci Monit. 2016;22:2144-51.

206. Britton LJ, Subramaniam VN, Crawford DH. Iron and non-alcoholic fatty liver disease. World J Gastroenterol. 2016;22(36):8112-22.

207. Dongiovanni P, Ruscica M, Rametta R, Recalcati S, Steffani L, Gatti S, et al. Dietary iron overload induces visceral adipose tissue insulin resistance. Am J Pathol. 2013;182(6):2254-63.

208. Aigner E, Felder TK, Oberkofler H, Hahne P, Auer S, Soyal S, et al. Glucose acts as a regulator of serum iron by increasing serum hepcidin concentrations. J Nutr Biochem. 2013;24(1):112-7.

209. Valenti L, Fracanzani AL, Bugianesi E, Dongiovanni P, Galmozzi E, Vanni E, et al. HFE genotype, parenchymal iron accumulation, and liver fibrosis in patients with nonalcoholic fatty liver disease. Gastroenterology. 2010;138(3):905-12.

210. Maliken BD, Nelson JE, Klintworth HM, Beauchamp M, Yeh MM, Kowdley KV. Hepatic reticuloendothelial system cell iron deposition is associated with increased apoptosis in nonalcoholic fatty liver disease. Hepatology. 2013;57(5):1806-13.

211. Adams LA, Crawford DH, Stuart K, House MJ, St Pierre TG, Webb M, et al. The impact of phlebotomy in nonalcoholic fatty liver disease: A prospective, randomized, controlled trial. Hepatology. 2015;61(5):1555-64.

212. Laine F, Ruivard M, Loustaud-Ratti V, Bonnet F, Cales P, Bardou-Jacquet E, et al. Metabolic and hepatic effects of bloodletting in dysmetabolic iron overload syndrome: A randomized controlled study in 274 patients. Hepatology. 2017;65(2):465-74.

213. Corradini E, Pietrangelo A. Iron and steatohepatitis. J Gastroenterol Hepatol. 2012;27 Suppl 2:42-6.

214. Corradini E, Bernardis I, Dongiovanni P, Buzzetti E, Caleffi A, Artuso L, et al. Rare ceruloplasmin variants are associated with hyperferritinemia and increased hepatic iron in NAFLD patients: results from a NGS study. In: Hepatology Jo, editor. The International Liver Congress ILC; 2018; Paris2018. p. S58.

215. Valenti L, Rametta R, Dongiovanni P, Motta BM, Canavesi E, Pelusi S, et al. The A736V TMPRSS6 polymorphism influences hepatic iron overload in nonalcoholic fatty liver disease. PLoS One. 2012;7(11):e48804.

216. Ryan JD, Armitage AE, Cobbold JF, Banerjee R, Borsani O, Dongiovanni P, et al. Hepatic iron is the major determinant of serum ferritin in NAFLD patients. Liver Int. 2017.

217. Avila F, Echeverria G, Perez D, Martinez C, Strobel P, Castillo O, et al. Serum Ferritin Is Associated with Metabolic Syndrome and Red Meat Consumption. Oxid Med Cell Longev. 2015;2015:769739.

218. Nelson JE, Brunt EM, Kowdley KV, Nonalcoholic Steatohepatitis Clinical Research N. Lower serum hepcidin and greater parenchymal iron in nonalcoholic fatty liver disease patients with C282Y HFE mutations. Hepatology. 2012;56(5):1730-40.

219. Handa P, Vemulakonda AL, Maliken BD, Morgan-Stevenson V, Nelson JE, Dhillon BK, et al. Differences in hepatic expression of iron, inflammation and stress-related genes in patients with nonalcoholic steatohepatitis. Ann Hepatol. 2017;16(1):77-85.

220. Ruddell RG, Hoang-Le D, Barwood JM, Rutherford PS, Piva TJ, Watters DJ, et al. Ferritin functions as a proinflammatory cytokine via iron-independent protein kinase C zeta/nuclear factor kappaB-regulated signaling in rat hepatic stellate cells. Hepatology. 2009;49(3):887-900.

221. Graham RM, Chua AC, Carter KW, Delima RD, Johnstone D, Herbison CE, et al. Hepatic iron loading in mice increases cholesterol biosynthesis. Hepatology. 2010;52(2):462-71.

222. Lu S, Natarajan SK, Mott JL, Kharbanda KK, Harrison-Findik DD. Ceramide Induces Human Hepcidin Gene Transcription through JAK/STAT3 Pathway. PLoS One. 2016;11(1):e0147474.

223. Patil VA, Fox JL, Gohil VM, Winge DR, Greenberg ML. Loss of cardiolipin leads to perturbation of mitochondrial and cellular iron homeostasis. J Biol Chem. 2013;288(3):1696-705.

224. Liu J, Han L, Zhu L, Yu Y. Free fatty acids, not triglycerides, are associated with non-alcoholic liver injury progression in high fat diet induced obese rats. Lipids Health Dis. 2016;15:27.

225. Ogawa Y, Imajo K, Honda Y, Kessoku T, Tomeno W, Kato S, et al. Palmitate-induced lipotoxicity is crucial for the pathogenesis of nonalcoholic fatty liver disease in cooperation with gut-derived endotoxin. Sci Rep. 2018;8(1):11365.

226. Britton L, Bridle K, Reiling J, Santrampurwala N, Wockner L, Ching H, et al. Hepatic iron concentration correlates with insulin sensitivity in nonalcoholic fatty liver disease. Hepatol Commun. 2018;2(6):644-53.